

# Validation of Gyratory Mix Design in Iowa – Phase II

**Final Report**  
**August 2021**



---

**IOWA STATE UNIVERSITY**  
**Institute for Transportation**

**Sponsored by**  
Iowa Highway Research Board  
(IHRB Project TR-742)  
Iowa Department of Transportation  
(InTrans Project 18-642)

## **About the Asphalt Materials and Pavements Program**

The Asphalt Materials and Pavements Program (AMPP) at InTrans specializes in improving asphalt materials and pavements through research and technology transfer and in developing students' technical skills in asphalt.

## **About the Institute for Transportation**

The mission of the Institute for Transportation (InTrans) at Iowa State University is to save lives and improve economic vitality through discovery, research innovation, outreach, and the implementation of bold ideas.

## **Iowa State University Nondiscrimination Statement**

Iowa State University does not discriminate on the basis of race, color, age, ethnicity, religion, national origin, pregnancy, sexual orientation, gender identity, genetic information, sex, marital status, disability, or status as a US veteran. Inquiries regarding nondiscrimination policies may be directed to the Office of Equal Opportunity, 3410 Beardshear Hall, 515 Morrill Road, Ames, Iowa 50011, telephone: 515-294-7612, hotline: 515-294-1222, email: eooffice@iastate.edu.

## **Disclaimer Notice**

The contents of this report reflect the views of the authors, who are responsible for the facts and the accuracy of the information presented herein. The opinions, findings and conclusions expressed in this publication are those of the authors and not necessarily those of the sponsors.

The sponsors assume no liability for the contents or use of the information contained in this document. This report does not constitute a standard, specification, or regulation.

The sponsors do not endorse products or manufacturers. Trademarks or manufacturers' names appear in this report only because they are considered essential to the objective of the document.

## **Iowa DOT Statements**

Federal and state laws prohibit employment and/or public accommodation discrimination on the basis of age, color, creed, disability, gender identity, national origin, pregnancy, race, religion, sex, sexual orientation or veteran's status. If you believe you have been discriminated against, please contact the Iowa Civil Rights Commission at 800-457-4416 or the Iowa Department of Transportation affirmative action officer. If you need accommodations because of a disability to access the Iowa Department of Transportation's services, contact the agency's affirmative action officer at 800-262-0003.

The preparation of this report was financed in part through funds provided by the Iowa Department of Transportation through its "Second Revised Agreement for the Management of Research Conducted by Iowa State University for the Iowa Department of Transportation" and its amendments.

The opinions, findings, and conclusions expressed in this publication are those of the authors and not necessarily those of the Iowa Department of Transportation.

**Technical Report Documentation Page**

<b>1. Report No.</b> IHRB Project TR-742	<b>2. Government Accession No.</b>	<b>3. Recipient's Catalog No.</b>	
<b>4. Title and Subtitle</b> Validation of Gyratory Mix Design in Iowa – Phase II		<b>5. Report Date</b> August 2021	
		6. Performing Organization Code	
<b>7. Author(s)</b> R. Christopher Williams (orcid.org/0000-0002-8833-6232), Ashley Buss (orcid.org/0000-0002-8563-9553), Joseph Podolsky (orcid.org/0000-0003-1834-5026), Hosin "David" Lee (orcid.org/0000-0001-9766-1232), and Kai Xin (orcid.org/0000-0002-4061-191X)		<b>8. Performing Organization Report No.</b> InTrans Project 18-642	
<b>9. Performing Organization Name and Address</b> Asphalt Materials and Pavement Program Iowa State University 2711 South Loop Drive, Suite 4700 Ames, IA 50010-8664		<b>10. Work Unit No. (TRAIS)</b>	
		<b>11. Contract or Grant No.</b>	
<b>12. Sponsoring Organization Name and Address</b> Iowa Highway Research Board and Iowa Department of Transportation 800 Lincoln Way Ames, IA 50010		<b>13. Type of Report and Period Covered</b> Final Report	
		<b>14. Sponsoring Agency Code</b> IHRB Project TR-742	
<b>15. Supplementary Notes</b> Visit <a href="https://intrans.iastate.edu/">https://intrans.iastate.edu/</a> for color pdfs of this and other research reports.			
<b>16. Abstract</b> <p>Optimizing the asphalt mixture design process to produce mixes that balance excellent performance with economical materials, requires addressing the current <math>N_{design}</math> values. <math>N_{design}</math> is where differences between the laboratory mix design compaction effort and the air voids that are ultimately achieved in the field can be improved. Validating this relationship for Iowa asphalt mix designs will lead to better correlations between mix design target voids, field voids, and performance.</p> <p>As a result of the Phase I study, the <math>N_{design}</math> specifications were changed in October 2016. In addition to the mix design changes, the Iowa Department of Transportation (DOT) implemented new asphalt binder grading criteria. Phase II is primarily a validation study of the new mix design specifications.</p> <p>The main purpose of this study was to evaluate and compare differences in performance between mix designs made using old and new <math>N_{design}</math> values (different optimal binder contents) for low, medium, and high traffic. Performance comparisons were made for three mix designs with one for each traffic level (low, medium, and high) using tests such as Hamburg wheel tracking for rutting and moisture susceptibility, flow number for rutting, disk-shaped compact tension for low-temperature cracking, -point beam fatigue for fatigue cracking, and dynamic modulus for characterizing asphalt mix stiffness with changing temperatures. Lastly this study used results from the dynamic modulus and dynamic shear rheometer, along with site location information, for use in AASHTOWare Pavement ME Design, to forecast long-term pavement performance impacts by changing the asphalt content <math>N_{design}</math> value and comparing performance to field distress surveyed performance.</p> <p>When produced with new <math>N_{design}</math> values (higher optimal binder content), the three mix designs were observed to perform better against rutting, fatigue cracking, and low-temperature cracking than that of mixtures made using old <math>N_{design}</math> values. Significant differences were shown between old and new <math>N_{design}</math> for IA 4 using flow number results and IA 330 and I-235 for Hamburg wheel tracking test results in terms of resistance against rutting. Laboratory results appear to validate that changing to new <math>N_{design}</math> value specifications does improve mix performance.</p> <p>When comparing predicted performance from AASHTOWare Pavement ME Design against field performance in the Iowa DOT's Pavement Management Information System, there were significant differences for both old and new <math>N_{design}</math> produced mixtures. A possible reason for this is a need for more level 1 input data in ME Design such that predicted performance can be better correlated to field performance.</p>			
<b>17. Key Words</b> air voids—AASHTOWare Pavement ME Design—asphalt pavement design—binders—fatigue cracking—gyratory compaction cycles—low-temperature cracking—moisture susceptibility—new $N_{design}$ validation—pavement performance comparisons—rutting		<b>18. Distribution Statement</b> No restrictions.	
<b>19. Security Classification (of this report)</b> Unclassified.	<b>20. Security Classification (of this page)</b> Unclassified.	<b>21. No. of Pages</b> 105	<b>22. Price</b> NA



# **VALIDATION OF GYRATORY MIX DESIGN IN IOWA – PHASE II**

**Final Report  
August 2021**

## **Principal Investigator**

R. Chris Williams, Director  
Asphalt Materials and Pavements Program  
Institute for Transportation, Iowa State University

## **Research Assistant**

Kai Xin

## **Authors**

R. Chris Williams, Ashley Buss, Joseph Podolsky, Hosin “David” Lee, and Kai Xin

Sponsored by  
Iowa Highway Research Board and  
Iowa Department of Transportation  
(IHRB Project TR-742)

Preparation of this report was financed in part  
through funds provided by the Iowa Department of Transportation  
through its Research Management Agreement with the  
Institute for Transportation  
(InTrans Project 18-642)

A report from  
**Institute for Transportation**  
**Iowa State University**  
2711 South Loop Drive, Suite 4700  
Ames, IA 50010-8664  
Phone: 515-294-8103 / Fax: 515-294-0467  
<https://intrans.iastate.edu/>



## TABLE OF CONTENTS

ACKNOWLEDGMENTS .....	xi
EXECUTIVE SUMMARY .....	xiii
Background and Problem Statement.....	xiii
Study Overview and Objectives.....	xiii
Experimental Plan Summary .....	xiii
Key Findings.....	xiv
Implementation Readiness and Benefits.....	xiv
CHAPTER 1: INTRODUCTION .....	1
Background.....	1
Project Objectives and Experimental Plan Summary .....	2
Report Content.....	3
CHAPTER 2: LITERATURE REVIEW .....	4
Background of Superpave Mix Design.....	4
Gyratory Compaction.....	4
Iowa $N_{design}$ .....	5
$N_{design}$ in Other States .....	6
CHAPTER 3: EXPERIMENTAL PLAN AND TESTING METHODS .....	9
Introduction and Overview .....	9
Volumetrics and Compaction Curves .....	10
Dynamic Modulus Tests .....	13
E* Shifted Results Using Sigmoidal Model .....	14
Flow Number Tests.....	15
Hamburg Wheel Tracking Tests .....	16
Beam Fatigue Tests.....	17
Project Selection .....	18
Evaluation of Existing Pavement Conditions .....	20
Determination of Mixture Volumetrics .....	21
Determination of Optimal Asphalt Content using Laboratory-Compacted Mixes.....	22
Mix Design.....	22
CHAPTER 4: RESULTS AND ANALYSES .....	28
Optimal Binder Content Selection.....	28
Dynamic Modulus Results and Master Curves.....	30
Flow Number Results .....	33
Hamburg Wheel Tracking Results.....	36
DCT Results.....	41
Beam Fatigue Results .....	43
ME Design Performance Prediction .....	45
PMIS Research Results.....	50
PMIS and ME Design Comparisons.....	50

CHAPTER 5: CONCLUSIONS AND RECOMMENDATIONS .....	57
REFERENCES .....	59
APPENDIX A: MIXTURE FORMULA INFORMATION .....	63
APPENDIX B: QC/QA FIELD VOIDS DATA.....	69
APPENDIX C: DYNAMAIC MODULUS TEST RESULTS .....	71
APPENDIX D: HAMBURG WHEEL TRACKING TEST RESULTS.....	77
APPENDIX E: DCT RESULTS.....	79
APPENDIX F: BEAM FATIGUE TEST RESULTS.....	81
APPENDIX G: AASHTOWARE PAVEMENT ME DESIGN INPUTS .....	85



## LIST OF FIGURES

Figure 1. Field-mix/laboratory-compacted (FMLC) versus field-mixed/field-compacted (FMFC) air voids after 3 years .....	7
Figure 2. Flowchart of experimental plan for the study.....	10
Figure 3. VMA and VFA for three roadways .....	11
Figure 4. IA 4 compaction curves .....	12
Figure 5. IA 330 compaction curves.....	12
Figure 6. I-235 compaction curves .....	13
Figure 7. Predicted E* master curve from existing data.....	14
Figure 8. Estimated E* values of -10°C and 54°C from predicted E* master curve.....	15
Figure 9. Estimate and existing E* values .....	15
Figure 10. Permanent shear strain versus number of loading cycles .....	16
Figure 11. Project locations in Iowa .....	19
Figure 12. Water bath used in conventional method .....	21
Figure 13. Metal bucket method .....	22
Figure 14. IA 4 aggregate gradation .....	26
Figure 15. IA 330 aggregate gradation .....	26
Figure 16. I-235 aggregate gradation.....	27
Figure 17. IA 4 percent air void versus percent binder content.....	28
Figure 18. IA 330 percent air void versus percent binder content.....	29
Figure 19. I-235 percent air void versus percent binder content .....	29
Figure 20. IA 4 dynamic modulus data.....	31
Figure 21. IA 330 dynamic modulus data.....	31
Figure 22. I-235 dynamic modulus data .....	32
Figure 23. Flow number results .....	34
Figure 24. Creep slope, stripping slope, and SIP .....	37
Figure 25. IA 4 rutting depth versus passes .....	38
Figure 26. IA 330 rutting depth versus passes .....	38
Figure 27. I-235 rutting depth versus passes .....	39
Figure 28. Fracture energy and peak load results .....	41
Figure 29. Beam fatigue curves .....	44
Figure 30. Transverse cracking results and reliability .....	46
Figure 31. IRI results .....	47
Figure 32. AC top-down fatigue cracking results.....	48
Figure 33. AC rutting results .....	49
Figure 34. IA 4 PMIS vs. ME Design IRI comparison.....	51
Figure 35. IA 330 PMIS vs. ME Design IRI comparison.....	52
Figure 36. I-235 PMIS vs. ME Design IRI comparison .....	52
Figure 37. IA 4 PMIS vs. ME Design rutting depth comparison .....	53
Figure 38. IA 330 PMIS vs. ME Design rutting depth comparison .....	53
Figure 39. I-235 PMIS vs. ME Design rutting depth comparison .....	54
Figure 40. IA 4 PMIS vs. ME Design transverse cracking comparison .....	55
Figure 41. IA 330 PMIS vs. ME Design transverse cracking comparison .....	55
Figure 42. I-235 PMIS vs. ME Design transverse cracking comparison.....	56
Figure 43. IA 4 formula .....	63

Figure 44. IA 4 formula (continued).....	64
Figure 45. IA 330 formula .....	65
Figure 46. IA 330 formula (continued).....	66
Figure 47. I-235 formula.....	67
Figure 48. I-235 formula (continued) .....	68

## LIST OF TABLES

Table 1. AASHTO R 35 Superpave gyratory compaction specifications .....	5
Table 2. Newly implemented asphalt mix design and asphalt binder grading criteria .....	6
Table 3. Volumetric details for three Iowa roadways.....	10
Table 4. Mixtures and mixture properties included in this study .....	17
Table 5. Project details.....	19
Table 6. Level of severity corresponding to type of distress .....	20
Table 7. IA 4 aggregate gradation.....	23
Table 8. IA 330 aggregate gradation.....	24
Table 9. I-235 aggregate gradation .....	25
Table 10. $N_{design}$ compaction gyrations .....	28
Table 11. Summary of new $N_{design}$ optimal asphalt content for all levels of traffic .....	30
Table 12. IA 4 ANOVA results .....	32
Table 13. IA 330 ANOVA results .....	33
Table 14. I-235 ANOVA results .....	33
Table 15. Tentative flow number criteria .....	34
Table 16. Experimental design for flow number .....	34
Table 17. IA 4 flow number ANOVA results.....	35
Table 18. IA 330 flow number ANOVA results.....	35
Table 19. I-235 flow number ANOVA results .....	36
Table 20. Hamburg wheel tracking test results.....	36
Table 21. IA 4 rutting depth ANOVA results.....	40
Table 22. IA 330 rutting depth ANOVA results.....	40
Table 23. I-235 rutting depth ANOVA results .....	40
Table 24. DCT test results .....	41
Table 25. IA 4 fracture energy ANOVA results .....	42
Table 26. IA 330 fracture energy ANOVA results .....	42
Table 27. I-235 fracture energy ANOVA results.....	42
Table 28. Beam fatigue test results .....	43
Table 29. IA 4 cycles to failure ANOVA results.....	44
Table 30. IA 330 cycles to failure ANOVA results.....	45
Table 31. I-235 cycles to failure ANOVA results .....	45
Table 32. 2018 PMIS information .....	50
Table 33. PMIS results in 2014 and 2016.....	51
Table 34. QC/QA data .....	69
Table 35. Dynamic modulus results.....	71
Table 36. Dynamic modulus results (continued) .....	72
Table 37. Dynamic modulus results (continued) .....	73

Table 38. Dynamic modulus results (continued) .....	74
Table 39. Dynamic modulus results (continued) .....	75
Table 40. Dynamic modulus results (continued) .....	76
Table 41. HWTT results .....	77
Table 42. HWTT results (continued) .....	78
Table 43. DCT Results.....	79
Table 44. Beam fatigue results.....	81
Table 45. Beam fatigue results (continued) .....	82
Table 46. Beam fatigue results (continued) .....	83
Table 47. Binder input .....	85
Table 48. 2014 ME Design inputs summary .....	86
Table 49. 2014 ME Design inputs summary (continued) .....	87
Table 50. 2016 ME Design inputs summary .....	88
Table 51. 2016 ME Design inputs summary (continued) .....	89



## **ACKNOWLEDGMENTS**

The authors would like to thank the Iowa Department of Transportation (DOT) and the Iowa Highway Research Board (IHRB) for sponsoring this project. They would also like to thank the technical advisory committee (TAC) members, Jon Arjes and Chris Brakke, and the rest of the staff in the Central Materials Laboratory at the Iowa DOT for their support and assistance with asphalt mixture testing during the duration of the project. Finally, the authors would like to acknowledge Paul Ledtje and the staff of the Advanced Asphalt Materials Laboratory at Iowa State University for their time in assisting with specimen preparation and testing.



## **EXECUTIVE SUMMARY**

### **Background and Problem Statement**

The use of asphalt pavements, which cover about 94% of paved roads, have gradually increased since the late 19th century (Roberts et al. 1991). The mix design of asphalt pavements has undergone continual evolution since initial development, relying heavily on empirical knowledge. In the US, the Superior Performing Asphalt Pavement (Superpave) mix design method is used in most states.

One of the most important factors in mix design is the compaction effort, or number of gyrations of the asphalt mixture, which is denoted as the design number of gyrations ( $N_{\text{design}}$ ).  $N_{\text{design}}$  is one of the most significant design considerations/parameters in the laboratory and is selected based on the corresponding number of equivalent single-axle loads (ESALs) for the proposed pavement structure.

### **Study Overview and Objectives**

All mixes used for this study were field-produced and laboratory-compacted for both new and old  $N_{\text{design}}$  values. The field-produced mixes were collected from Iowa Department of Transportation (DOT) storage units, and asphalt remix and compaction were according to Superpave mix design and Iowa local performance testing.

Performance tests will help to evaluate the effect of changing the  $N_{\text{design}}$  value on mixture performance. The laboratory-compacted mixes were used for all performance tests. The key objective of the study was using performance tests at the optimal binder content for a given  $N_{\text{design}}$  to indicate the differences due to changing the number of gyrations.

Performance tests such as dynamic modulus, flow number, Hamburg wheel track, 4-pt beam fatigue and disk-shaped compact tension were used to evaluate stiffness, rutting/moisture susceptibility, fatigue resistance, and resistance to low-temperature cracking; the results helped in determining if significant differences exist between the old and new  $N_{\text{design}}$  specifications.

The last objective of the laboratory study was to take results from dynamic modulus testing and site location information to use in The American Association of State Highway and Transportation Officials' (AASHTO's) AASHTOWare Pavement Mechanistic-Empirical (ME) Design software to forecast long-term pavement performance impacts in changing the asphalt content or  $N_{\text{design}}$ . The mixture properties and binder data from the supplier were used to forecast the pavement performance in 20 years. If differences were detected between material properties, the computer model helped to show how material properties would influence performance over time.

## Experimental Plan Summary and Goal

This Phase II study included performance evaluation of the field mixes being produced to ensure performance expectations were being met for rutting, moisture susceptibility, fatigue and low-temperature cracking. Phase II was conducted as a laboratory study with the goal of addressing the mix design process and identifying how changes in  $N_{\text{design}}$  influence performance over a pavement's lifetime. The differences between AASHTOWare Pavement ME Design software predictions and Iowa DOT Pavement Management Information System (PMIS)-field performance data were also investigated.

Loose mixes were sampled for subsequent testing. Concurrently, a mix design analysis for each of the new ESAL levels using the source aggregates and binder from the field construction projects were re-evaluated for mixture design. The  $N_{\text{design}}$  was validated using traditional mix design procedures by varying asphalt content to compact to 4% air voids. The four tasks that were part of the first and second objectives in the study were about the mix design analysis, as follows:

- Evaluate the ultimate in-place densities by performing volumetric testing on  $\leq 1$  million ESALs (on IA 4 pavements), 1–10 million ESALs (on IA 330 pavements), and  $>10$  million ESALs (on I-235 pavements) for design level surface mixes
- Determine the compatibility of the mixes under the existing mix design procedures by recalculating the gyratory slope from the quality control and quality assurance (QC/QA) data
- Estimate and compare the post-construction compaction effort for each selected project and determine the theoretical  $N_{\text{design}}$  at construction and post-construction
- Evaluate the optimal asphalt contents and aggregate structures due to different  $N_{\text{design}}$  values adopted for the mixtures under the three different traffic levels

## Key Findings

- New  $N_{\text{design}}$  mixtures had higher dynamic modulus than old  $N_{\text{design}}$  mixtures. However, the differences were not significant according to statistical analysis.
- New  $N_{\text{design}}$  mixtures had better rutting resistance than old  $N_{\text{design}}$  mixtures according to flow number test results. The statistical analysis showed only IA 4 (lowest traffic level) mixtures had a significant difference between old and new  $N_{\text{design}}$  specifications. IA 330 and I-235 (with medium and highest traffic level) mixtures showed no statistical differences.
- With the Hamburg wheel tracking tests, new  $N_{\text{design}}$  mixtures showed better performance and lower rutting than old  $N_{\text{design}}$  mixtures. IA 330 and I-235 had statistical differences between the two specifications. No significant difference was found with IA 4 specimens.



- New  $N_{\text{design}}$  mixtures showed better low-temperature performance than old  $N_{\text{design}}$  specimens according to DCT results. New  $N_{\text{design}}$  specimens had higher fracture energy than old  $N_{\text{design}}$  specimens.
- Better fatigue cracking resistance was observed in new  $N_{\text{design}}$  mixes based on beam fatigue test results. New  $N_{\text{design}}$  mixtures afforded more cycles to failure than old  $N_{\text{design}}$  mixtures.

### **Implementation Readiness and Benefits**

The results of this study provide detailed information verifying current  $N_{\text{design}}$  levels in Iowa and provide glimpses into how  $N_{\text{design}}$  might be improved based on performance testing data and  $N_{\text{design}}$  correlations to field density. The advantages of the new  $N_{\text{design}}$  included reduced gyratory compaction cycles and increased binder content, while the binder type and gradation did not change within specimens made using the old and new  $N_{\text{design}}$  levels.

The results also showed how changes to  $N_{\text{design}}$  impact rutting and mixture stiffness as well as predicted pavement performance. However, Iowa DOT PMIS and AASHTOWare Pavement ME Design result comparisons were not perfect.

The possible reasons could be that there is insufficient level 1 input data into ME Design or there could be other reasons that need to be further investigated. In this study, only laboratory-measured values such as dynamic modulus and dynamic shear rheometer (DSR) were used in ME Design as level 1 inputs. Additional research should be undertaken.



## CHAPTER 1: INTRODUCTION

### Background

The use of asphalt pavement has increased since the late 19th century (Roberts et al. 1991). Hot-mix asphalt (HMA) mixture design parameters are critical in making safe and cost-effective asphalt pavements. Nowadays, the Superior Performing Asphalt Pavement (Superpave) mix design is widely used in the US. The design number of gyrations ( $N_{\text{design}}$ ) is one of the most critical factors used in Superpave mix design (Prowell and Brown 2007). The  $N_{\text{design}}$  parameter is selected based on the traffic volume or equivalent single-axle load (ESAL) levels. The asphalt  $N_{\text{design}}$  parameter helps to control the optimal asphalt content.

During mixture design, the laboratory-compaction effort must match achievable field-compaction conditions on the roadway during construction and subsequent compaction from traffic. Achieving density is essential to ensuring excellent pavement performance and economical material costs (Newcomb et al. 2001). A comprehensive review of Iowa Department of Transportation's (DOT's) current  $N_{\text{design}}$  was performed to study the correlation between laboratory air voids and field air voids for asphalt pavements. This study examines existing mixes and pavements constructed at previously specified  $N_{\text{design}}$  levels and investigates field performance data.

During the asphalt mixture design process in the laboratory, the gyratory compaction level controls how the aggregates interact with the binder content to affect the percentage of air voids within a mixture (Williams et al. 2016, Button et al. 2004). In other words, when the gradation of the mix stays constant, changing the gyration level results in air void and binder content changes based on Superpave mix design to achieve 4% air voids. Design compaction level, or  $N_{\text{design}}$ , requirements correspond to a traffic level. The intent is to compact the mixture to 7–8% air voids in the field and densify the roadway further through traffic (Butcher 1998).

In this study, the new  $N_{\text{design}}$  gyration levels for each traffic classification are lower than the old  $N_{\text{design}}$  gyration levels. However, the biggest concern in reducing gyratory compaction levels is increased roadway rutting. To meet the minimum air void requirement, increasing binder content for lower gyration levels is necessary. The purpose of this work was to analyze how mix performance changes when adjusting gyration levels from the Iowa DOT's old  $N_{\text{design}}$  levels to their new  $N_{\text{design}}$  levels. Furthermore, if a given traffic level is needed to increase compaction, a new mix design may need created to meet the density requirements.

Studying how binder content changes with compaction is an excellent method to develop good asphalt mix performance. The asphalt mixture's voids in mineral aggregate (VMA) control(s) the overall voids in the asphalt mixture, and asphalt binder fills the air voids in asphalt concrete. The purpose of the new  $N_{\text{design}}$  levels (changing gyration numbers) was not to change the required volumetrics but to change the binder content to minimize VMA by selecting the best gyration number (Ceylan et al. 2015).

In this study, the mixture's gradation was held constant. Increased binder content was used to meet VMA and air-void requirements for the new  $N_{\text{design}}$  specifications due to gyratory compaction reductions.

This study sought to determine, quantify, and evaluate how HMA performance is affected by differences in the  $N_{\text{design}}$  gyrations levels from the American Association of State Highway and Transportation Officials (AASHTO 2008). The Iowa DOT had implemented a new asphalt mix design of 50 gyrations for traffic levels of <1M equivalent single-axle loads (ESALs), 75 gyrations for 1M to 10M ESALs, and 95 gyrations for >10M ESALs. Three highway pavements were selected to represent the three traffic levels: IA 4 for <1M ESALs, IA 330 for 1–10M ESALs, and I-235 for >10M ESALs. By analyzing the predicted performance of IA 4, IA 330, and I-235, the asphalt performance could be estimated based on the new  $N_{\text{design}}$  specification. In addition, this could also help validate the new mix design specification based on field mix performance parameters, such as rutting, complex shear modulus, and low-temperature cracking.

AASHTO's AASHTOWare Pavement Mechanistic-Empirical (ME) Design can be used to establish a forecast of pavement field performance (Kennedy et al. 1994). The AASHTOWare Pavement ME Design software. (called ME Design for short) can calculate future pavement responses, such as stresses, strain, and deflections (FHWA 2014).

In this study, ME Design was used to help estimate field performance of mixtures designed with new and old  $N_{\text{design}}$  asphalt mixture parameters. The traffic volume, location, climate, and material properties are the factors that influence pavement response. ME Design can be used with advanced material mechanics and engineers' experience (Harmelink and Aschenbrener 2002). The software provides a tool to optimize pavement design and estimate the various distresses. Researchers can develop better validation models by evaluating the model's sensitivity to input values (Iowa DOT 2012). In ME Design, the distresses such as the international roughness index (IRI), asphalt concrete (AC) top-down cracking, and AC rutting can be predicted.

## **Project Objectives and Experimental Plan Summary**

Phase II was primarily a validation study of the new mix design specifications. The first objective of the Phase II study was to evaluate performance of the field mixes produced with the 2016 specifications to ensure performance expectations were being met for rutting, moisture susceptibility, and low-temperature cracking; loose mixes were used for subsequent specimen preparation and testing.

The second objective was to evaluate the new mix design specifications in terms of performance and constructability. A mix design analysis for each of the new ESAL levels using the source aggregates and binder from three field construction projects were re-evaluated based on mixture design. The  $N_{\text{design}}$  was validated using traditional mix design procedures by varying asphalt content to compact to 4% air voids. Measuring strength in the design process would directly correlate  $N_{\text{design}}$  with performance tests.

The third objective of the study entailed performance testing of each mix at the optimal binder content in each  $N_{\text{design}}$  level (categorized by aggregate gradation and ESAL level) using tests such as dynamic modulus, Hamburg wheel tracking, and disk-shaped compact tension to evaluate the stiffness, rutting moisture susceptibility, and resistance to low-temperature cracking.

The last objective of the laboratory study was to take results from the dynamic modulus testing and site location information to use in ME Design to forecast long-term pavement performance impacts by changing the asphalt content or  $N_{\text{design}}$  values. The mixture properties and binder data from the supplier was used to forecast the pavement performance in 20 years. If differences were detected between material properties, the computer model helped to show how the properties would influence performance over time.

The results of this study provide detailed information verifying current  $N_{\text{design}}$  levels in Iowa and provide recommendations on how  $N_{\text{design}}$  can be improved based on performance testing data and  $N_{\text{design}}$  correlations with field density. The results also show how changes to  $N_{\text{design}}$  impact rutting and moisture susceptibility, resistance to fatigue and low temperature cracking and mixture stiffness as well as predicted pavement performance. Phase II was conducted as a laboratory study with the goal of addressing the mix design process and identifying how changes in  $N_{\text{design}}$  will influence performance over a pavement's lifetime.

## **Report Content**

Chapter 1 introduced background information and the project objectives. Chapter 2 contains the literature review and summarizes information about  $N_{\text{design}}$  and how  $N_{\text{design}}$  specifications have changed in Iowa. Chapter 3 introduces the experimental methods for testing and analysis of data. Chapter 4 presents binder information, results from mixture performance testing, and a discussion of the asphalt materials test results. Chapter 4 also includes the comparison of the mix performance test results and ME Design results. Finally, Chapter 5 presents conclusions and recommendations about the new  $N_{\text{design}}$  levels. Seven appendices (A through G) include supplementary information complete result tables of data from the study.

## CHAPTER 2: LITERATURE REVIEW

### Background of Superpave Mix Design

In 1987, the Federal Highway Administration (FHWA) improved the management of HMA pavement and provided the innovation for the Superpave system (Asphalt Institute 2001). This system provided practical tools for engineers and contractors to improve the performance of HMA pavements. The Superpave system consists of two parts: asphalt binder specification and mix design system. Superpave provides the technology to ensure pavement mixtures perform successfully on the roadway with appropriate binder and aggregation corporations (FHWA 2013).

Superpave mix design helps in evaluating the volumetric properties of compacted specimens. It includes several parameters: VMA, air voids ( $V_a$ ), voids filled with asphalt binder (VFA), and dust-to-binder ratio. The criteria for those values are also different.  $V_a$  needs to be 4% at  $N_{\text{design}}$ ; VMA includes the air voids and the effective asphalt content, expressed as a percent of the total volume; and VFA is the percentage of the voids in the mineral aggregate that are filled with asphalt, not including absorbed asphalt. These volumetric parameters consist of the void structure, and the properties make the void requirement of the asphalt mix (Dhir et al. 2017).

Cominsky et al. 1994 provided a detailed background and overview of the Superpave mix design system that was developed (Kennedy et al. 1994). The design of asphalt mixtures is a complex process that requires the proper proportioning of materials to satisfy mixture volumetric and mechanical properties. Most of the time spent in the mix design process is used to evaluate and select aggregate gradations to meet project requirements (Anderson and Bahia 1997). The aggregate requirements are based on traffic volume and gyration compaction number. The aggregate mixes with asphalt binder are compacted by a gyratory compactor using a certain number of gyrations, and then the volumetric properties are evaluated to check if volumetric requirements are met. The asphalt aggregate gradation selection will meet the minimum volume and densification criteria and determine an aggregate structure that will provide sufficient resistance to permanent deformation, fatigue, and thermal cracking (NHI 2000).

### Gyratory Compaction

The laboratory compaction effort replicates the ultimate compaction condition of pavement under several years of traffic loading. Practical experience shows that pavements compacted to an air void content of 4% maintain the best long-term performance in the field (Asphalt Institute 2015). Therefore, choosing an appropriate level of compaction in the laboratory is critical to ensure excellent field asphalt pavement performance.

Asphalt binder is the most expensive component in a mixture and about 70% of HMA production cost (Copeland 2011). The gyratory compaction level used in the laboratory mixture design is critical for determining the optimal binder content. Many agencies have recently reduced the design gyratory compaction levels for a given traffic level. Reduced compaction

allows for more void space between the aggregates and, if air voids and gradation are kept the same, this can lead to higher binder content and improved film thickness, but it could result in lower rutting resistance. Engineers must develop designs to meet the minimum binder content and increase the resistance to plastic deformations (Tashman et al. 2001).

Asphalt mix compaction should create the best air void condition. Low air void content can cause damage to the mixture and even cause flushing. Excessive air void content can lead to a porous asphalt mixture layer, accelerating the asphalt binder’s oxidation and resulting in raveling and rutting. Adequate air voids limit permeability and provide long-lasting performance. To guarantee adequate compaction, the load applied by the roller press or laboratory compactor must be higher than the traffic loading because, during construction and compaction, the mixture is transformed from a very loose state to a tighter condition to afford the traffic load.

The internal resistance of asphalt concrete determines if compaction is efficient. The resistance includes aggregate interlocking, frictional resistance, and viscous resistance (Swanson et al. 1965). Another reason to compact the asphalt pavement is to make it watertight and impermeable to air (Smith 1979). To achieve good compaction means air-void content is lower, permeability is lower, and water intrusion is reduced, causing fewer instances of freeze- thaw damage. Increasing the mixture’s density usually results in a stiffer mix but does not necessarily make the pavement stronger and could cause brittle pavement. However, optimal density compaction is associated with the optimal combination of strength and ductility (Smith 1979).

### **Iowa $N_{design}$**

$N_{design}$  is the design number of gyration or compaction values used in Superpave HMA. The designated  $N_{design}$  or design revolutions of the gyratory compactor are used to simulate the roadway’s ESALs. The optimal  $N_{design}$  values are based on two factors: the improvement of pavement fatigue life and the benefits of increasing binder content (increased film thickness) in the mix (Qarouach 2013). Increasing the film thickness can improve pavement durability in terms of thermal cracking. The existing AASHTO R 35 specification has five traffic levels with four gyratory design levels, as shown in Table 1.

**Table 1. AASHTO R 35 Superpave gyratory compaction specifications**

<b>20-Year Design Traffic, ESALs (millions)</b>	<b><math>N_{design}</math> (gyration number)</b>
<0.3	50
0.3 to <3	75
3 to <10	100
10 to <30	100
$\geq 30$	125

The Iowa  $N_{\text{design}}$  specifications were changed in October 2016. In addition to the mix design changes, the Iowa DOT has implemented new asphalt binder grading criteria. The new specifications are summarized in Table 2.

**Table 2. Newly implemented asphalt mix design and asphalt binder grading criteria**

ASPHALT MIX TYPE			PERFORMANCE GRADE BINDER					
Traffic Millions of ESALs	Traffic (T) Level	Number of Design Gyrations	Traffic (ESALs)		Design Speed (MPH)	Class I Projects		Class II Projects
						North	South	
≤ 1 M	ST	50	≤ 1 M	and/or	> 45	58-28S	58-34S	58-28S
1 - 10 M	HT	75	1 - 10 M	and/or	15-45	58-28H	58-34H	58-28H
>10 M	VT	95	>10 M	or	<15	58-28V	58-34V	58-28V
			>10 M	and	<15	58-28E	58-34E	58-28E

ST = standard traffic, HT = high traffic, VT = very high traffic  
Source: Iowa DOT Mixture Design Criteria I.M. 510

The Asphalt Institute developed an original  $N_{\text{design}}$  table through the SHRP-A-408 Task F project (Cominsky et al. 1994). This task aims to determine the number of gyrations that produce the same density on the constructed road (92% of the theoretical maximum density) and the active highway (96% of the theoretical maximum density). The  $G_{\text{mm}}$  of the mixture is the specific gravity of HMA, excluding air voids (Brown et al. 2009).

Asphalt concrete's initial goal was to compact to 7% of the air void in the field. Over time, the traffic loads further densified the pavement to 4% of the target void (Anderson et al. 2002).  $N_{\text{design}}$  is crucial in the optimal asphalt content, because a mixture with too much asphalt will cause permanent deformation. Simultaneously, too little asphalt will cause difficulty in on-site compaction, which usually leads to early fatigue cracks (VMA will be affected later). In general, achieving target pavement density and excellent construction quality are critical to producing durable and long-lasting pavement structures.

### **$N_{\text{design}}$ in Other States**

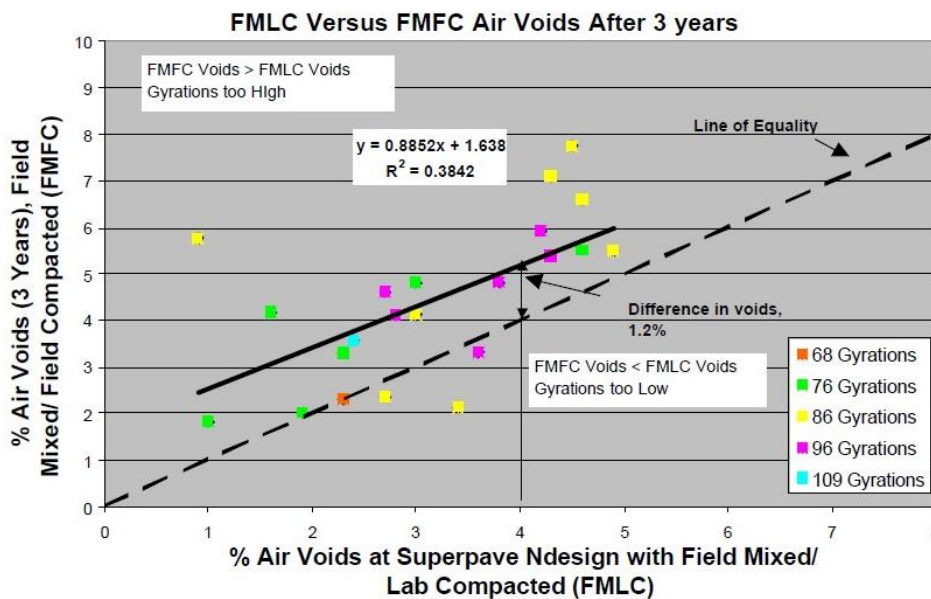
The Superpave mix design of gyration ( $N_{\text{design}}$ ) produces a mixture with the same density to represent the field conditions for different traffic volumes. Lowering the number of design gyrations could increase optimal asphalt binder content if the design aggregate gradation stays constant. Using lower binder content in asphalt pavements helps against rutting. However, it can also cause early fatigue cracking on the pavement surface. Repeated traffic loading applied on pavement surface causes pavement interconnected cracks through fatigue failure. Several factors cause fatigue cracking: traffic load increase, inadequate compaction during construction, poor structure design, and possible loss of supporting base, subbase, and subgrade layers (Schaefer et al. 2008).

National Cooperative Highway Research Program (NCHRP) Report 573 concluded that mixes with higher gyration levels provided better rutting resistance but may lack sufficient durability (Prowell and Brown 2007). In the Phase I report for this study, the researchers concluded that



asphalt mixes with high gyratory compaction levels would perform better against rutting, but that high gyratory compaction levels could lead to low pavement durability (Williams et al. 2016). According to the Phase I report, many states conducted various tests to verify the existing design number of gyrations. The states evaluated the effect on pavement performance to validate the  $N_{\text{design}}$  for their specific regions. The primary interest was in validating current  $N_{\text{design}}$  specifications to meet the requirement over five to six years. Many states developed their gyratory compaction number, including Colorado, Georgia, Ohio, Virginia, and others.

According to Colorado DOT (CDOT) research, none of the pavements randomly selected reached the design air void content after six years. Harmelink and Aschenbrener (2002) found an average of 1.2% difference in air voids for years 3, 4, 5, and 6 between the line of equality at 4% air voids, as shown in Figure 1.



Harmelink and Aschenbrener 2002, Colorado DOT

**Figure 1. Field-mix/laboratory-compacted (FMLC) versus field-mixed/field-compacted (FMFC) air voids after 3 years**

The line of equality was used to contrast the percent air void difference at Superpave  $N_{\text{design}}$  specification with the percent air voids after specific years of construction. Figure 1 shows a 1.2% air void difference between 3 years of in-place field pavement and the equality line. The difference in air voids (1.2%) indicated that the current gyration level was too high, and traffic loading was not enough to compact pavement to meet the 4% air void requirement. CDOT determined that, by reducing gyration levels by 30 design gyrations, pavement mixtures in the laboratory would match the in-place ultimate pavement density.

Pavement performance was also evaluated throughout the study; low to moderate rutting was detected, but no major distresses were observed. The final recommendations were that 75 gyrations were to be used for lower traffic levels and 100 gyrations for higher traffic levels.

The Georgia DOT (GDOT) selected the design gyration number of 65 to match the in-place densities in Georgia. The Ohio DOT (ODOT) used annual average daily traffic (AADT) to select the design number of gyrations of about 65 (Grogg et al. 2020). The Virginia DOT (VDOT) provided better pavement serviceability while controlling rutting or bleeding in the pavements in Virginia. VDOT used a Superpave mix design to accommodate low gyratory compaction numbers with low optimal binder content.

## CHAPTER 3: EXPERIMENTAL PLAN AND TESTING METHODS

### Introduction and Overview

This study used performance tests to evaluate the differences between the old  $N_{\text{design}}$  gradation levels and the new, reduced  $N_{\text{design}}$  specifications for HMA mixture design in Iowa. The performance of old and new  $N_{\text{design}}$  mixtures designed for traffic volumes of low, medium, and high were evaluated.

This research primarily focused on the differences between the two specifications and compared the performance gained in the laboratory to in-field performance. The evaluation of existing pavement conditions was accomplished by using data from the Iowa DOT Pavement Management Information System (PMIS). ME Design was used to help predict field conditions by using mix and binder information as level 1 input, including aggregate gradation, dynamic modulus results, and binder dynamic shear rheometer (DSR) results. Level 1 input means the results are directly measured from testing. Level 2 input is empirically derived results from mix tests. Level 3 input refers to results that are entirely empirically derived. Thus, the AASHTOWare Pavement ME Design system provides a framework in which the engineer determines design inputs for traffic, pavement materials, climate, pavement structure, and reliability.

Several mixtures from pavement projects designed under the old Iowa DOT specification were chosen for this study. IA 4, IA 330, and I-235 were selected to represent low, medium, and high traffic levels. The mixtures were recompacted in the laboratory according to old and new  $N_{\text{design}}$  gradation levels. Performance testing was performed on the mixtures for each traffic level to evaluate performance differences between the two specifications. Dynamic modulus test results, binder values, and pavement section information from the PMIS were used as input for ME Design to predict roadway conditions. Besides evaluation of the ME Design predicted data, measured field data from the PMIS were also evaluated in this study. Figure 2 summarizes the experimental plan for this Phase II study.

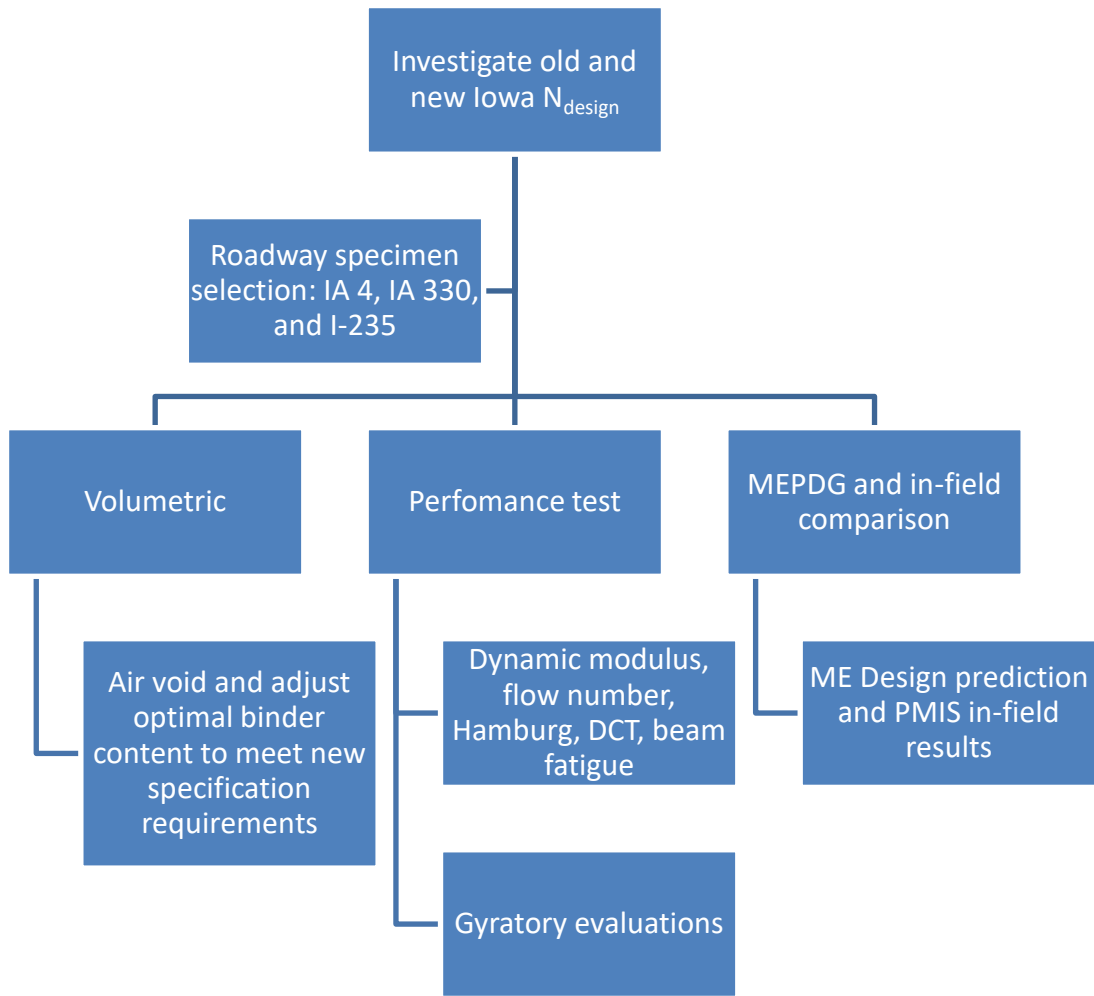


**Figure 2. Flowchart of experimental plan for the study**

## Volumetrics and Compaction Curves

### *Volumetrics*

Table 3 shows the volumetric details of the three traffic roadway mixtures at optimal binder content.

**Table 3. Volumetric details for three Iowa roadways**

	P <sub>b</sub>	P <sub>s</sub>	G <sub>b</sub>	G <sub>se</sub>	G <sub>sb</sub>	G <sub>mm</sub>	Measure G <sub>mb</sub>	% Air voids	VMA	VFA
hwy 4 old Ndesign	5.73	94.27	1.030	2.670	2.558	2.449	2.348	4.12	13.47	69.38
hwy 4 new Ndesign	5.73	94.27	1.030	2.670	2.558	2.447	2.351	3.92	13.36	70.63
hwy 330 old Ndesign	6.33	93.67	1.033	2.789	2.708	2.518	2.412	4.21	16.57	74.58
hwy 330 new Ndesign	6.33	93.67	1.033	2.789	2.708	2.518	2.419	3.93	16.33	75.91
I-235 old Ndesign	5.68	94.32	1.022	2.710	2.612	2.478	2.377	4.06	14.17	71.35
I-235 new Ndesign	5.68	94.32	1.022	2.710	2.612	2.478	2.381	3.90	14.02	72.20

P<sub>b</sub> is the asphalt binder content in percent, P<sub>s</sub> is aggregate content in percent, G<sub>b</sub> is asphalt binder specific gravity, G<sub>se</sub> is effective specific gravity of aggregate coated with asphalt, G<sub>sb</sub> is bulk density of aggregate, G<sub>mm</sub> is maximum theoretical specific gravity, VMA is voids in mineral aggregate, and VFA is percent voids filled with asphalt binder

According to Table 3, the new  $N_{design}$  mixtures for all three roadways had lower VMA values than the old  $N_{design}$  VMA values. As air voids decrease, the VFA increases. The new  $N_{design}$  mixtures had lower air void values but they ha higher VFA values than mixtures made using the old  $N_{design}$  levels. Figure 3 presents the average VMA and VFA for each roadway and new vs. old  $N_{design}$  levels, where the error bars in each direction signify one standard deviation.

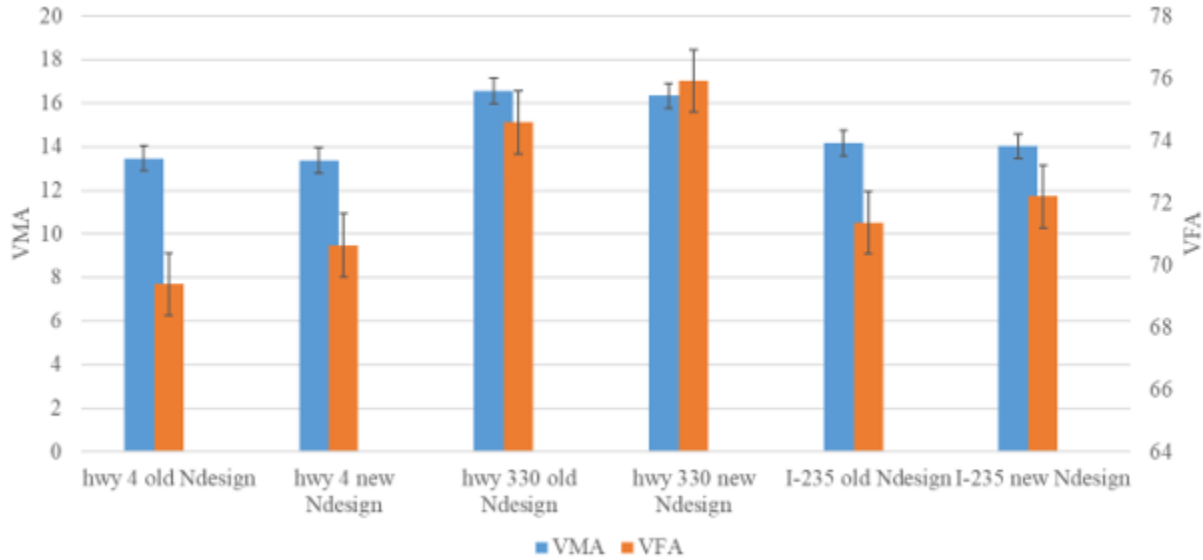


**Figure 3. VMA and VFA for three roadways**

According to Table 3 values, new  $N_{design}$  mixes had lower VMA and higher VFA; however, all the error bars overlap for the VMA and VFA in Figure 3. In this case, the new and old  $N_{design}$  mixes appear to have no significant differences.

*Compaction Curves*

Figures 4 through 6 show the compaction curves for IA 4, IA 330, and I-235, respectively.

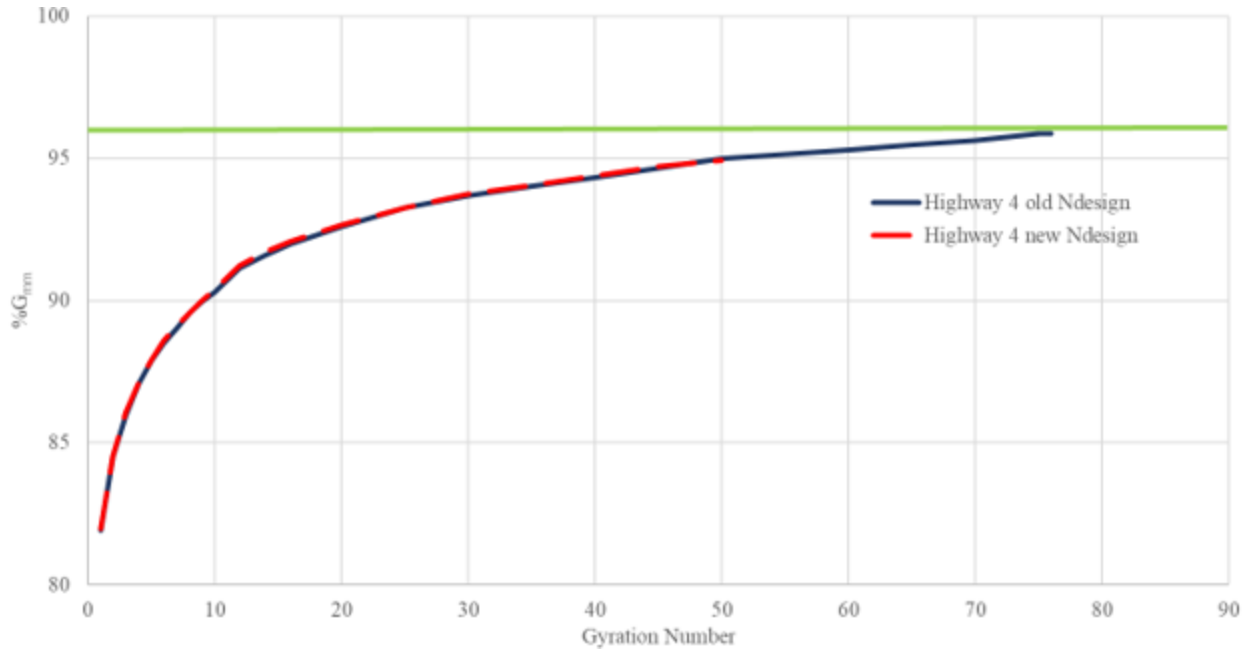


**Figure 4. IA 4 compaction curves**

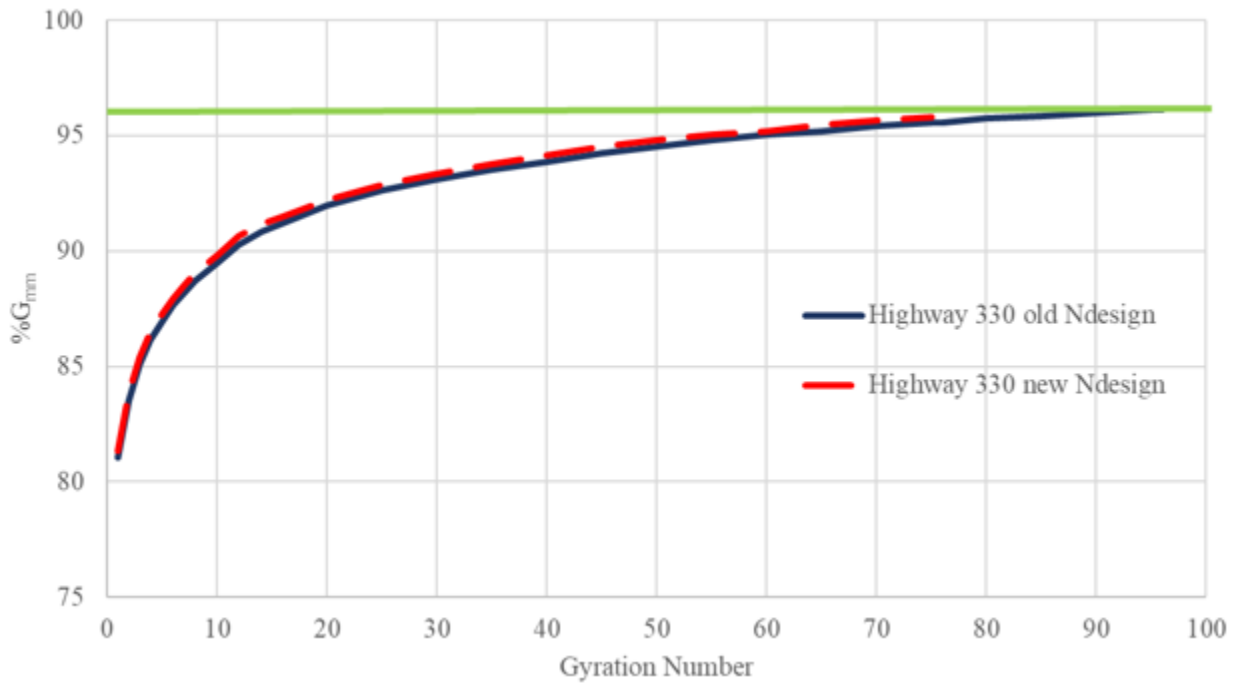


**Figure 5. IA 330 compaction curves**

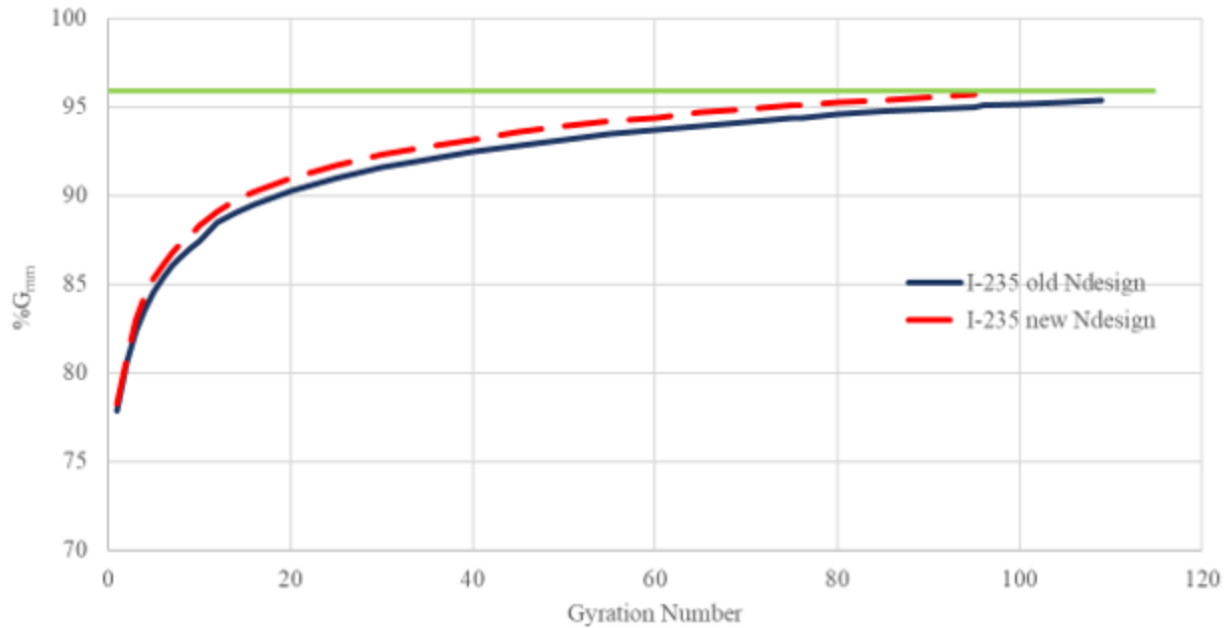


**Figure 6. I-235 compaction curves**

The gyratory compaction curves show that both IA 330 and I-235 old and new  $N_{\text{design}}$  mixtures meet 4% air voids at  $N_{\text{design}}$  gyrations. According to the figures, new  $N_{\text{design}}$  mixes have higher % $G_{\text{mm}}$ , which means lower air void values than the old  $N_{\text{design}}$  mixes. This proves that when more binder is used, the air voids in the asphalt mix are reduced. It also shows new  $N_{\text{design}}$  mixtures are less sensitive to the gyration level compared to the old  $N_{\text{design}}$  mixes. However, for IA 4, there appeared to be no visual differences between the old and new  $N_{\text{design}}$  mixes.

### Dynamic Modulus Tests

Six dynamic modulus specimens were produced and tested in the laboratory for each mix representing each  $N_{\text{design}}$  level. The six experimental groups were IA 4 old and new  $N_{\text{design}}$ , IA 330 old and new  $N_{\text{design}}$ , and I-235 old and new  $N_{\text{design}}$ . The binders used to adjust optimal asphalt content in the laboratory were the original binders used during field production of each highway pavement. The dynamic modulus specimens were mixed with additional binder to reach optimal binder content and then compacted to  $7\% \pm 1\%$  air voids. The compaction procedures followed the AASHTO T 312 standard. The loose mixes were heated for two hours conditioning at  $140 \pm 5^\circ\text{C}$ , and a Superpave gyratory compactor was used to compact the specimens to 4 in. (100 mm) diameter and 6 in. (150 mm) height.

Six replicate specimens were also produced and tested for each group. For these, dynamic modulus specimen preparation was done according to the AASHTO T 342 standard. The asphalt mix specimens were conditioned for two hours before testing at three temperatures,  $4^\circ\text{C}$ ,  $21^\circ\text{C}$ , and  $37^\circ\text{C}$ , and frequencies of 25, 20, 10, 5, 2, 1, 0.5, 0.2, and 0.1 Hz. Dynamic modulus values were recorded at each given temperature and frequency.

## E\* Shifted Results Using Sigmoidal Model

The measured E\* values that were obtained from the dynamic modulus tests at temperatures of 4°C, 21°C, and 37°C were subsequently used to create E\* master curves using the sigmoidal model, as shown in Equations 1 and 2. From this model and using back calculation with Excel Solver, the E\* values for temperatures of -10°C and 54°C were obtained. The sigmoidal function is described as follows:

$$\log|E^*| = \delta + \frac{(\alpha)}{1+e^{\beta+\gamma\log f_r}} \quad (1)$$

$$\text{Error}^2 = \sum_{i=1}^n [\log(\text{Predicted}E_i^*) - \log(\text{Measured}E_i^*)]^2 \quad (2)$$

where E\* = dynamic modulus,  $\delta$  = minimum modulus value,  $\alpha$ ,  $\beta$ ,  $\delta$ , and  $\gamma$  = fitting parameter using sigmoid function, and  $f_r$  = reduced frequency. A new master curve can be created using E\* values from sigmoid function to match laboratory-tested E\* values. The reference temperature was set at 21°C.

The dynamic modulus input used sigmoid function-shifted values. E\* values at -10°C, 4°C, 21°C, 37°C, and 54°C and six frequencies were used to represent the master curves. From laboratory work, the E\* values at 4°C, 21°C, and 37°C and at nine frequencies were measured during testing. The existing E\* values can help establish the master curve to estimate values for temperature -10°C and 54°C at six frequencies. Figure 7 shows the predicted E\* master curve according to the laboratory test results.

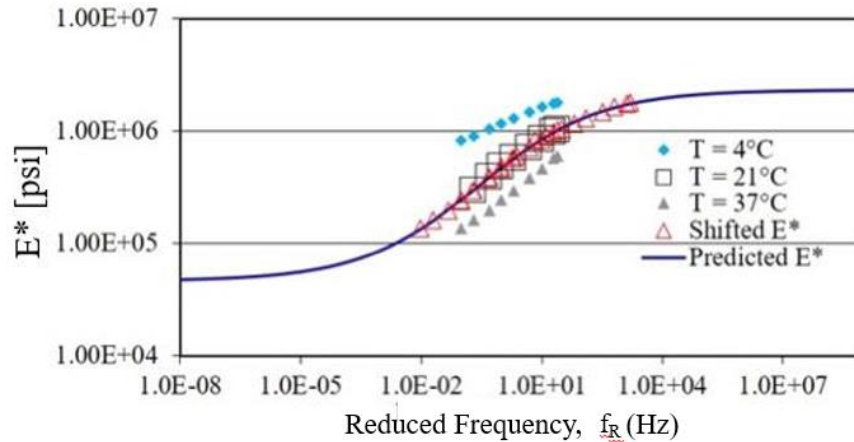


**Figure 7. Predicted E\* master curve from existing data**

Once the master curve was established, the values for temperature -10°C and 54°C could be estimated by using the shift factor  $a(T)$ . Equations 3 and 4 were used to determine the shift factor (Newcomb et al. 2001).



$$f_r = \frac{f}{a(T)} \rightarrow \log(f_r) = \log(f) - \log(a(T)) \quad (3)$$

$$\log(a(T)) = aT^2 + bT + c \quad (4)$$

where  $f_r$  = reduced frequency,  $f$  = loading frequency,  $a(T)$  = shift factor, and  $a$ ,  $b$ , and  $c$  are coefficients to obtain the shift factor. Figure 8 shows the estimated values for  $-10^\circ\text{C}$  and  $54^\circ\text{C}$  from the existing predicted master curve.

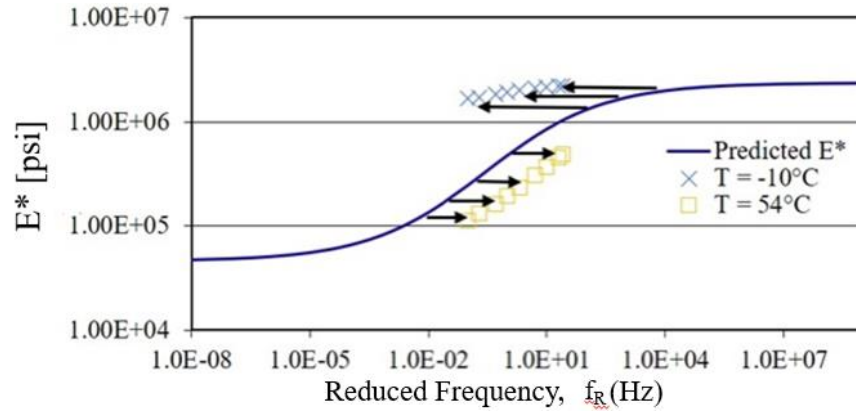


**Figure 8. Estimated  $E^*$  values of  $-10^\circ\text{C}$  and  $54^\circ\text{C}$  from predicted  $E^*$  master curve**

Once  $E^*$  values at five temperatures were obtained, the data was used in ME Design. Figure 9 shows the unshifted  $E^*$  values at  $-10^\circ\text{C}$ ,  $4^\circ\text{C}$ ,  $21^\circ\text{C}$ ,  $37^\circ\text{C}$ , and  $54^\circ\text{C}$ .

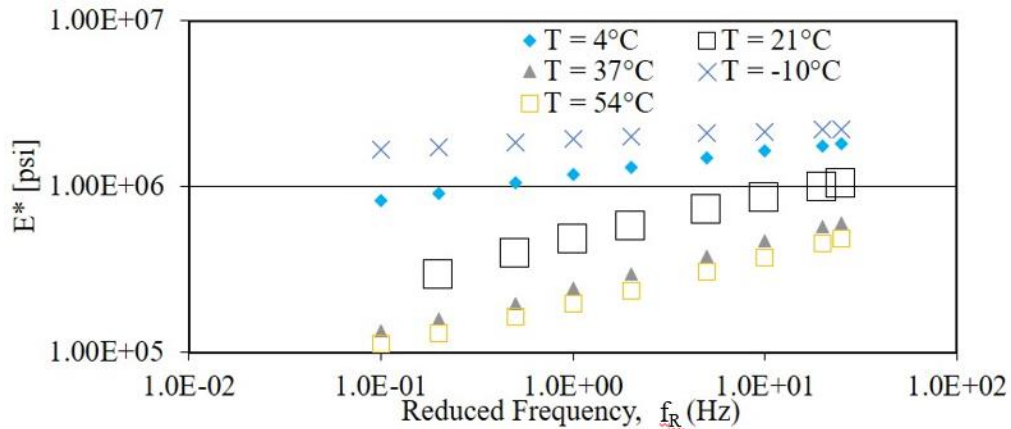


**Figure 9. Estimate and existing  $E^*$  values**

### Flow Number Tests

Non-destructive dynamic modulus testing allows researchers to perform other tests on the same specimen. The dynamic modulus specimens were also used for the flow tests. The flow test is a destructive test that can measure the rutting potential of an asphalt mix.

The test procedure for the flow number test is based on the repeated load permanent deformation test described in NCHRP reports 465 and 513 (Witczak et al. 2002, Bonaquist et al. 2003). A typical graph is shown in Figure 10, which illustrates how the accumulated permanent deformation increases with the number of applied load cycles.

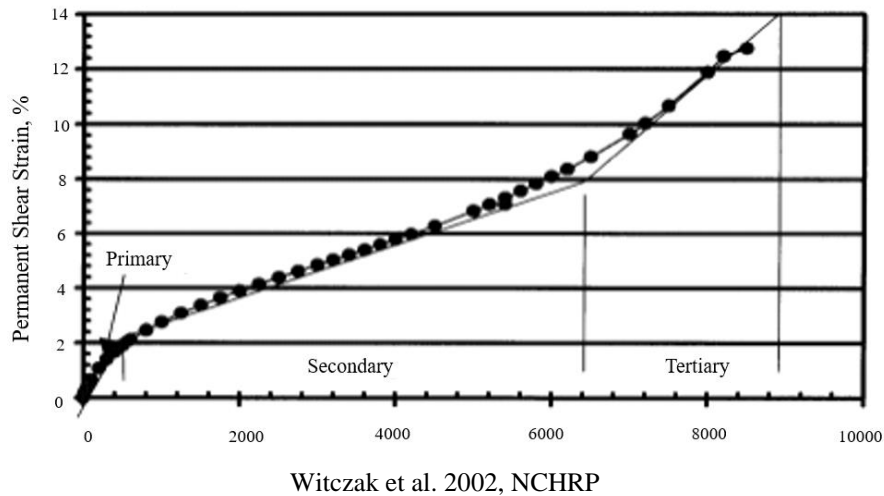


**Figure 10. Permanent shear strain versus number of loading cycles**

The three types of deformation that occur during the test are primary, secondary, and tertiary flows. The number of flows is defined as the number of loads.

The flow test was performed under the conditions of 37°C, frequency of 1 Hz, loading time of 0.1 second, and rest time of 0.9 second. The load level was 600 kPa. Once 10,000 pulses had been reached, or a 5.5% strain had occurred, the test was complete. The relationship curve between deformation and pulse number was drawn, and the relationship curve between strain rate and pulse number was also drawn. The flow rate was determined by the minimum strain rate and the corresponding number of pulses.

### Hamburg Wheel Tracking Tests

The Hamburg wheel tracking test (HWTT) was originally developed in Hamburg, Germany, in the mid-1970s to prevent pavement distresses caused by heavy trucks. During the 1990s, the HWTT gained popularity as a mixture evaluation tool in the US. Over the years, the HWTT has proved to be an effective method to measure pavement rutting and moisture susceptibility in asphalt mixtures in various regions and for many types of mixtures.

The HWTT procedure followed AASHTO T 324, where a rolling steel wheel loads a submerged asphalt mixture specimen at a specified temperature. The HWTT specimens have an air void content of  $7\pm 1\%$ , and the testing temperature typically ranges between 40°C and 60°C, depending on the climate. In this study, all mixtures followed AASHTO T 324 and the Iowa DOT's Instructional Memorandum. During the test, the wheel loading is applied, and

deformation of the HWTT specimen is collected by linear variable differential transformers measuring 11 locations along the specimen (Bahia et al. 2016). The test results provide performance-related information for rutting potential and moisture damage. Results were analyzed according to recommendations by Schram et al. (2014) and considering Gibson et al.’s (2012) approach as well. This study also introduced the capability of HWTT to characterize laboratory results and compare new and old  $N_{design}$  results.

The Iowa DOT specifications require a minimum stripping inflection point of 10,000 for standard traffic and 14,000 for both high traffic and very high traffic (Schram et al. 2014). Other significant HWTT results include rutting depth, stripping inflection point (SIP), stripping slope, creep slope, and ratio between strip slope and creep slope. The SIP is found at the intersection of the creep slope and the stripping slope with the value being the number of passes/cycles (Aschenbrener 1995). While this report presents comparisons between old and new  $N_{design}$  specimens, a study in Wisconsin investigated use of a reduced test temperature for Hamburg testing of mixtures (Buss et al. 2014).

Many factors influence asphalt mixture design. Still, some of the most important include aggregate angularity, aggregate gradation, traffic loading (number of ESALS), design gyrations, binder grade, recycled binder content, and film thickness, as all of these can influence mixture properties. Table 4 lists the essential properties for the mixtures included in this study.

**Table 4. Mixtures and mixture properties included in this study**

Iowa DOT Designation	Mixture Designation	Pavement Lift	NMAS	ESALS	Binder Performance Grade	Effective Binder Content Old $N_{design}$	Effective Binder Content New $N_{design}$
IA 4	1/2 in. Int-1M HMA	Inter-mediate	1/2 in.	1M	58-28	4.66	5.73
IA 330	1/2 in. Surf-10M HMA	Surface	1/2 in.	10M	64-22	5.05	6.33
I-235	1/2 in. Surf-30M HMA	Surface	1/2 in.	30M	64-22	4.27	5.68

Each mixture tested had five HWTT observations. Additional mixture formula information is included in Appendix A.

### Beam Fatigue Tests

Fatigue cracking is a load/structural-related distress and is measured in the laboratory using a four-point beam loading machine that produces a constant bending moment over the center one-third of a beam to evaluate the fatigue resistance parameter. The prediction of fatigue cracking uses high microstrain levels to simulate accelerated traffic (traffic would be closer to 35–50 microstrain).

The strain levels used in this study were 500, 700, and 900 microstrain. The test temperature was 68°F (20°C). The temperature is considered as an intermediate temperature at which fatigue cracking is more likely to occur. The loading frequency was 10 Hz, and it did not change as a level 1 input factor.

The beam fatigue test was to evaluate the stress and strain relationship under continuous sinusoidal loading. The maximum tensile stress,  $\sigma_t$ , at each load cycle interval can be computed using Equation 5.

$$\sigma_t = \frac{0.357P}{bh^2} \quad (5)$$

where  $\sigma_t$  = tensile stress (psi),  $P$  = load applied by actuator (N),  $b$  = average specimen width (m), and  $h$  = average specimen height (m).

The maximum tensile strain,  $\varepsilon_t$ , can be computed using Equation 6.

$$\varepsilon_t = \frac{12\delta h}{3L^2 - 4a^2} = \frac{12\delta h}{0.325703} \quad (6)$$

where  $\varepsilon_t$  = maximum tensile strain (m/m),  $\delta$  = maximum deflection at center of beam (m),  $a$  = space between inside clamps (0.119 m), and  $L$  = length of beam between outside clamps (0.357 m).

The flexural stiffness,  $S$ , is then computed by the ratio of the maximum tensile stress and the maximum tensile strain, as shown in Equation 7.

$$S = \frac{\sigma_t}{\varepsilon_t} \quad (7)$$

In addition, the number of cycles to failure,  $N_f$ , is represented in Equation 8.

$$N_f = K_1 \left( \frac{1}{\varepsilon_t} \right)^{K_2} \quad (8)$$

where  $N_f$  = number of cycles to failure,  $\varepsilon_t$  = flexural strain, and  $K_1$ ,  $K_2$  = regression constants.

## Project Selection

Three traffic levels were used in this research. IA 4 represented low traffic volume roadways, IA 330 represented medium traffic volume roadways, and I-235 represented high traffic volume roadways. The PMIS and project plan provided the project details, including AADT, ESALs, and  $N_{\text{design}}$  value, as shown in Table 5.

**Table 5. Project details**

<b>Project Location (County and Highway)</b>	<b>Year</b>	<b>Location</b>	<b>Milepost</b>	<b>AADT</b>	<b>ESALs</b>	<b>N<sub>design</sub></b>
Calhoun IA 4	2005	0.16 miles north of US 30 North to IA 175	20.95	1,200	1M	76
Jasper IA 330	2006	0.5 miles south of F-17 to 1,000 ft S. of 285th St. and SB from Glick Ave. to US 30	19.4	7,400	10M	96
Polk* I-235	2015	73rd/8th St. E. to 63rd St.	0.84	108,600	30M	109

\*More specifically, West Des Moines

Figure 11 shows the general locations of the three traffic levels.

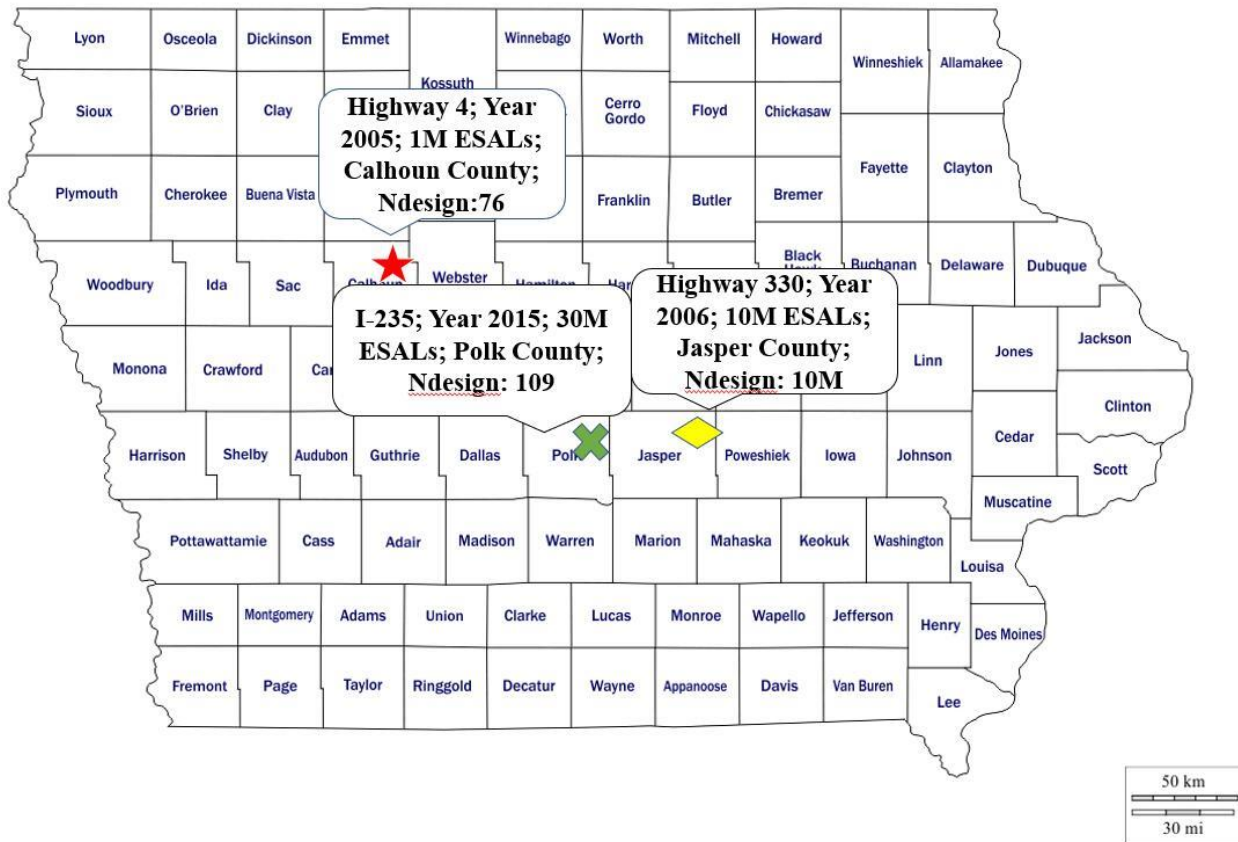


**Figure 11. Project locations in Iowa**

Additional project information is shown in Appendix B.

## Evaluation of Existing Pavement Conditions

Distresses are critically important considerations in asphalt design; they are the initial indication of pavement surface failure. The *Distress Identification Manual for the Long-Term Pavement Performance Program* (Miller and Bellinger 2003) shows pavement distresses for flexible pavement. Table 6 includes information for the severity levels of these distress types: fatigue cracking, transverse cracking, longitudinal cracking, and patch/patch deterioration.

**Table 6. Level of severity corresponding to type of distress**

Type	Severity Levels
<b>Fatigue</b>	Low: A small percentage of cracks present; not spalled or sealed.
	Moderate: An initial formation of interconnecting cracks developing into a pattern; somewhat spalled; possible cracks sealed
	High: Moderate to high interconnected cracks form complete pattern; severely spalled; possible cracks sealed; possible pumping present.
<b>Transverse</b>	Low: Unsealed crack with a mean width of 1/4 in. (6 mm) or less; a decent condition sealed crack with sealant material, mean width unable to determine.
	Moderate: Any cracks with a mean width greater than 1/4 in. (6 mm) but less than or equal to 3/4 in. (19 mm); or any cracks adjacent to low severity with a mean width of 3/4 in. (19 mm) or less.
	High: Any cracks with a mean width greater than 3/4 in. (19 mm); or any cracks adjacent to moderate to high severity with a mean width of 3/4 in. (19 mm) or less.
<b>Longitudinal</b>	Low: Unsealed crack with a mean width of .25 in. (6 mm) or less; a decent condition sealed crack with sealant material, mean width unable to determine.
	Moderate: Any cracks with a mean width greater than 1/4 in. (6 mm) but less than or equal to 3/4 in. (19 mm); or any cracks adjacent to low severity with a mean width of 3/4 in. (19 mm) or less.
	High: Any cracks with a mean width greater than 3/4 in. (19 mm); or any cracks adjacent to moderate to high severity with a mean width of 3/4 in. (19 mm) or less.
<b>Patch/Patch deterioration</b>	Low: Patch has low severity distress (rutting less than 1/4 in. [6 mm]); pumping is not present.
	Moderate: Patch has moderate severity distress (rutting less than 1/4 in. [6 mm] to 1/2 in. [12 mm]); pumping not present.
	High: Patch has high severity distress (rutting greater than 1/2 in. [12 mm]); or additional patch material within original patch; pumping present.

Source: Miller and Bellinger 2003

Note that ME Design will estimate different types of distresses according to pavement information.

## Determination of Mixture Volumetrics

Field-produced mixes for the three traffic levels were collected from storage units. All of the test specimens were then made in the laboratory based on the old and new  $N_{\text{design}}$  specifications. The volumetrics were determined and calculated in the laboratory, and then compared with the given mix design information. If the difference between laboratory measured volumetric and given field volumetric was significant, a correction factor was used to adjust the laboratory volumetrics. The detailed QC/QA data is shown in Appendix B.

The  $G_{\text{mb}}$  of specimens was determined in accordance with ASTM D6752/D6752M (2011) and AASHTO T 166-13 (2013). For this study, the conventional method (Figure 12) was used to determine the bulk specific gravity of each mixture.



**Figure 12. Water bath used in conventional method**

AASHTO T 09 was used to determine the  $G_{\text{mm}}$  in the laboratory using the apparatus shown in Figure 13.



**Figure 13. Metal bucket method**

For this study, the metal bucket method was used to measure  $G_{mm}$ . Each loose field-produced mix was heated in the oven at  $135 \pm 5^\circ\text{C}$  for one hour or until the mix was tender enough to break apart. A total 2,000 grams of mix were tested for each experimental group and for changes occurring from additional binder content.

### **Determination of Optimal Asphalt Content using Laboratory-Compacted Mixes**

#### **Mix Design**

The Superpave mix design consists of four steps: material selection, aggregate structure design, optimal binder content, and moisture susceptibility testing. To identify the influence of the gyration level on the mix design, this study's efforts were focused on performing mix design evaluations for the three traffic levels (IA 4, IA 330, and I-235). The aggregate gradations for the three traffic levels are summarized in Tables 7 through 9, respectively, and are plotted in Figures 14 through 16, respectively.



**Table 7. IA 4 aggregate gradation**

Aggregate			Martin Marietta (Ames)	Martin Marietta (Ames)	Vecker Gravel (Ames)	Hallet (Ames)	Trial Blend
			3/4 stone	3/8 stone chips	3/4 screen gravel	1/4 core sand	
U.S. Sieve	Sieve, mm	% Used	25%	20%	37%	18%	100%
		Sieve <sup>.45</sup>	% Passing	% Passing	% Passing	% Passing	% Passing
1"	25	4.257	100.0	100.0	100.0	100.0	100.0
3/4"	19	3.762	100.0	100.0	100.0	100.0	100.0
1/2"	12.5	3.116	77.0	100.0	91.0	100.0	90.9
3/8"	9.5	2.754	63.0	100.0	88.0	100.0	86.3
#4	4.75	2.016	36.0	24.0	73.0	100.0	58.8
#8	2.36	1.472	25.0	8.0	59.0	92.0	46.2
#16	1.18	1.077	20.0	5.0	45.0	69.0	35.1
#30	0.60	0.795	17.0	3.5	29.0	32.0	21.4
#50	0.30	0.582	14.0	2.5	14.0	5.8	10.2
#100	0.15	0.426	10.0	2.2	6.9	1.1	5.7
#200	0.075	0.312	7.5	1.7	5.2	0.8	4.3

**Table 8. IA 330 aggregate gradation**

Aggregate			Cessford (Le Grand)	Cessford (Le Grand)	Linwood (Montpelier)	Martin Marietta (Marshall- town)	Trial Blend
			manf. sand	1/2 #220 lmst	5/8 8/8 #4 slag	3/8 cone sand	
U.S. Sieve	Sieve, mm	% Used	25%	38%	12%	25%	100%
		Sieve <sup>.45</sup>	% Passing	% Passing	% Passing	% Passing	% Passing
1"	25	4.257	100.0	100.0	100.0	100.0	100.0
3/4"	19	3.762	100.0	100.0	100.0	100.0	100.0
1/2"	12.5	3.116	100.0	99.0	96.0	100.0	99.1
3/8"	9.5	2.754	100.0	80.0	55.0	100.0	87.0
#4	4.75	2.016	100.0	41.0	3.2	98.0	65.5
#8	2.36	1.472	74.0	22.0	1.8	88.0	49.1
#16	1.18	1.077	41.0	16.0	1.6	73.0	34.8
#30	0.60	0.795	21.0	13.0	1.4	44.0	21.4
#50	0.30	0.582	11.0	11.0	1.3	9.2	9.4
#100	0.15	0.426	5.3	9.8	1.1	1.2	5.5
#200	0.075	0.312	3.5	8.8	1.0	0.8	4.5

**Table 9. I-235 aggregate gradation**

Aggregate			Everest (Dell Rapids)	Martin Marietta (Ames)	Martin Marietta (Ames)	Martin Marietta (Ames)	M.M. (John- ston)	Trial Blend
			1/2" cr. quartzite	1/2" crushed	3/8" chip	manf. sand	sand	
U.S. Sieve	Sieve, mm	% Used	15%	25%	20%	30%	10%	100%
		Sieve <sup>.45</sup>	% Passing	% Passing	% Passing	% Passing	% Passing	% Passing
1"	25	4.257	100.0	100.0	100.0	100.0	100.0	100.0
3/4"	19	3.762	100.0	100.0	100.0	100.0	100.0	100.0
1/2"	12.5	3.116	100.0	93.0	100.0	100.0	100.0	88.3
3/8"	9.5	2.754	83.0	74.0	90.0	100.0	100.0	89.0
#4	4.75	2.016	7.0	40.0	22.0	98.0	96.0	54.5
#8	2.36	1.472	1.3	23.0	3.0	66.0	87.0	35.0
#16	1.18	1.077	0.8	17.0	2.5	39.0	70.0	23.6
#30	0.60	0.795	0.7	13.0	1.5	21.0	44.0	14.4
#50	0.30	0.582	0.6	11.0	1.2	11.0	13.0	7.7
#100	0.15	0.426	0.5	8.8	1.1	4.0	1.1	3.8
#200	0.075	0.312	0.4	7.5	1.0	2.4	0.3	2.9

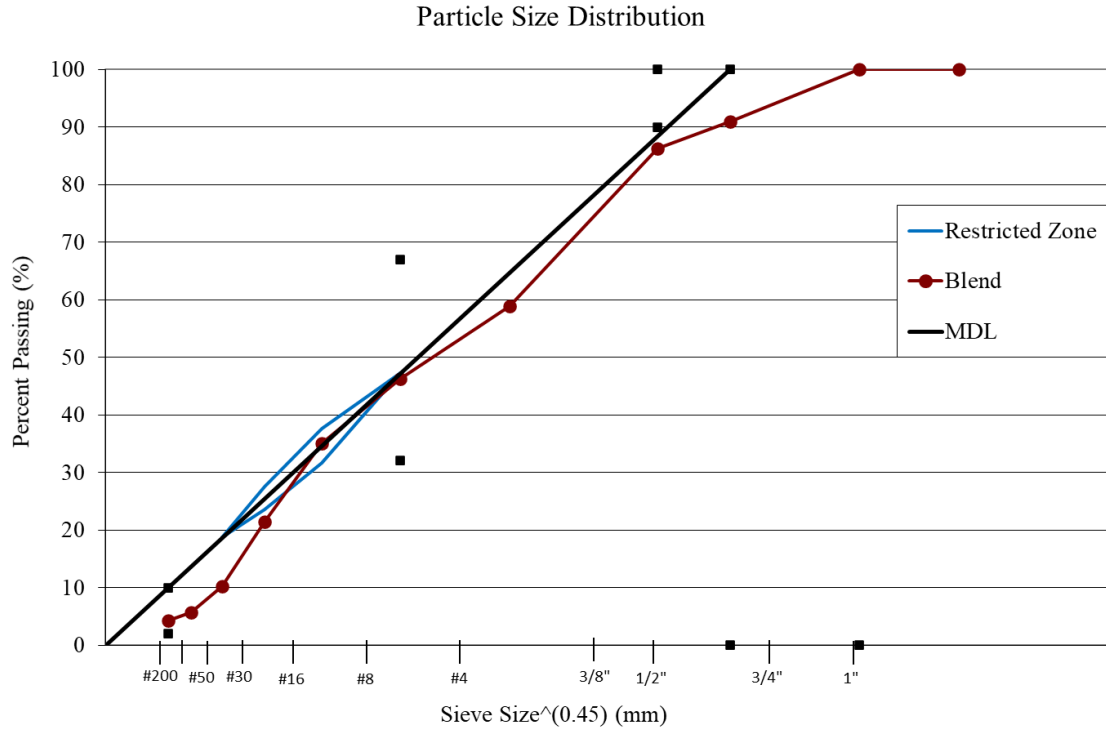


**Figure 14. IA 4 aggregate gradation**

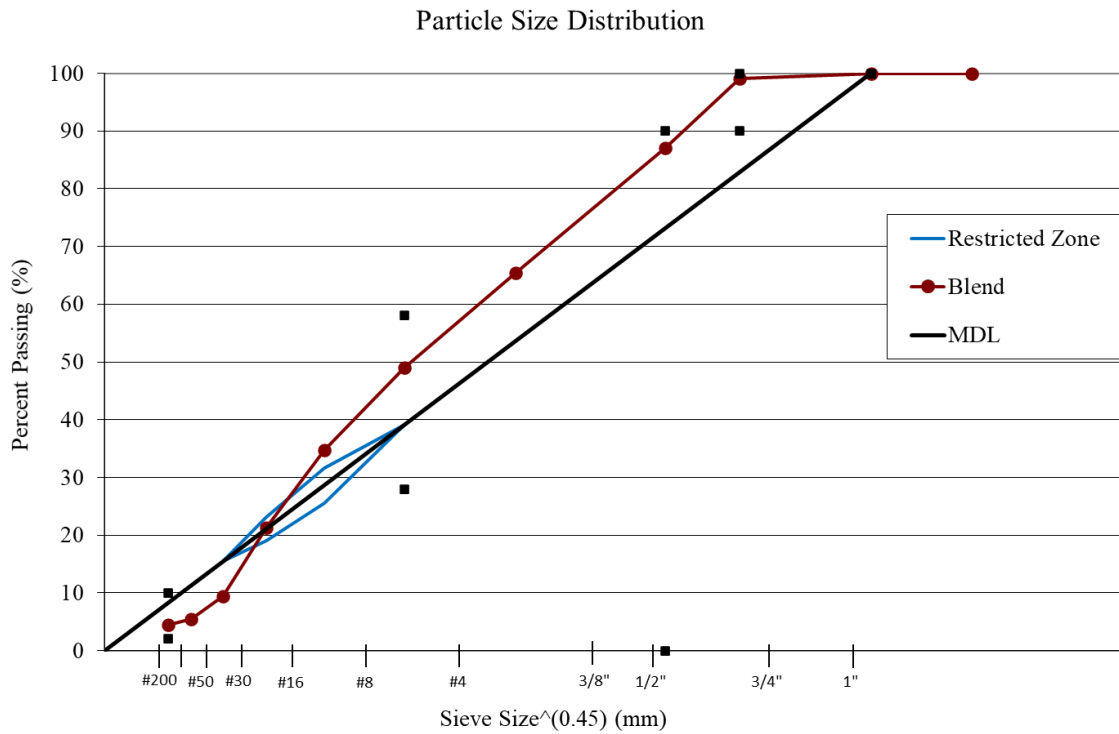


**Figure 15. IA 330 aggregate gradation**

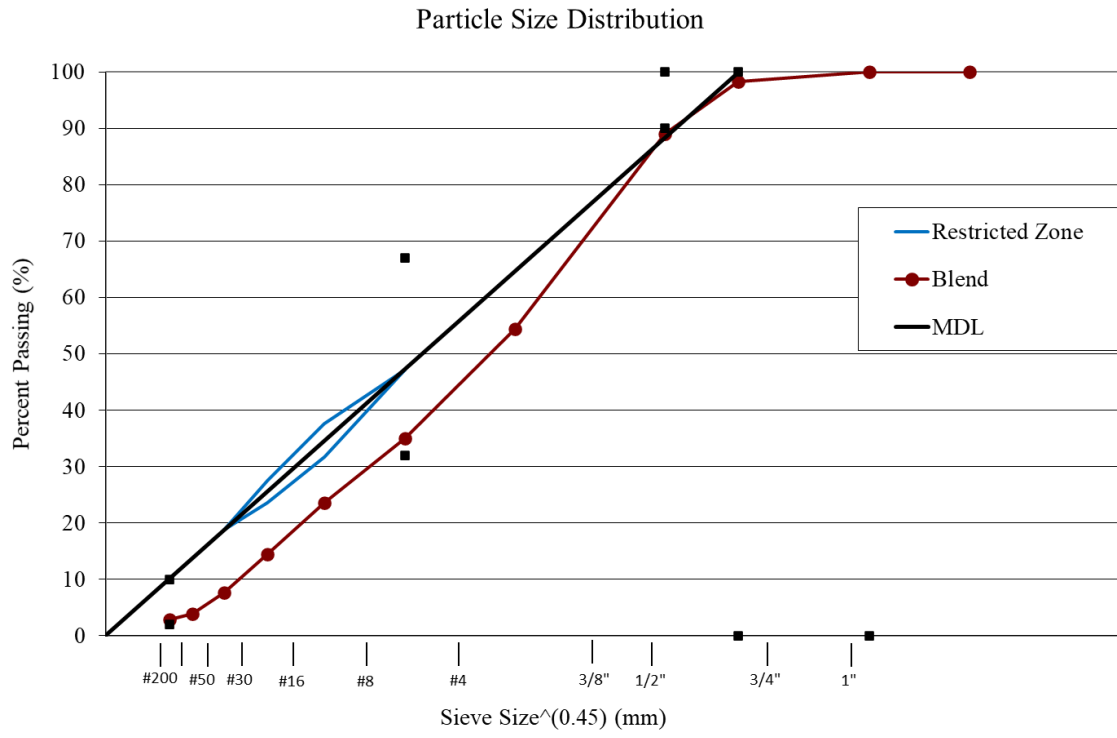


**Figure 16. I-235 aggregate gradation**

## CHAPTER 4: RESULTS AND ANALYSES

### Optimal Binder Content Selection

The optimal binder content is 4% air voids for these three traffic levels. The aggregate gradations are the same for the old and new  $N_{\text{design}}$  specimens. IA 4, IA 330, and I-235 represent the three different traffic levels with IA 4 (1M ESALs) for low traffic level, IA 330 (10M ESALs) for medium traffic level, and I-235 (30M ESALs) for high traffic level. The gyratory compaction curves can help illustrate the gyration difference between the old and new  $N_{\text{design}}$  values, and Table 10 lists the values.

**Table 10.  $N_{\text{design}}$  compaction gyrations**

Gyrations	IA 4	IA 330	I-235
old $N_{\text{design}}$	76	96	109
new $N_{\text{design}}$	50	75	95

Figures 17 through 19 show the new  $N_{\text{design}}$  percent air voids versus binder content for three traffic levels, respectively.

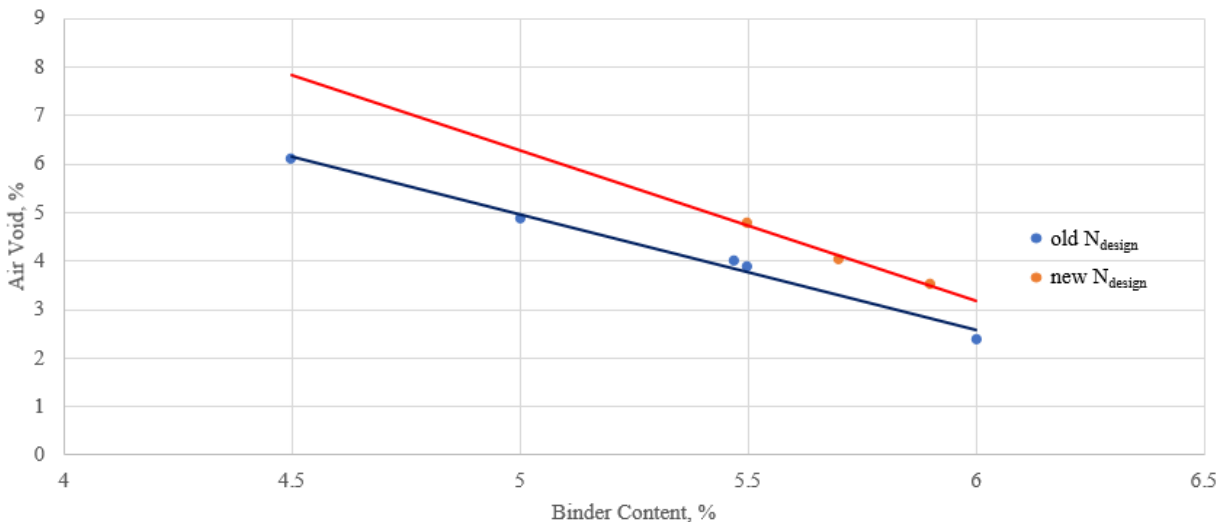


**Figure 17. IA 4 percent air void versus percent binder content**

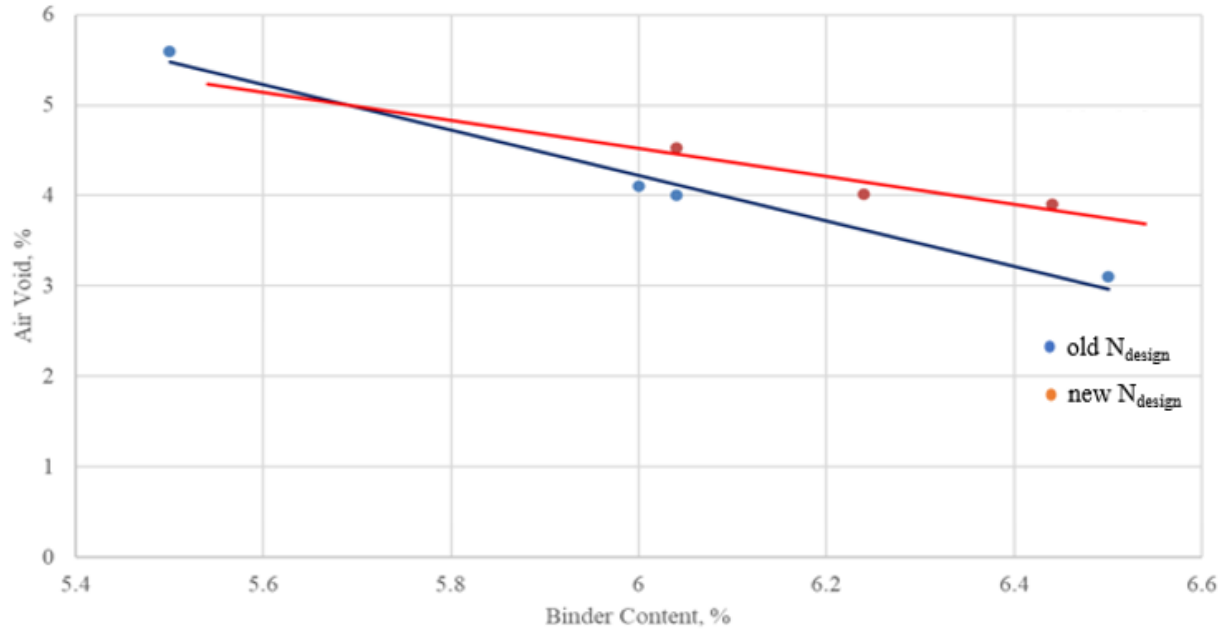


**Figure 18. IA 330 percent air void versus percent binder content**

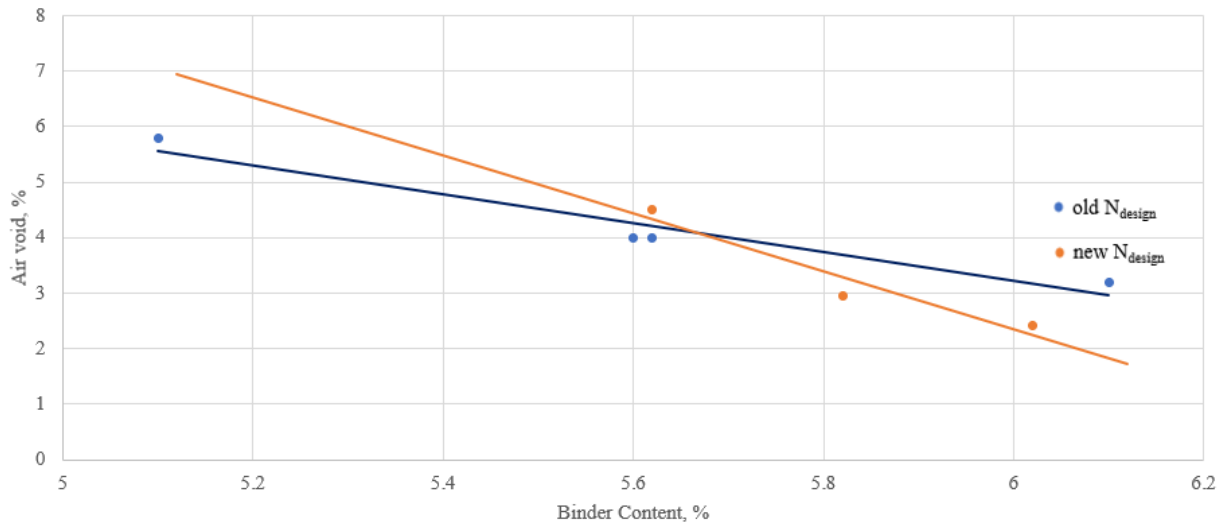


**Figure 19. I-235 percent air void versus percent binder content**

Table 11 summarizes the optimal asphalt content for IA 4, IA 330, and I-235 for the new  $N_{design}$  levels. As Figures 17 through 19 show, when the asphalt content is increased, the air voids decrease.

**Table 11. Summary of new  $N_{design}$  optimal asphalt content for all levels of traffic**

<b>Mixtures for Traffic Levels</b>	<b>Optimal Asphalt Content</b>
IA 4	5.7%
IA 330	6.3%
I-235	5.7%

### **Dynamic Modulus Results and Master Curves**

The visco-elastic test's dynamic modulus shows the difference of stiffness under sinusoidal loading for a range of frequencies and temperatures.  $E^*$  is defined as a complex number for HMA, and the absolute value of the complex modulus  $|E^*|$  is defined as the dynamic modulus.

The master curves for  $E^*$  were developed using measured data from frequency sweeps across multiple temperatures in combination with shift factors. The master curves recorded the average values of dynamic values under a wide range of frequencies for different temperatures. The left part of the master curve refers to the mixture stiffness behavior at low frequency and high temperature. The right portion of the master curve refers to the mixture stiffness behavior at high frequency and low temperature. The master curve is a log-log scale plot for the horizontal and vertical axes. The log-log scale plot is powerful in recognizing the complex number trend through the fundamental frequencies; it especially illustrates the difference between two mixtures at low and high frequencies.

Two factors of interest that need to be investigated are covered in this section. The dynamic modulus test specimens' first objective is to find the mixture stiffness difference between the old and new  $N_{design}$ . The second interest is to show the  $N_{design}$  change impact for different traffic volumes.

Five specimens were made for each group studied, for a total of 30 specimens. The dynamic modulus values for all 30 specimens are included in Appendix C. Figures 20 through 22 show the dynamic master curves for IA 4, IA 330, and I-235, respectively.



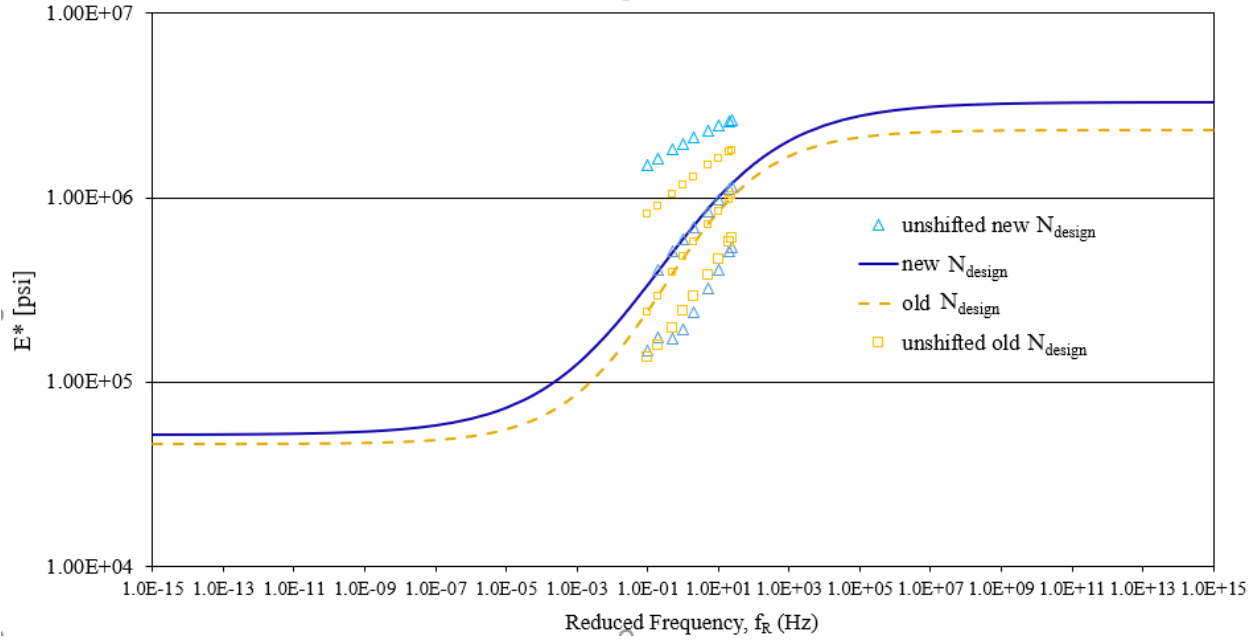


**Figure 20. IA 4 dynamic modulus data**

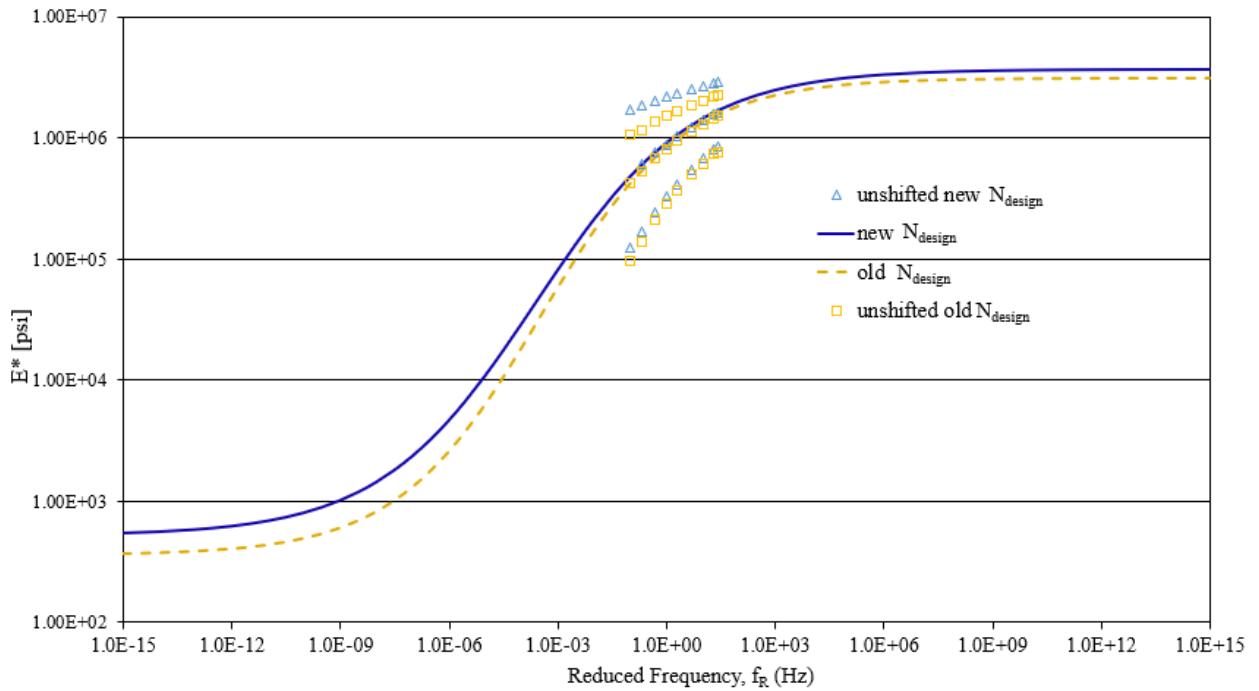


**Figure 21. IA 330 dynamic modulus data**

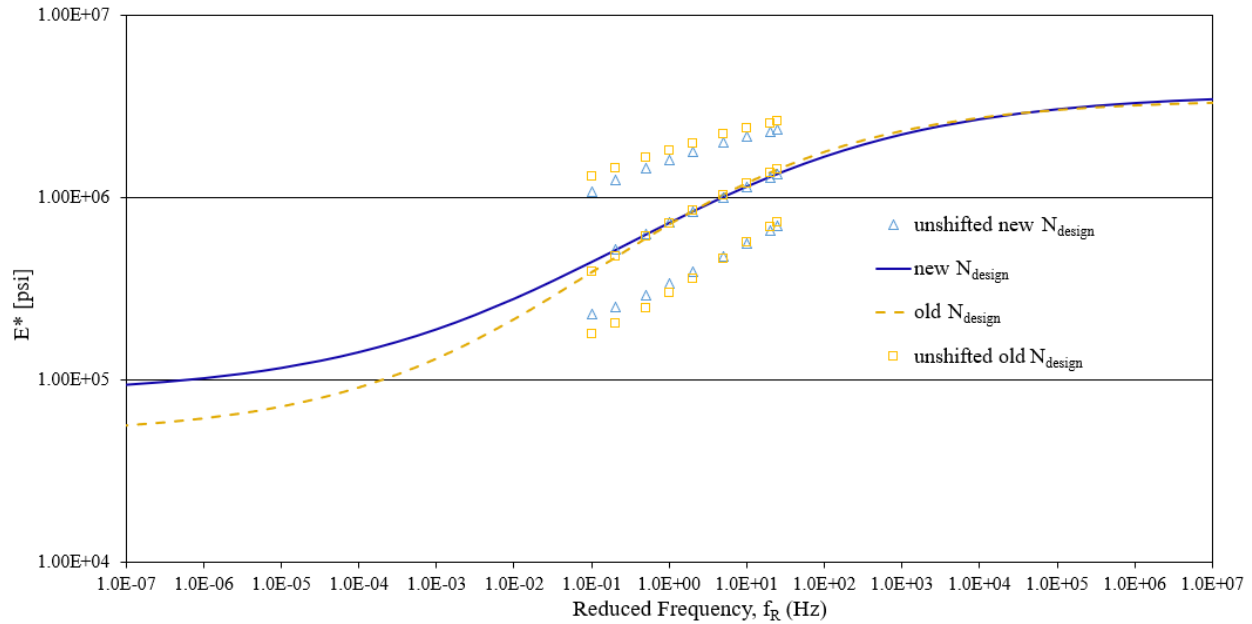


**Figure 22. I-235 dynamic modulus data**

The  $E^*$  values are the average number for the five specimens for each group. The results for the new  $N_{\text{design}}$  specimens are shown with a solid blue line, and the results for the old  $N_{\text{design}}$  specimens are shown with a dashed yellow line. The new  $N_{\text{design}}$  specimens appear to have a higher modulus for low frequency or high temperature for all three traffic levels. For high frequency or low temperature, the new  $N_{\text{design}}$  specimens for IA 4 and IA 330 appear to have higher modulus. There is little difference between the old and new  $N_{\text{design}}$  for I-235. The log-log scale plot can only show the image trend of complex values. The statistical analysis is essential to illustrate the detail and the difference between two  $N_{\text{design}}$  mixtures.

Due to three test temperatures (4°C, 21°C, and 37°C) and nine frequencies (0.1, 0.2, 0.5, 1, 2, 5, 10, and 25 Hz) being used to test the two  $N_{\text{design}}$  specifications (old and new) using the dynamic modulus test, a three-way split-plot analysis of variance (ANOVA) test was used to evaluate the statistical analysis results. Tables 12 through Table 14 show the ANOVA test results.

**Table 12. IA 4 ANOVA results**

Source	N	DF	Sum of Squares	F Ratio	Prob>F
Temperature	3	3	841548900	353.6093	<.0001
Hz	9	9	146945739	61.7449	<.0001
Temperature*Hz	27	27	12173823	5.1153	0.0285
Ndesign	2	2	53441850	22.4557	<.0001
Temperature*Ndesign	6	6	72715392	30.5542	<.0001
Hz*Ndesign	18	18	14434	0.0061	0.9383
Temperature*Hz*Ndesign	54	54	205322	0.0863	0.7703

**Table 13. IA 330 ANOVA results**

Source	N	DF	Sum of Squares	F Ratio	Prob>F
Temperature	3	3	1056654890	481.1133	<.0001
Hz	9	9	239849092	109.2074	<.0001
Temperature*Hz	27	27	6242985.49	2.8425	0.0986
Ndesign	2	2	45491124.2	20.7129	<.0001
Temperature*Ndesign	6	6	40585468.7	18.4793	<.0001
Hz*Ndesign	18	18	61954.8819	0.0282	0.8674
Temperature*Hz*Ndesign	54	54	65510.1766	0.0298	0.8636

**Table 14. I-235 ANOVA results**

Source	N	DF	Sum of Squares	F Ratio	Prob>F
Temperature	3	3	911661098	419.0308	<.0001
Hz	9	9	205594384	94.4982	<.0001
Temperature*Hz	27	27	18513996	8.5097	0.0054
Ndesign	2	2	3294980	1.5145	0.2247
Temperature*Ndesign	6	6	5936889	2.7288	0.1054
Hz*Ndesign	18	18	583784	0.2683	0.6069
Temperature*Hz*Ndesign	54	54	25658	0.0118	0.914

The default assumed value of 95% reliability was used in the ANOVA tests. The three-way ANOVA test in statistical analysis was used in this section to evaluate dynamic modulus test results and determine the differences between new and old  $N_{\text{design}}$  specifications. The null hypothesis stands for equal mean values, and significant difference refers to not equal mean values. It can be seen as an asymptotic version of the well-known ANOVA F-test (Dave et al. 2019). In the ANOVA analysis, the difference was found to be significant if the p-value was less or equal to 0.05. From Tables 12 through 14, the main factor and interaction of interest were temperature\*Hz\*  $N_{\text{design}}$ , which showed no significant difference for any of the three traffic volume levels (IA 4, IA 330, or I-235). The F ratio values for all three roadways were smaller than their Prob F values according to the ANOVA test. This indicates no significant differences were found between old and new  $N_{\text{design}}$  specifications.

### Flow Number Results

The flow number test is the performance test related to the rutting resistance of asphalt concrete mixtures. The primary factor of interest to investigate is the flow number difference between the old and new  $N_{\text{design}}$  specifications. The effect of traffic level on flow numbers for the old and new  $N_{\text{design}}$  were also investigated. The tentative flow number criteria were developed from NCHRP Project 9-33, A Mix Design Manual for Hot Mix Asphalt (HMA) (Advanced Asphalt Technologies, LLC 2011 for the final report). Table 15 shows the tentative flow number criteria.

**Table 15. Tentative flow number criteria**

M ESAL	Flow Number
3	--
3 to <10	340
10 to <30	460
≥30	590

As covered in this section, the flow number values for the old and new  $N_{design}$  mixtures were determined from the testing data. Table 16 outlines the experimental design.

**Table 16. Experimental design for flow number**

Mix	Specification	Binder Grade	Replicates
IA 4	old $N_{design}$	PG 58-28	XXXX
	new $N_{design}$		XXXX
IA 330	old $N_{design}$	PG 64-22	XXXX
	new $N_{design}$		XXXX
I-235	old $N_{design}$	PG 64-22	XXXX
	new $N_{design}$		XXXX

Four specimens were reused after dynamic modulus testing for each group for a total of 24 test specimens in the flow number test. Figure 23 shows the average measured flow number values for each mix group’s four specimens.

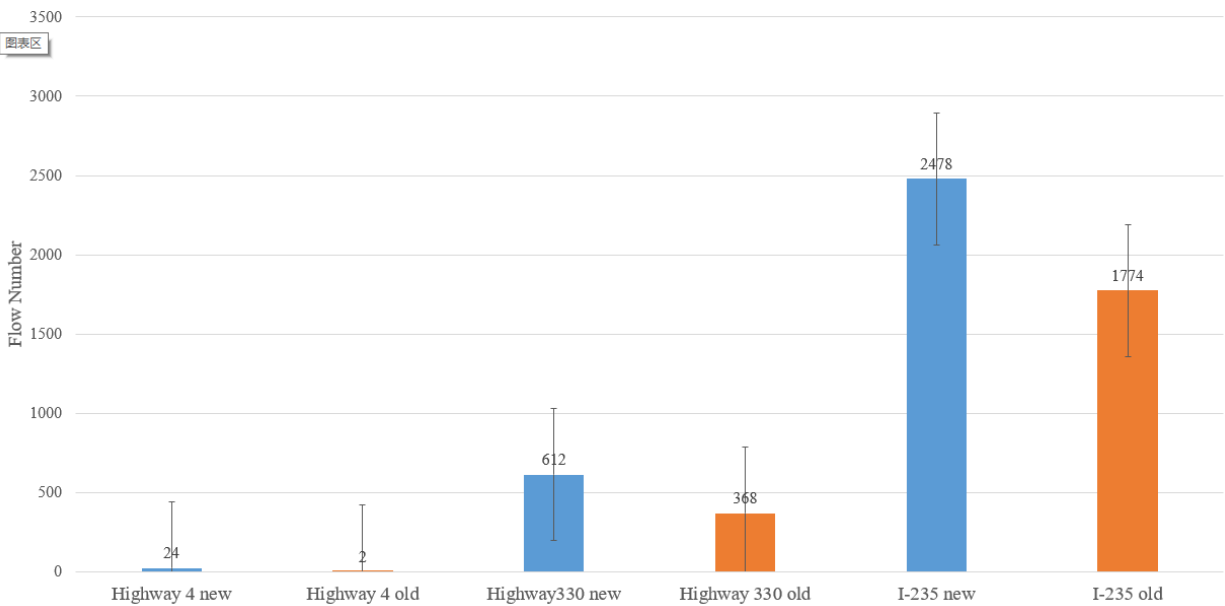


**Figure 23. Flow number results**

According to Table 15 tentative flow number criteria and Figure 23 flow number results, all test specimens met the minimum flow number requirement according to NCHRP Project 9-33. Based on the values in Figure 23, new  $N_{design}$  flow number values are greater than old  $N_{design}$  values for all traffic levels. The increased flow number indicates a significant increase in stiffness for the new  $N_{design}$  mixtures. New  $N_{design}$  had more binder used compared to old  $N_{design}$ . I-235 had the largest flow number value, followed by IA 330, with IA 4 being the smallest. This indicates that high traffic volume roadways were designed with stiffer mixtures to meet the demand of higher traffic volumes.

To better understand the flow number difference between old and new  $N_{design}$ , the F-test one-way ANOVA statistical analysis was used. The alpha values of the F-test were assumed as 0.05, which is commonly used. If the F-value is greater than F-critical, it means the two group numbers have a significant difference. The smaller P-value indicates the significant difference between the two groups. Tables 17 through 19 show the ANOVA results for the three traffic levels.

**Table 17. IA 4 flow number ANOVA results**

Highway 4 Flow Number Anova: Single Factor						
<b>SUMMARY</b>						
Groups	Count	Sum	Average	Variance		
old Ndesign	4.00	94.00	23.50	29.67		
New Ndesign	4.00	8.00	2.00	0.00		
<b>ANOVA</b>						
Source of Variation	SS	df	MS	F	P-value	F crit
Between Groups	924.50	1.00	924.50	62.33	0.00022	5.98738
Within Groups	89.00	6.00	14.83		F crit > P-value	
Total	1013.50	7.00				

**Table 18. IA 330 flow number ANOVA results**

Highway 330 Flow number Anova: Single Factor						
<b>SUMMARY</b>						
Groups	Count	Sum	Average	Variance		
Old Ndesign	4.00	2447.00	611.75	42452.92		
New Ndesign	4.00	1470.00	367.50	6228.33		
<b>ANOVA</b>						
Source of Variation	SS	df	MS	F	P-value	F crit
Between Groups	119316.1	1.0	119316.1	4.9	0.069	5.987
Within Groups	146043.8	6.0	24340.6		F crit > P-value	
Total	265359.9	7.0				

**Table 19. I-235 flow number ANOVA results**

I-235 Flow number Anova: Single Factor						
<b>SUMMARY</b>						
Groups	Count	Sum	Average	Variance		
Old N <sub>design</sub>	4	9911	2477.75	7418854.917		
New N <sub>design</sub>	4	12007	3001.75	6292297.583		
<b>ANOVA</b>						
Source of Variation	SS	df	MS	F	P-value	F crit
Between Groups	549152.00	1.00	549152.00	0.08	0.79	5.99
Within Groups	41133457.50	6.00	6855576.25		F crit > P-value	
Total	41682609.50	7.00				

The IA 4, IA 330, and I-235 F-values were 62.33, 4.9, and 0.08, respectively. The F critical values for the three traffic levels was about 6.0 and F-values lower than 6.0 cannot reject the null hypothesis. Therefore, only the IA 4 flow number showed a significant difference between the old and new N<sub>design</sub>; IA 330 and I-235 were not significantly different between old and new N<sub>design</sub> according to the ANOVA test. The possible reason is that IA 4 is a low traffic volume roadway. The P-values also indicated the impact of the traffic level on old and new N<sub>design</sub>. IA 4 had the smallest p-value of 0.0002, followed by IA 330 with a p-value of 0.069, and I-235 with the largest p-value of 0.79.

### Hamburg Wheel Tracking Results

This section presents the HWTT results. The most important comparison is between old and new N<sub>design</sub> specimens for all traffic levels. Four specimens were made for each group studied for a total of 24 specimens. Additional Hamburg test information is included in Appendix D. Table 20 and Figure 24 show the average Hamburg test result values for the six groups with their three traffic levels.

**Table 20. Hamburg wheel tracking test results**

Mix		No. of Wheel Passes	Rut Depth (mm)				Max Impression (mm)	Creep Slope (mm/1000 passes)	SIP
			8,000 passes	10,000 passes	15,000 passes	20,000 passes			
IA 4	new N <sub>design</sub>	20,000	1.96	2.12	2.43	2.73	3.285	0.0463	20,000
	old N <sub>design</sub>	20,000	1.95	2.12	2.39	2.61	3.198	0.0445	20,000
IA 330	new N <sub>design</sub>	20,000	2.44	2.66	3.08	3.57	3.910	0.0757	20,000
	old N <sub>design</sub>	19,813	1.98	2.16	2.53	3.09	4.313	0.0639	20,000
I-235	new N <sub>design</sub>	20,000	2.52	2.70	3.09	3.51	4.208	0.0687	20,000
	old N <sub>design</sub>	20,000	2.05	2.17	2.43	2.61	3.260	0.0361	20,000

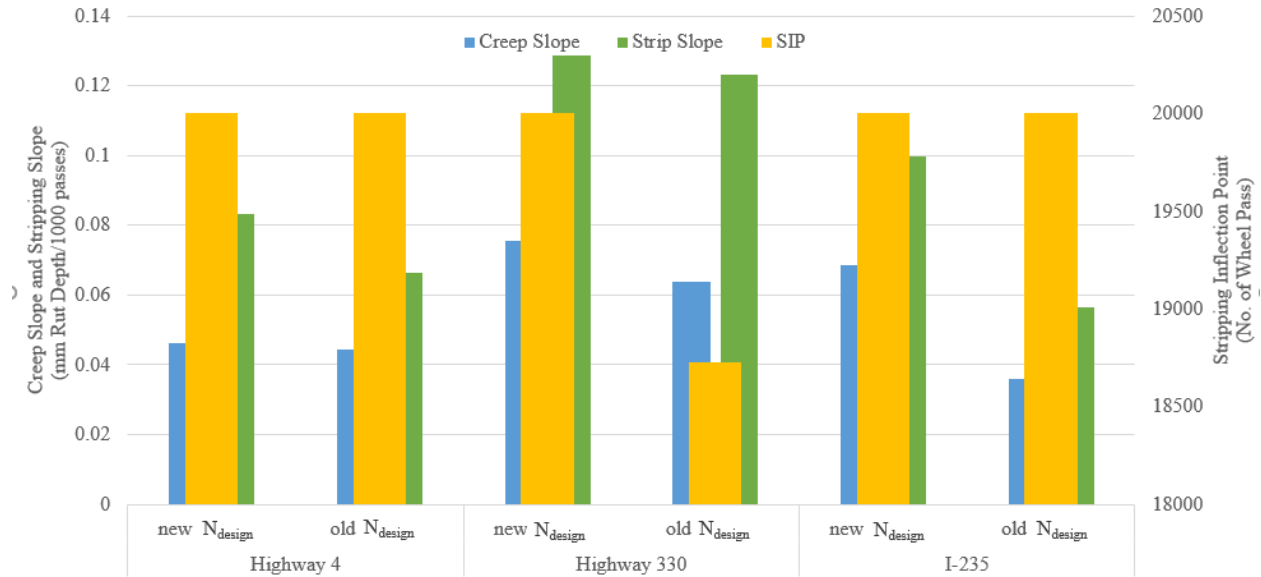


**Figure 24. Creep slope, stripping slope, and SIP**

According to Table 20 values, specimens passed the Hamburg test, which measured deformation for up to 20,000-wheel passes. The creep slope and strip slope are still suitable parameters to evaluate rutting performance. The strip slope and creep slope for the new  $N_{design}$  specimens were more significant for all traffic levels than for the old  $N_{design}$  specimens. Lower creep slope and strip slope indicate there could be more severe rutting and moisture damage experienced by these old  $N_{design}$  pavements. The rutting depths for new  $N_{design}$  mixtures were slightly lower than for old  $N_{design}$  mixtures. This also proves that new  $N_{design}$  mixes have better performance and rutting resistance. Additional evidence will be provided through ANOVA analysis.

Figures 25 through 27 indicate the rutting depth versus the number of passes for the three roadways/traffic volumes.

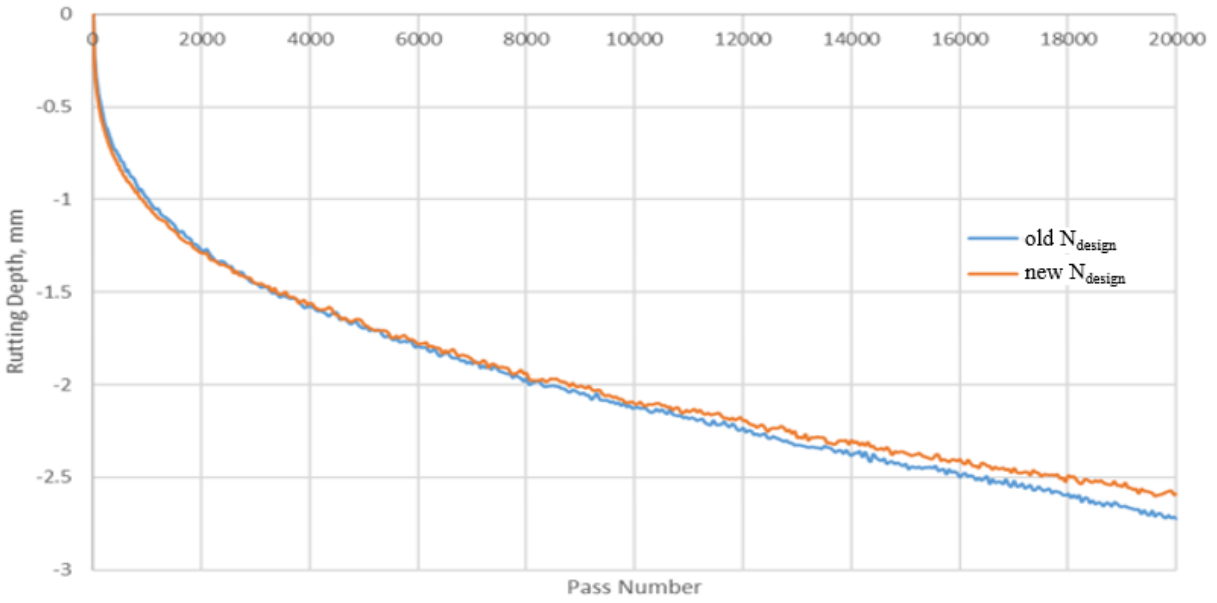


**Figure 25. IA 4 rutting depth versus passes**

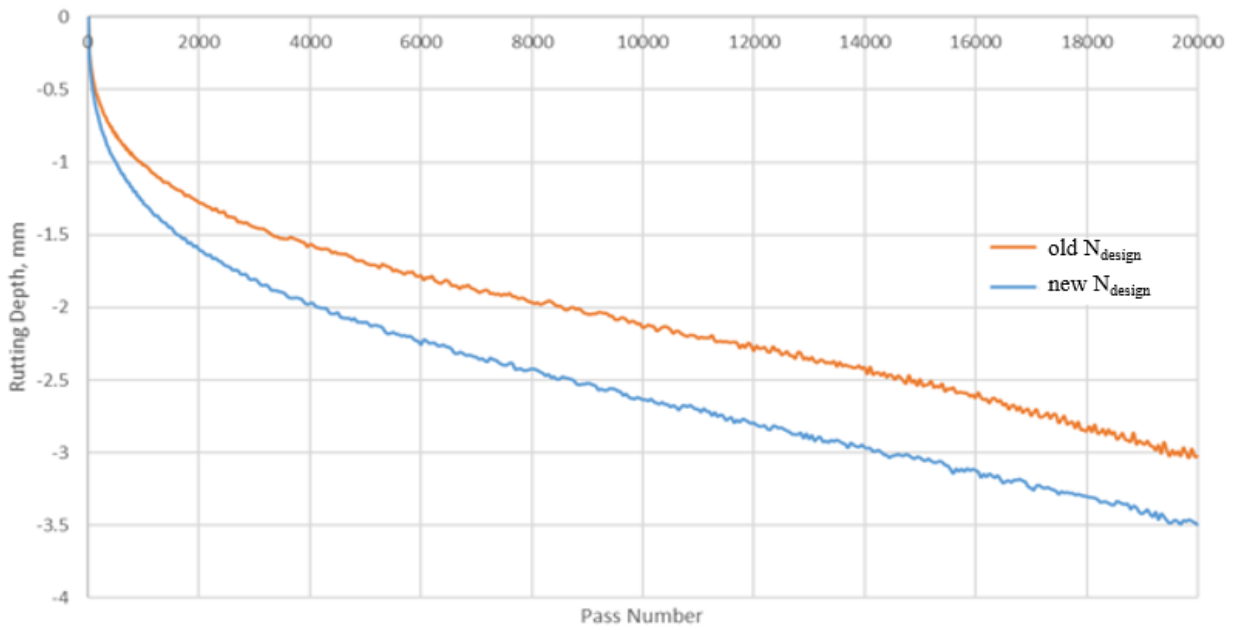


**Figure 26. IA 330 rutting depth versus passes**



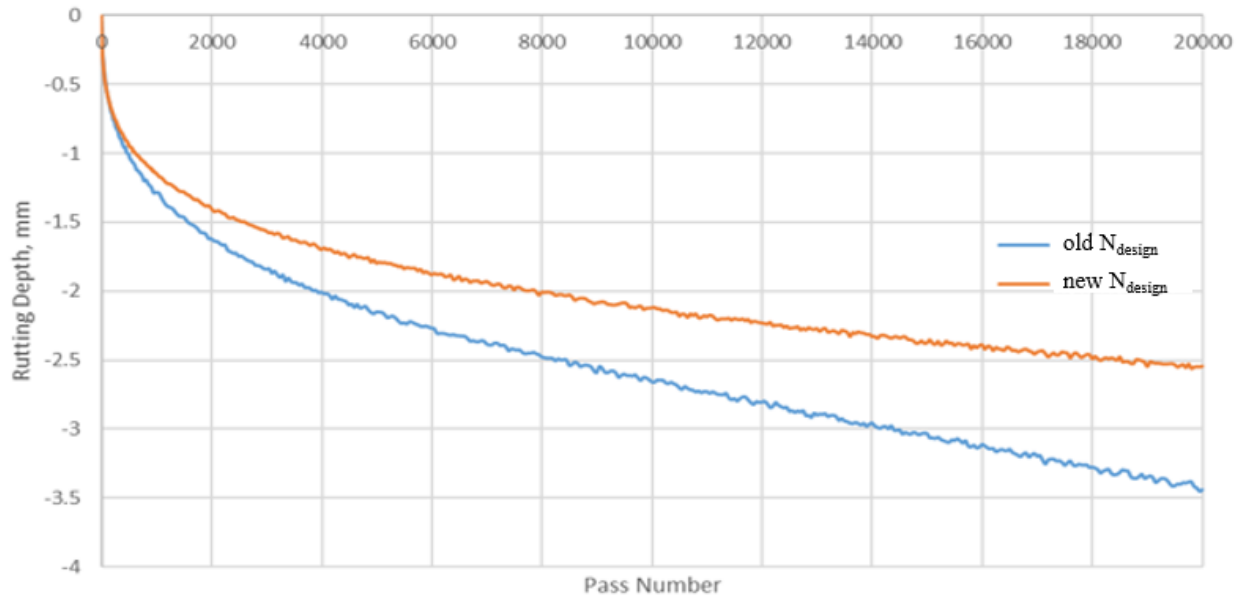


**Figure 27. I-235 rutting depth versus passes**

The orange line indicates average number of four new  $N_{design}$  specimens; the blue line indicates the average for old  $N_{design}$  specimens. According to the trend shown in the figures, new  $N_{design}$  mixtures have less rutting than old  $N_{design}$  mixtures. The possible reason is new  $N_{design}$  mixtures used more binder, and additional binder improves asphalt performance. The IA 4 specimens showed a slight difference between the old and new  $N_{design}$ , but IA 330 and I-235 had significant differences.

Statistical analysis also helps to illustrate whether groups perform significantly different from one another. In general, increases in binder content make asphalt film thickness increase and make a stiffer asphalt mix. However, for old  $N_{design}$  mixtures, higher binder content and lower gyrations make “softer” material according to the indicators shown in the figures. Appropriate binder content establishes stable pavement with good shape and a smooth surface under traffic loading. However, excessive binder content could result in a stiffer pavement that could be less durable at lower temperatures.

Tables 21 through 23 show the ANOVA test results for the three traffic levels.

**Table 21. IA 4 rutting depth ANOVA results**

Highway 4 Rutting depth Anova: Single Factor						
SUMMARY						
Groups	Count	Sum	Average	Variance		
old $N_{design}$	431.00	-828.11	-1.92	0.36		
new $N_{design}$	431.00	-815.10	-1.89	0.31		
ANOVA						
Source of Variation	SS	df	MS	F	P-value	F crit
Between Groups	0.20	1.00	0.20	0.58	0.45	3.85
Within Groups	292.27	860.00	0.34		F crit > P - value	
Total	292.46	861.00				

**Table 22. IA 330 rutting depth ANOVA results**

Highway 330 Rutting Depth Anova: Single Factor						
SUMMARY						
Groups	Count	Sum	Average	Variance		
old $N_{design}$	431.00	-1039.74	-2.41	0.58		
New $N_{design}$	431.00	-852.14	-1.98	0.43		
ANOVA						
Source of Variation	SS	df	MS	F	P-value	F crit
Between Groups	40.83	1.00	40.83	80.54	1.75635E-18	3.852294
Within Groups	435.95	860.00	0.51		F crit > P - value	
Total	476.78	861.00				

**Table 23. I-235 rutting depth ANOVA results**

I-235 Rutting depth Anova: Single Factor						
SUMMARY						
Groups	Count	Sum	Average	Variance		
old $N_{design}$	431.00	-1044.93	-2.42	0.56		
new $N_{design}$	431.00	-836.39	-1.94	0.27		
ANOVA						
Source of Variation	SS	df	MS	F	P-value	F crit
Between Groups	50.45	1.00	50.45	121.19	1.84558E-26	3.852294
Within Groups	358.03	860.00	0.42		F crit > P - value	
Total	408.48	861.00				

The default alpha value was set at 0.05. From the F-values, it can be concluded that there was not a significant difference between the old and new  $N_{design}$  for IA 4, in which the F-value of 0.58 is less than the F-critical of 3.85. However, significant differences were found for both IA 330 and I-235, in which their F-values were much larger than F-critical. IA 4 had the largest Pp-value of 0.45, IA 330 had a p-value of 1.8E-18, and I-235 had a p-value of 1.8E-26. The lower the p-

value is meaning the two data sets are much more significantly different from one another. Therefore, lower traffic volume has less impact on  $N_{\text{design}}$  specifications.

### DCT Results

The disk-shaped compaction tension (DCT) test addresses HMA mixture thermal cracking at low temperatures (Cuevas et al. 2004). DCT test results are highly dependent on asphalt film thickness and the low temperature durability of the asphalt binder used in the asphalt mix design. The standard DCT test temperature was recommended to be 10°C warmer than the PG low-temperature limit (Marasteanu et al. 2007). Table 24 shows the DCT results and test temperatures for the three traffic levels.

**Table 24. DCT test results**

Mix	Test Temperature (°C)	$N_{\text{design}}$	Fracture Energy (J/m <sup>2</sup> )	Coefficient of variation	Peak Load (kN)	Coefficient of variation
IA 4	-18	old	247	0.055	2.53	0.011
		new	267		2.49	
IA 330	-12	old	250.3	0.088	2.48	0.028
		new	283.8		2.58	
I-235	-12	old	356	0.224	2.46	0.024
		new	490.3		2.544	

The binder grade for IA 4, IA 330, and I-235 was PG 58-28, PG 64-22, and PG 64-22, respectively. The required test temperatures for the three traffic levels were -18°C, -12°C, and -12°C, respectively. Four specimens were made for each category studied for a total of 24 specimens. Full DCT results for the 24 tested specimens are shown in Appendix E. Figure 28 shows fracture energy and peak load.

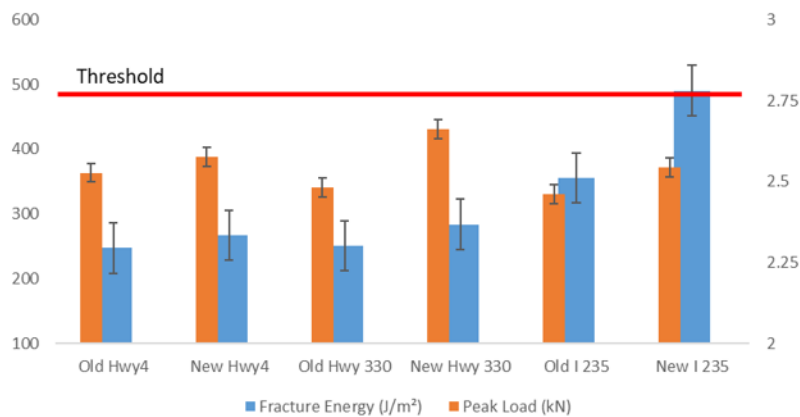


**Figure 28. Fracture energy and peak load results**

The previous Table 24 shows the average value of the four specimens for each group. The results show that new  $N_{\text{design}}$  mixtures have higher fracture energy than old  $N_{\text{design}}$  mixtures for all traffic levels. They indicate that new  $N_{\text{design}}$  specimens have better performance than old  $N_{\text{design}}$  specimens at low temperatures.

Statistical analysis also helps to illustrate whether the differences are significant between the old and new  $N_{\text{design}}$ . Tables 25 through 27 show the ANOVA F-test results for all traffic levels.

**Table 25. IA 4 fracture energy ANOVA results**

Highway 4 Fracture Energy Anova: Single Factor						
<b>SUMMARY</b>						
Groups	Count	Sum	Average	Variance		
old $N_{\text{design}}$	4.00	1128.00	282.00	1020.67		
new $N_{\text{design}}$	4.00	955.00	238.75	454.25		
<b>ANOVA</b>						
Source of Variation	SS	df	MS	F	P-value	F crit
Between Groups	3741.13	1.00	3741.13	5.07	0.07	5.99
Within Groups	4424.75	6.00	737.46		F crit > P - value	
Total	8165.88	7.00				

**Table 26. IA 330 fracture energy ANOVA results**

Highway 330 Fracture Energy Anova: Single Factor						
<b>SUMMARY</b>						
Groups	Count	Sum	Average	Variance		
old $N_{\text{design}}$	4.00	1001.00	250.25	2608.92		
new $N_{\text{design}}$	4.00	1135.00	283.75	1640.25		
<b>ANOVA</b>						
Source of Variation	SS	df	MS	F	P-value	F crit
Between Groups	2244.50	1.00	2244.50	1.06	0.34	5.99
Within Groups	12747.50	6.00	2124.58		F crit > P - value	
Total	14992.00	7.00				

**Table 27. I-235 fracture energy ANOVA results**

I-235 Fracture Energy Anova: Single Factor						
<b>SUMMARY</b>						
Groups	Count	Sum	Average	Variance		
old $N_{\text{design}}$	4.00	1635.00	408.75	14424.25		
new $N_{\text{design}}$	4.00	2164.00	541.00	11061.33		
<b>ANOVA</b>						
Source of Variation	SS	df	MS	F	P-value	F crit
Between Groups	34980.13	1.00	34980.13	2.75	0.15	5.99
Within Groups	76456.75	6.00	12742.79		F crit > P - value	
Total	111436.88	7.00				

If the F-value is smaller than F-critical, there is no significant difference between the two data groups. F-values for IA 4, IA 330, and I-235 were 5.07, 1.06, and - 2.74, respectively, all of which are smaller than F-critical of 5.99. This means that no significant differences were found between old and new  $N_{design}$  compaction criteria based on the F-test. However, only the I-235 new  $N_{design}$  specimens passed the 400 J/m<sup>2</sup> fracture energy threshold (Marasteanu et al. 2012). Additional work on adjusted specimens between old and new  $N_{design}$  levels needs to be conducted.

## Beam Fatigue Results

The beam fatigue test is used to test flexural stiffness and asphalt fatigue life. The four-point beam fatigue test was used to test asphalt beams at microstrain levels of 900, 700, and 500. A total of 36 specimens were tested to obtain average beam fatigue results. The results for the three traffic levels and two  $N_{design}$  specifications are summarized in Table 28, and the detailed beam fatigue results are included in Appendix F.

**Table 28. Beam fatigue test results**

Mix Type		Macro-strain ( $\mu\epsilon$ )	Initial Flexural Stiffness (MPa)	50% of Initial Flexural Stiffness (MPa)	Flexural Stiffness at end of test (MPa)	Cycles to Failure ( $N_f$ )	Cumulative dissipated energy (MJ/m <sup>3</sup> )
IA 4	old $N_{design}$	900	3,520.0	1,760.0	1,422.0	7,385	23.5
		700	4,340.5	2,170.3	1,860.0	19,140	48.0
		500	4,266.5	2,133.3	1,916.0	56,230	153.9
	new $N_{design}$	900	4,299.0	2,149.5	1,726.5	7,875	30.9
		700	3,632.0	1,816.0	1,559.5	31,355	54.7
		500	4,545.7	2,272.8	2,045.5	58,120	90.9
IA 330	old $N_{design}$	900	5,548.0	2,774.0	2,314.0	5,360	29.9
		700	6,233.0	3,116.5	2,796.5	8,185	31.7
		500	5,518.5	2,759.3	2,576.0	62,200	71.6
	new $N_{design}$	900	5,341.0	2,670.5	2,198.5	3,930	20.5
		700	5,829.5	2,914.8	2,570.0	15,615	54.8
		500	6,237.5	3,118.8	2,876.0	66,505	104.9
I-235	old $N_{design}$	900	3,725.5	1,862.8	1,534.0	12,370	43.8
		700	2,726.5	1,363.3	1,225.0	54,725	87.7
		500	2,978.5	1,489.3	1,330.0	521,115	427.5
	new $N_{design}$	900	3,436.0	1,718.0	1,379.0	9,900	30.1
		700	3,348.5	1,674.3	1,451.5	41,995	81.6
		500	3,757.5	1,878.8	1,727.5	522,290	591.9

Each value is the average for two specimens. IA 4, IA 330, and I-235 refer to 1M, 10M, and 30M ESAL traffic levels, respectively, and test results can be used to predict the pavement endurance limit. Only the old and new  $N_{design}$  levels for I-235 at  $500 \mu\epsilon$  passed 3 million cycles without failing. Figure 29 shows the microstrain versus cycles to failure curves for all mixes and is a log-log scale chart that can provide a better visual indication for cycles to failure versus microstrain relationships.

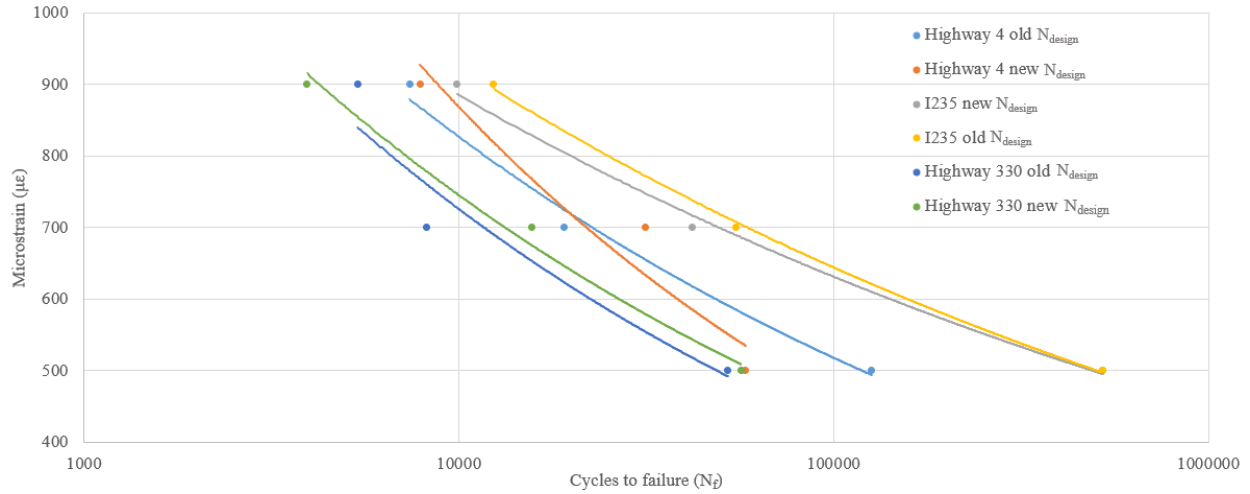


**Figure 29. Beam fatigue curves**

Based on the number of cycles to failure, all new  $N_{design}$  mixtures had more cycles than the old  $N_{design}$  mixtures. This means the new  $N_{design}$  mixtures have better fatigue life than the old  $N_{design}$  mixtures. According to Figure 29, there was a slight difference for old versus new  $N_{design}$ , and statistical analysis is needed to compare the detail between the two specifications. Table 29 through Table 31 show the ANOVA F-test results for cycles to failure for the three traffic levels.

**Table 29. IA 4 cycles to failure ANOVA results**

Highway 4 Cycles to failure Anova: Single Factor						
<b>SUMMARY</b>						
Groups	Count	Sum	Average	Variance		
old $N_{design}$	3	152755	50918.33333	4288430358		
new $N_{design}$	3	97350	32450	632039275		
<b>ANOVA</b>						
Source of Variation	SS	df	MS	F	P-value	F crit
Between Groups	511619004.2	1	511619004.2	0.21	0.67	7.71
Within Groups	9840939267	4	2460234817			
Total	10352558271	5				
					F crit > P - value	

**Table 30. IA 330 cycles to failure ANOVA results**

I-235 Cycles to failure Anova: Single Factor						
SUMMARY						
Groups	Count	Sum	Average	Variance		
old N <sub>design</sub>	3	588210	196070	79689175525		
new N <sub>design</sub>	3	574185	191395	82376148025		
ANOVA						
Source of Variation	SS	df	MS	F	P-value	F crit
Between Groups	32783437.5	1	32783437.5	0.00	0.98	7.71
Within Groups	3.24131E+11	4	81032661775		F crit > P - value	
Total	3.24163E+11	5				

**Table 31. I-235 cycles to failure ANOVA results**

Highway 330 Cycles to failure Anova: Single Factor						
SUMMARY						
Groups	Count	Sum	Average	Variance		
old N <sub>design</sub>	3	65745	21915	689881075		
new N <sub>design</sub>	3	76050	25350	762110325		
ANOVA						
Source of Variation	SS	df	MS	F	P-value	F crit
Between Groups	17698837.5	1	17698837.5	0.02	0.88	7.71
Within Groups	2903982800	4	725995700		F crit > P - value	
Total	2921681638	5				

If the F-value is smaller than F-critical, there is no significant difference between the two data groups. The IA 4, IA 330, and I-235 F-values were 0.2, 0.8, and almost 0, respectively, while F-critical for all three traffic levels was 7.7. Therefore, there was no significant difference between the new and old N<sub>design</sub>. In other words, the statistical analysis showed that the new and old N<sub>design</sub> specifications did not significantly affect the dynamic modulus results.

### ME Design Performance Prediction

*Transverse Cracking: Thermal Cracking + Reflective Cracking*

Figure 30 shows the transverse cracking results using ME Design.

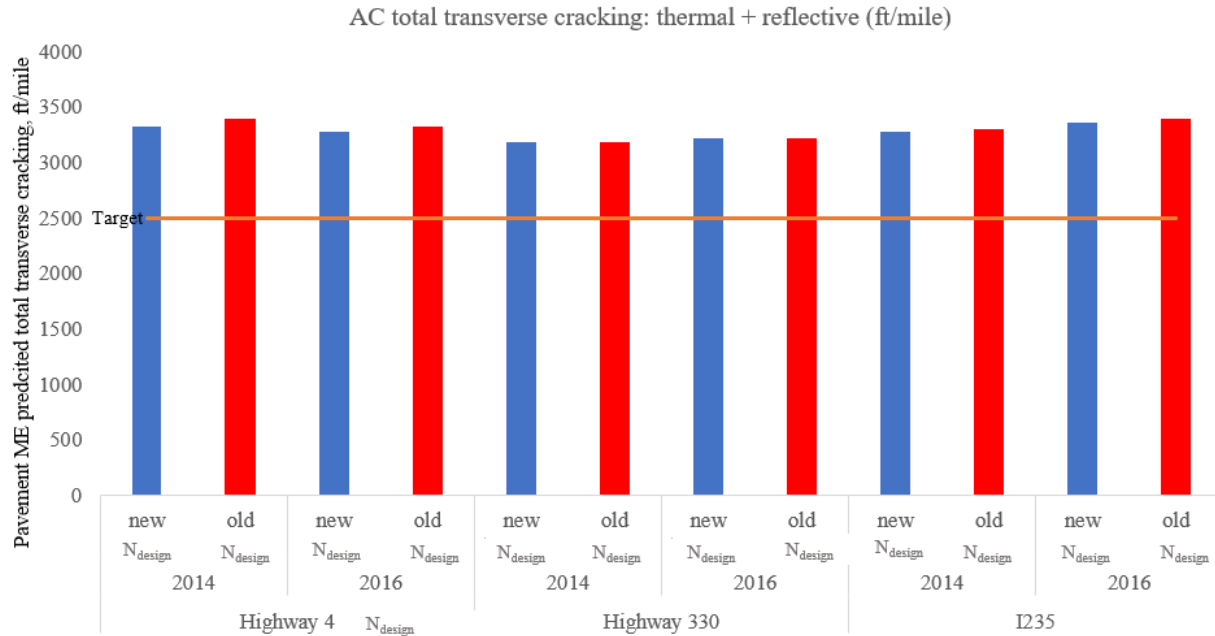


**Figure 30. Transverse cracking results and reliability**

For this section, transverse cracking was calculated using the sum of thermal cracking and reflective cracking. The leading causes of transverse cracking are low-temperature thermal cracking of the asphalt surface and reflective cracking. As Figure 30 shows, all traffic levels met the requirement for transverse cracking. However, the required reliability for transverse cracking is 90; ME Design predicted reliability for all traffic levels was lower than 90. Therefore, the overall transverse cracking prediction failed. However, the transverse cracking difference between the new and old  $N_{design}$  was not significant. Keep in mind, transverse cracking is non-load related and is mainly caused by low-temperature thermal cracking. As far as the reflective cracking prediction using ME Design, it was still problematic due to climate, and additional research for transverse cracking still needs to be conducted.

*International Roughness Index (IRI)*

Figure 31 presents an illustration of the average IRI values with standard deviations from ME Design.



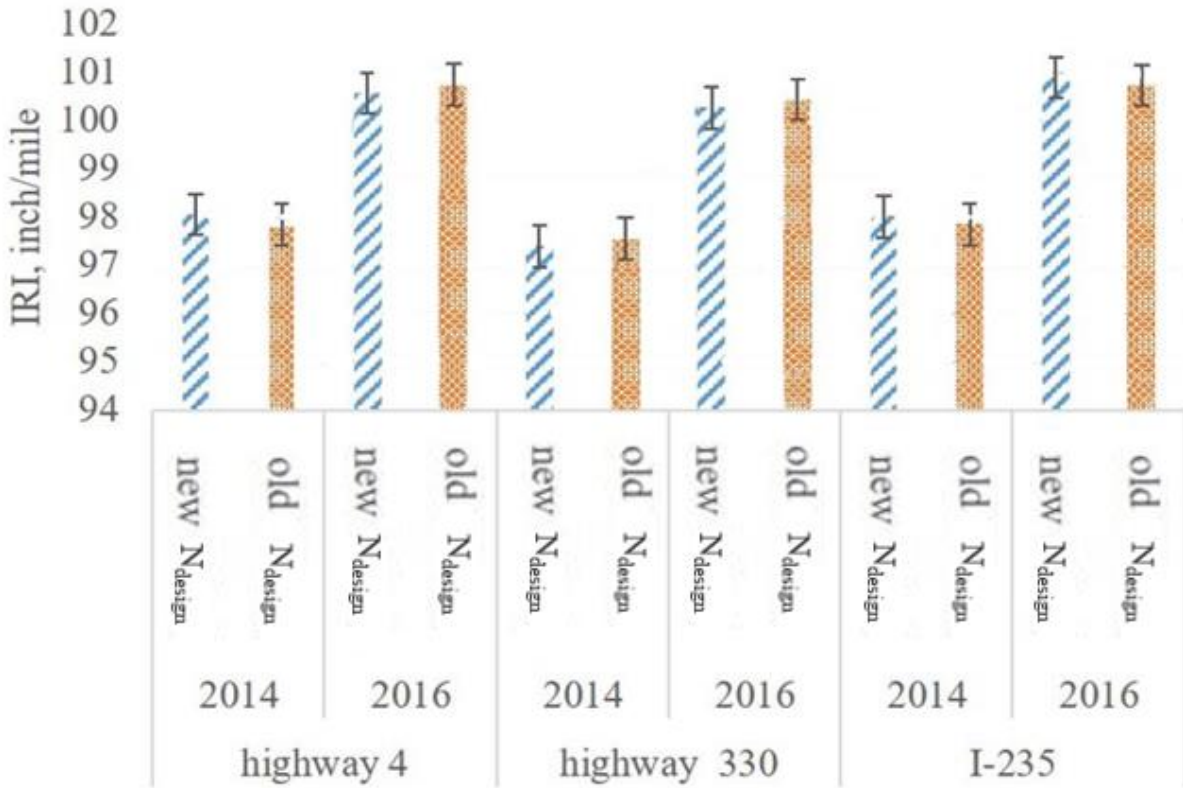


**Figure 31. IRI results**

From the chart, it appears that there are no visual differences between the new and old  $N_{design}$  results for the three traffic levels. Several factors can influence IRI, including climate, asphalt binder, asphalt binder content, etc. Colder weather influences changes in IRI (NHI 2000). However, for this study, all three roadways are within the same climatic region in Iowa, and, thus, there does not appear to be differences between IRI values for the three highways and their associated traffic levels.

Asphalt binder type and asphalt binder content can also significantly influence IRI. However, with the combination of asphalt type, weather, and binder content, a single factor is not enough to affect the overall pavement performance. That is why the ME Design predicted IRI values were not statistically different for the three highway pavements and two  $N_{design}$  specifications. The new  $N_{design}$  specification has lower gyratory compaction and higher binder content, and the results show it provides the same roughness as the old  $N_{design}$  specification.

#### *AC Top-Down Fatigue Cracking*

Figure 32 shows the average AC top-down fatigue cracking results.

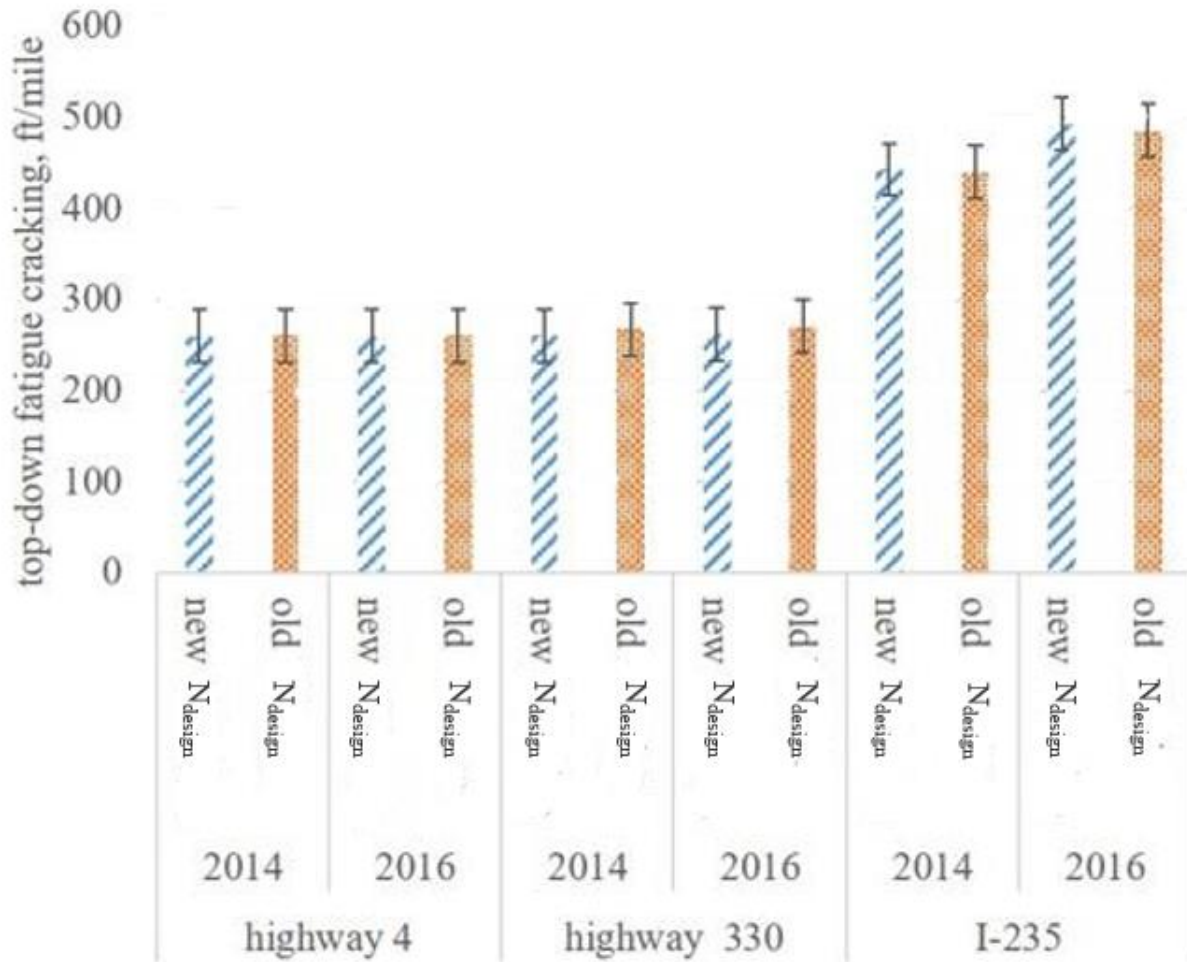


**Figure 32. AC top-down fatigue cracking results**

Horizontal loading can cause top-down cracking and AC failure (Asphalt Institute 2014). Because the aggregate gradations did not change for the new and old  $N_{design}$  mixes, the pavement structure inputs in ME Design were the same.

From the chart, I-235 (PG 64-22) had higher average top-down cracking compared to IA 330 (PG 64-22) and IA 4 (PG 58-28). The binder type difference significantly differs between I-235 and IA 4, but is not significantly different between IA 330 and I-235. However, this similarity does not transfer over into similar top-down cracking between the two pavements. I-235 is designed for high volume traffic (>30 million ESALs) compared to IA 330 (1–10 million ESALs) and IA 4 (<1 million ESALs).

Again, climate location influences temperature, and temperature affects top-down cracking; however, the locations of the three highways studied are close to each other and have the same weather conditions. That is why IA 330 and IA 4 had similar top-down cracking.

According to the E\* master curves, the new  $N_{\text{design}}$  specification produces a stiffer pavement than the old  $N_{\text{design}}$  specification, which means higher average top-down fatigue cracking should be predicted. However, according to the ME Design prediction, the new  $N_{\text{design}}$  mixes do not show differences from the old  $N_{\text{design}}$  mixes.

### AC Rutting

Asphalt rutting is a permanent deformation on the asphalt pavement surface (Copeland 2011). Figure 33 shows the average AC rutting results with standard deviations.

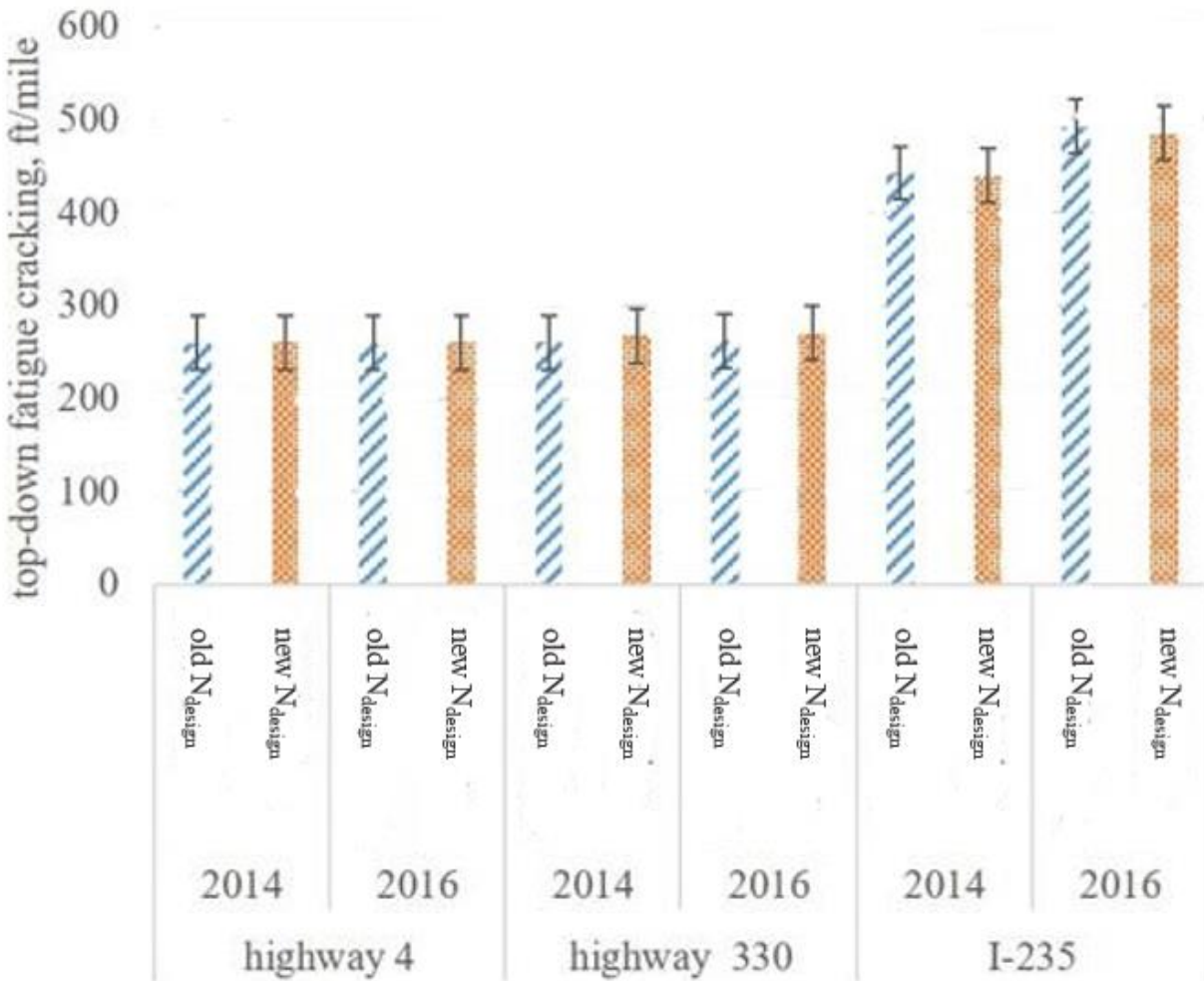


**Figure 33. AC rutting results**

As shown in the chart, there is a small difference between I-235 and IA 4 and between I-235 and IA 330. The possible reasons are temperature, binder type, and binder content. For the temperature aspect, the warmer weather, the higher the AC rutting. The location of I-235 has about the same mean annual air temperature (50°C) as both IA 330 (49°C) and IA 4 (49°C). I-235 has higher traffic volume, and the mix is compacted with more gyratory compaction cycles

than the IA 330 and IA 4 mixes. However, asphalt binder type and binder content affect rutting resistance the most and binder type has a significant influence on rutting resistance and compatibility. That said, the new  $N_{\text{design}}$  specifications have higher binder content than the old  $N_{\text{design}}$  specifications. From Figure 33, for the three highway pavements, the new  $N_{\text{design}}$  mixtures had the same AC rutting results as the old mixtures.

Superpave mixture performance shows low rutting due to lower binder content use. In this case, the new  $N_{\text{design}}$  mixtures used fewer gyratory compaction cycles to increase binder content, and the mixes still performed the same as the old  $N_{\text{design}}$  mixtures. It can be concluded that the new  $N_{\text{design}}$  specifications were validated according to rutting performance predictions.

### PMIS Research Results

The Iowa PMIS is an automated system for reporting information on and searching pavement-related information processes. The PMIS database serves as an open data system for the Iowa DOT and for recording all roadway information in Iowa. The PMIS data used in this study was from the 2018 PMIS data website. Table 32 summarizes the 2018 PMIS information used for this study.

**Table 32. 2018 PMIS information**

<b>Performance</b>	<b>IA 4</b>	<b>IA 330</b>	<b>I-235</b>
Rutting Index	61	84	86
IRI	95.66	110.35	41.41
Cracking Index	86	86	98
Friction	61	52	31
Average Faulting	0.0015	0	0.001
Rut Depth	0.18	0.08	0.006
Transverse Cracking Index	60	59	96
Longitudinal Cracking Index	99	75	99

### PMIS and ME Design Comparisons

PMIS and ME Design results were compared to identify any differences between in-field distresses and predicted distress. ME Design indicated distresses using laboratory-measured material values as level 1 inputs. Table 33 shows the overall 2014 and 2016 PMIS results for the three traffic levels.

**Table 33. PMIS results in 2014 and 2016**

Roadway	Year	Rutting	IRI	Transverse Cracking
IA 4	2014	0.11	76	224
	2016	0.15	91	237
IA 330	2014	0.17	81	371
	2016	0.07	100.8	385
I-235	2014	0	89.34	0
	2016	0.07	92.71	21

The comparisons shown in the bar charts in this section for the three roadways have PMIS values shown with orange bars and ME Design results shown with blue bars.

*IRI Comparisons*

This section compared the difference in PMIS-determined IRI results and ME Design-predicted IRI values. The comparisons are shown in Figures 34 through 36 for the three highways.

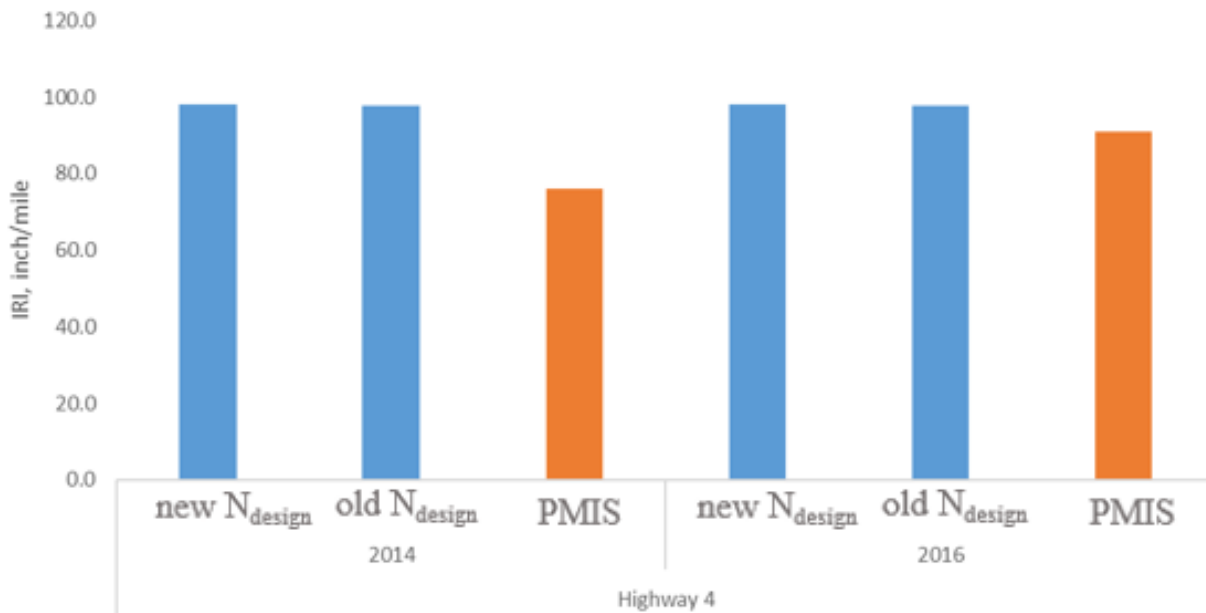


**Figure 34. IA 4 PMIS vs. ME Design IRI comparison**

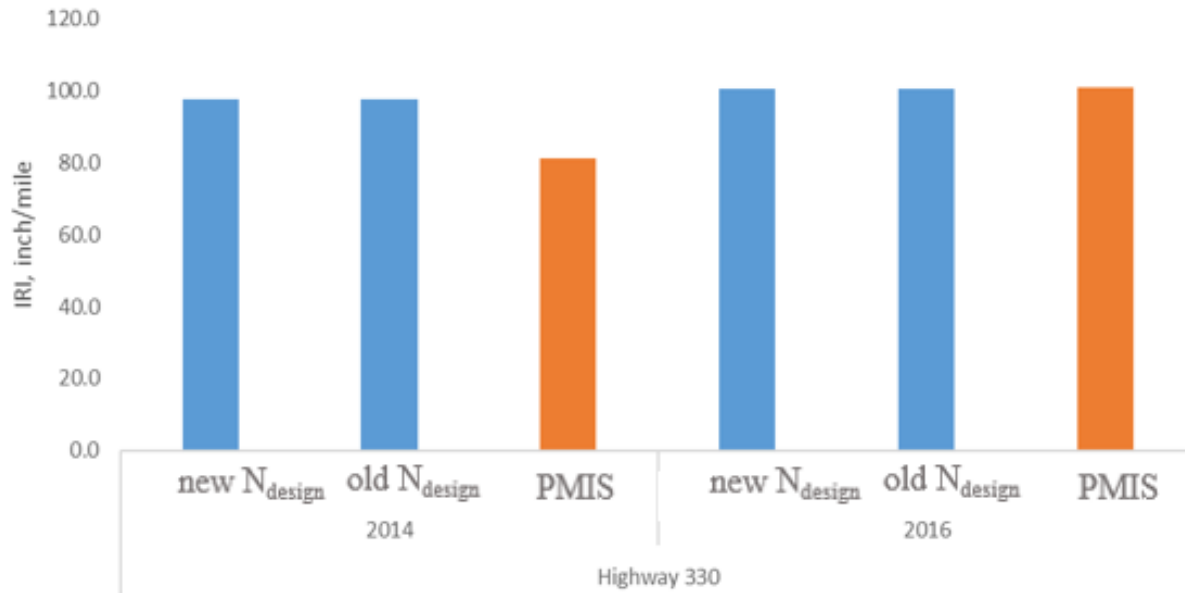


**Figure 35. IA 330 PMIS vs. ME Design IRI comparison**

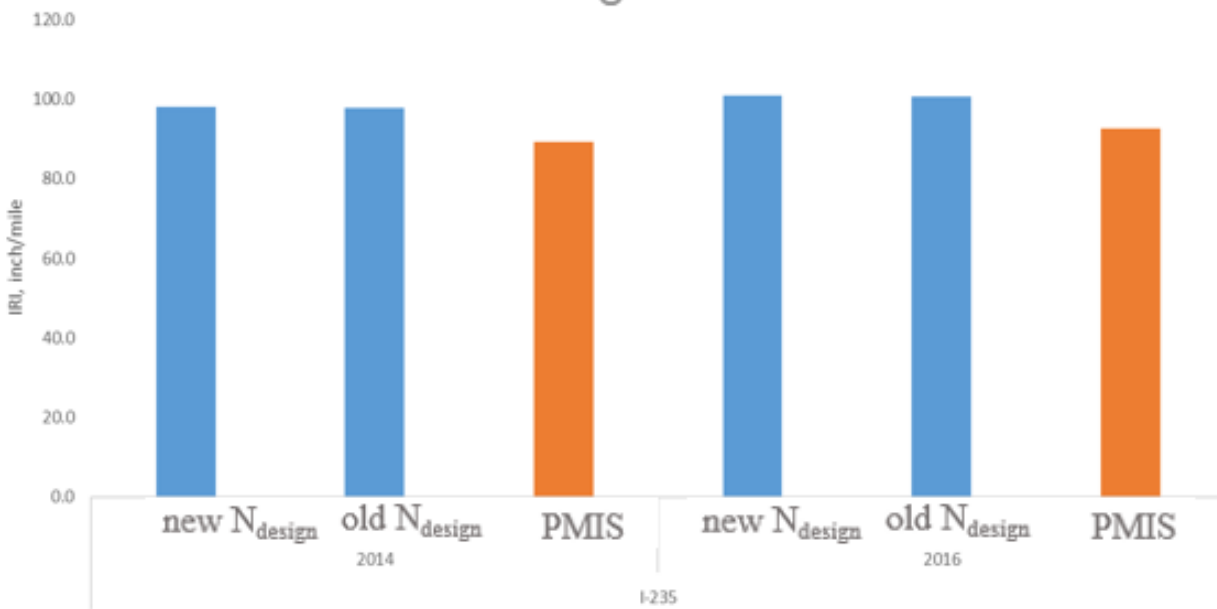


**Figure 36. I-235 PMIS vs. ME Design IRI comparison**

For all three traffic levels, 2016 PMIS and ME Design results were similar. However, 2014 PMIS values showed differences to ME Design results.

*Rutting Depth Comparisons*

This section compares the rutting depth differences between the PMIS data and ME Design predicted values. The comparisons are shown in Figures 37 through 39 for the three highways.

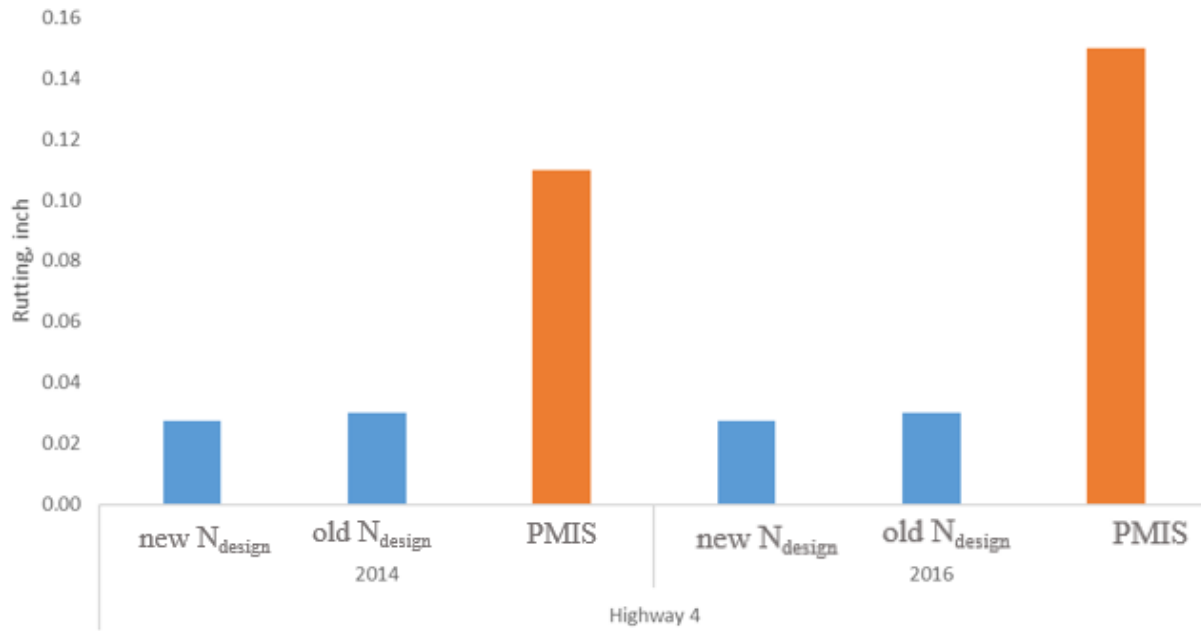


**Figure 37. IA 4 PMIS vs. ME Design rutting depth comparison**

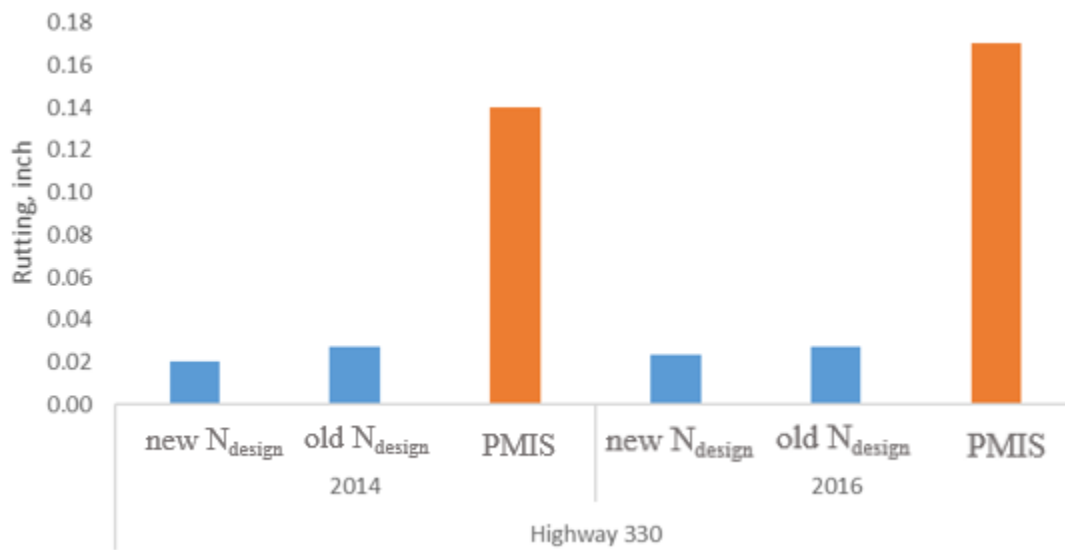


**Figure 38. IA 330 PMIS vs. ME Design rutting depth comparison**

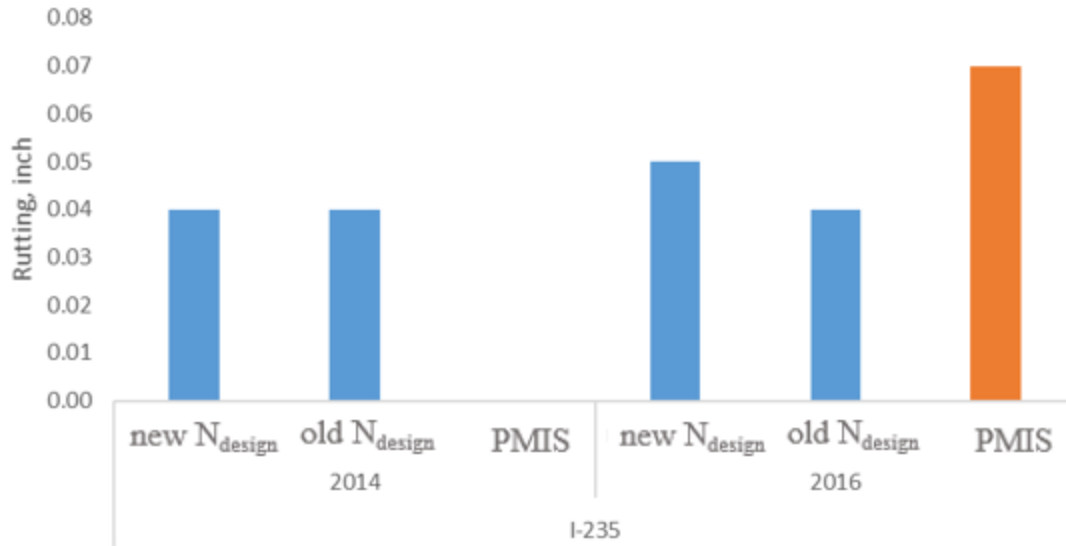


**Figure 39. I-235 PMIS vs. ME Design rutting depth comparison**

There were significant differences between the PMIS values and ME Design predicted values. Many factors can affect the formation of plastic deformation in AC pavements, including aggregates used in mix design, binder contents, additives, traffic loads, and temperatures. Environmental temperature could be the reason to cause huge rutting differences between PMIS data and ME Design predictions. In ME Design the climate data was an average value for each month. The PMIS test temperatures could have differences from Iowa's average temperatures used in ME Design.

*Transverse Cracking Comparisons*

This section compares transverse cracking between ME Design predicted values and PMIS results. The comparisons are shown in Figures 40 through 42 for the three highways.



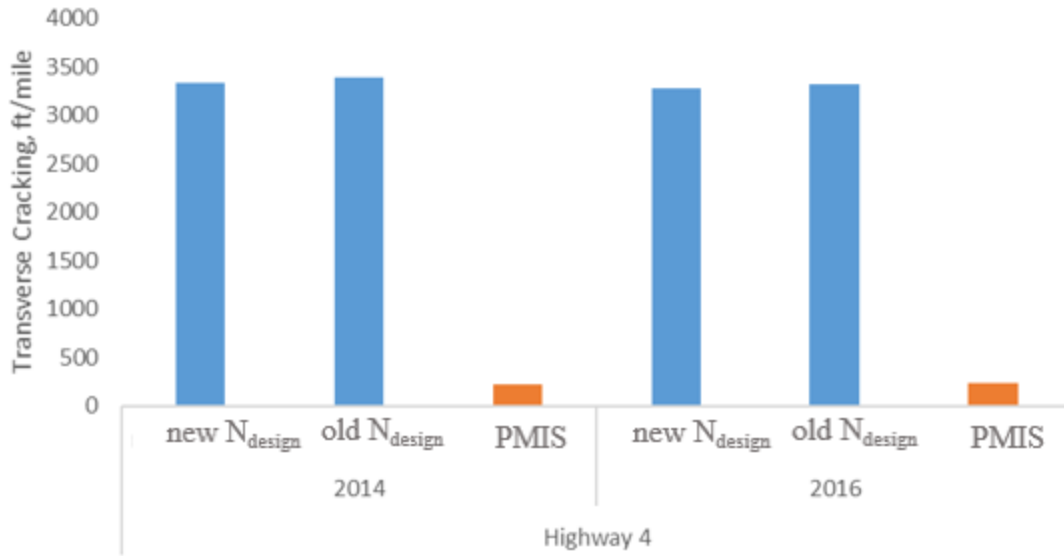


**Figure 40. IA 4 PMIS vs. ME Design transverse cracking comparison**

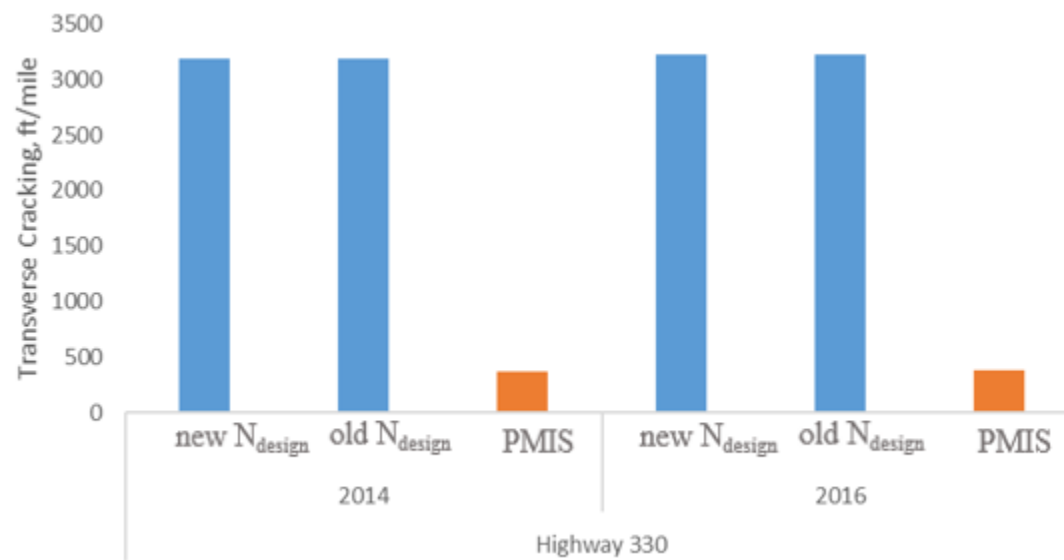
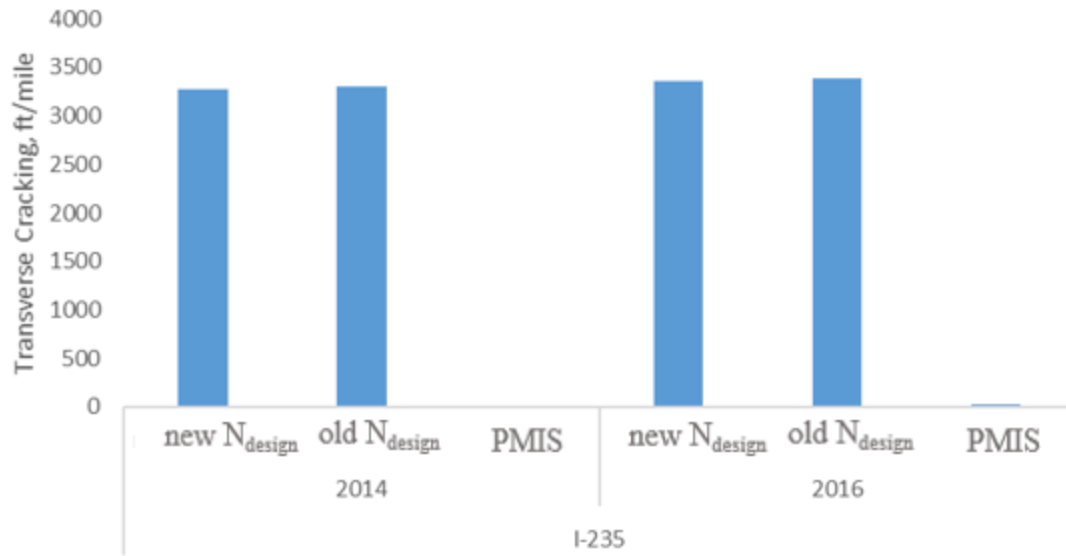


**Figure 41. IA 330 PMIS vs. ME Design transverse cracking comparison**



PMIS bars are either 0 or close to 0

**Figure 42. I-235 PMIS vs. ME Design transverse cracking comparison**

## CHAPTER 5: CONCLUSIONS AND RECOMMENDATIONS

The investigation of  $N_{\text{design}}$  with new and old Iowa DOT specifications studied three mix designs each designed for a different traffic level (low with <1M ESALs, medium with 1–10M ESALs, and high with >10M ESALs) in Iowa.

For each mix, specimens were compacted in a Superpave gyratory compacter in the laboratory. Each mix design was evaluated through performance testing for old  $N_{\text{design}}$  and new  $N_{\text{design}}$  levels. Dynamic modulus, flow number, DCT, Hamburg wheel tracking, and beam fatigue tests were performed on all mix specimens. Mixture properties were statistically compared, and factors within each mix were analyzed by performing an ANOVA F-test.

The advantages of the new  $N_{\text{design}}$  included reduced gyratory compaction cycles and increased binder content. The binder type and gradation did not change within specimens made using the old and new  $N_{\text{design}}$  levels. The old  $N_{\text{design}}$  optimal binder content for IA 4, IA 330, and I-235 was 5.47%, 6.04%, and 5.62%, respectively. The new  $N_{\text{design}}$  optimal binder content for IA 4, IA 330, and I-235 was 5.73%, 6.33%, and 5.68%, respectively.

For VMA, the new  $N_{\text{design}}$  mixtures have smaller VMA than the old  $N_{\text{design}}$  mixtures. IA 4's VMA for old and new  $N_{\text{design}}$  mixtures was 13.47 and 13.36, respectively. IA 330's VMA for old and new  $N_{\text{design}}$  mixtures was 16.57 and 16.33, respectively. I-235's VMA for old and new  $N_{\text{design}}$  mixtures was 14.17 and 14.02, respectively. However, there were concerns with reducing gyratory compaction levels as the binder content was increased, which can lead to increased rutting in roadways. According to results from the dynamic modulus, DCT, and flow number tests, the new  $N_{\text{design}}$  specimens still improved performance by increasing the asphalt content over the specimens produced based on the old  $N_{\text{design}}$  gyratory levels.

ANOVA F-tests identified few statistical differences between the old and new  $N_{\text{design}}$  in several mixture properties. However, it was still found that new  $N_{\text{design}}$  mixtures had slight improvement when comparing performance. On average, the ANOVA F-tests found no significant differences for dynamic modulus between the old and new  $N_{\text{design}}$  specifications.

The flow number tests showed that more binder added in the new  $N_{\text{design}}$  specification improved the rutting resistance. However, this difference was not found to be statistically significant. IA 4 did not show a significant difference according to the HWTT results between old and new  $N_{\text{design}}$  mixtures, but IA 330 and I-235 had significant rutting resistance improvement with these tests on the new  $N_{\text{design}}$  mixtures.

The beam fatigue tests showed no significant difference between the old and new  $N_{\text{design}}$  mixtures for the number of cycles to failure. This indicated that the new  $N_{\text{design}}$  specification did not change the pavement fatigue life a lot.

The comparison of PMIS data to predicted results using ME Design showed that future work should be continued based on both old and new  $N_{\text{design}}$  mix designs. The overall results showed

that there were significant differences. The possible reasons could be that there is insufficient level 1 input data into ME Design or there could be other reasons that need to be further investigated. In this study, only laboratory-measured values such as dynamic modulus and DSR were used in ME Design as level 1 inputs.

## REFERENCES

- AASHTO. 2008. *Mechanistic-Empirical Pavement Design Guide, Interim Edition: A Manual of Practice*. American Association of State Highway and Transportation Officials, Washington, DC.
- Advanced Asphalt Technologies, LLC 2011. *NCHRP Report 673: A Manual for Design of Hot Mix Asphalt with Commentary*. National Cooperative Highway Research Program, Washington DC.
- Anderson, R. M. and H. U. Bahia, 1997. Evaluation and Selection of Aggregate Gradations for Asphalt Mixtures Using Superpave. *Transportation Research Record: Journal of the Transportation Research Board*, No. 1583, pp. 91–97.
- Anderson, R. M., P. A. Turner, R. L. Peterson, and R. B. Mallick. 2002. *NCHRP Report 478: Relationship of Superpave Gyrotory Compaction Properties to HMA Rutting Behavior*. National Cooperative Highway Research Program, Washington, DC.
- Aschenbrenner, T. 1995. Evaluation of Hamburg Wheel-Tracking Device to Predict Moisture Damage in Hot-Mix Asphalt. *Transportation Research Record: Journal of the Transportation Research Board*, No. 1492, pp. 193–201.
- Asphalt Institute. 2001. *Superpave Mix Design: Superpave Series No. 2*. Asphalt Institute, Lexington, KY.
- Asphalt Institute. 2015. *MS-2 Asphalt Mix Design Methods*. 7th edition. Asphalt Institute, Lexington, KY.
- Bahia, H., P. Teymourpour, D. Swiertz, C. Ling, R. Varma, T. Mandal, P. Chaturabong, E. Lyngdal, and A. Hanz. 2016. *Analysis and Feasibility of Asphalt Pavement Performance-Based Specifications for WisDOT*. Wisconsin Highway Research Program and Wisconsin Department of Transportation, Madison, WI.
- Bonaquist, R. F., D. W. Christensen, and W. Stump, III. 2003. *NCHRP Report 513: Simple Performance Tester for Superpave Mix Design: First-Article Development and Evaluation*. National Cooperative Highway Research Program, Washington DC.
- Brown, E. R., S. P. Kandhal, L. F. Roberts, Y. R. Kim, D.-Y. Lee, and T. W. Kennedy. 2009. *Hot Mix Asphalt Materials, Mixture Design, and Construction*. 3rd edition. National Asphalt Pavement Association (NAPA) Education Foundation, Lanham, MD.
- Buss, A., A. Cascione, and R. C. Williams. 2014. Evaluation of Warm Mix Asphalt Containing Recycled Asphalt Shingles. *Construction and Building Materials*, Vol. 61, pp. 1–9.
- Butcher, M. 1998. Determining Gyrotory Compaction Characteristics Using Servopac Gyrotory Compactor. *Transportation Research Record: Journal of the Transportation Research Board*, No. 1630, pp. 89–97.
- Button, J. W., A. Chowdhury, and A. Bhasin. 2004. *Design of TxDOT Asphalt Mixtures Using the Superpave Gyrotory Compactor*. Texas Transportation Institute, Texas A&M University System, College Station, TX.
- Ceylan, H., S. Kim, O. Kaya, and K. Gopalakrishnan. 2015. *Investigation of AASHTOWare Pavement ME Design/DARWinME Performance Prediction Models for Iowa Pavement Analysis and Design*. Program for Sustainable Pavement Engineering & Research (PROSPER), Institute for Transportation, Iowa State University, Ames, IA.  
[https://intrans.iastate.edu/app/uploads/2018/03/AASHTOWare\\_performance\\_prediction\\_models\\_w\\_cvr.pdf](https://intrans.iastate.edu/app/uploads/2018/03/AASHTOWare_performance_prediction_models_w_cvr.pdf).

- Cominsky, R., R. B. Leahy, and E. T. Harrigan. 1994. *SHRP-A-408: Level One Mix Design: Materials Selection, Compaction, and Conditioning*. Strategic Highway Research Program, Washington, DC.
- Copeland, A. 2011. *Reclaimed Asphalt Pavement in Asphalt Mixtures: State of the Practice*. FHWA-HRT-11-021. Federal Highway Administration, Office of Research, Development, and Technology, Turner-Fairbank Highway Research Center, McLean, VA.
- Cuevas, A., M. Febrero, R. Fraiman. 2004. An Anova Test for Functional Data. *Computational Statistics & Data Analysis*, Vol. 47, No. 1, pp. 111–122.
- Dave, E. V., M. Oshone, A. Schokker, and C. E. Bennett. 2019. *Disc Shaped Compact Tension (DCT) Specifications Development for Asphalt Pavement*. Minnesota Department of Transportation, St. Paul, MN.
- Dhir, R. K. J. de Brito, R. Mangabhai, and C. Q. Lye. 2017. Chapter 7 – Use of Copper Slag in Road Pavement Applications. In *Sustainable Construction Materials: Copper Slag*. Woodhead Publishing, Elsevier Ltd. pp. 247–277.
- FHWA. 2013. *Asphalt Material Characterization for AASHTOWare Pavement ME Design Using an Asphalt Mixture Performance Tester*. Tech Brief. FHWA-HIF-13-060. Federal Highway Administration, Office of Pavement Technology, Washington, DC.
- FHWA. 2014. *Standard Specifications for Construction of Roads and Bridges on Federal Highway Projects*. FP-14. Federal Highway Administration, Office of Federal Lands - Highway, Washington, DC.
- Gibson, N., X. Qi, A. Shenoy, G. Al-Khateeb, M. E. Kutay, A. Andriescu, K. Stuart, J. Youtcheff, and T. Harman. 2012. *Performance Testing for Superpave and Structural Validation*. FHWA-HRT-11-045. Federal Highway Administration, Office of Research, Development, and Technology, Turner-Fairbank Highway Research Center, McLean, VA.
- Grogg, M., K. Smith, C. Williges, and S. Schram. 2020. Incorporating Pavement Smoothness Benefits to Enhance the Iowa Department of Transportation’s Pavement Type Determination Process. *Transportation Research Record: Journal of the Transportation Research Board*, Vol. 2674, No. 5, pp. 563–571.
- Harmelink, D. and T. Aschenbrener. 2002. *In-Place Voids Monitoring of Hot Mix Asphalt Pavements*. CDOT-DTD-R-2002-11. Colorado Department of Transportation, Research Branch, Denver, CO.
- Iowa DOT. October 16, 2012. *Hot Mix Asphalt (HMA) Design Criteria. Materials I.M. 510 Appendix A*. Iowa Department of Transportation, Ames, IA
- Kennedy, T. W., G. A. Huber, E. T. Harrigan, R. J. Cominsky, C. S. Hughes, H. Von Quintus, and J. S. Moulthrop. 1994. *SHRP-A-410: Superior Performing Asphalt Pavements (Superpave): The Product of the SHRP Asphalt Research Program*. Strategic Highway Research Program, Washington, DC.
- Marasteanu, M., A. Zofka, M. Turos, Xinjun Li, Raul Velasquez, X. Li, W. Buttlar, G. Paulino, A. Braham, E. Dave, J. Ojo, H. Bahia, C. Williams, J. Bausano, A. Kvasnak, A. Gallistel, and J. McGraw. 2007. *Investigation of Low Temperature Cracking in Asphalt Pavements: A Transportation Pooled Fund Study*, Minnesota Department of Transportation, St. Paul, MN.

- Marasteanu, M., W. Buttlar, H. Bahia, C. Williams, K. H. Moon, E. Z. Teshale, A. C. Falchetto, M. Turos, E. Dave, G. Paulino, S. Ahmed, S. Leon, A. Braham, B. Behnia, H. Tabatabaee, R. Velasquez, A. Arshadi, S. Puchalski, S. Mangiafico, A. Buss, J. Bausano, and A. Kvasnak. 2012. *Investigation of Low Temperature Cracking in Asphalt Pavements National Pooled Fund Study – Phase II*. Minnesota Department of Transportation, St. Paul, MN.
- Miller, J. S. and W. Y. Bellinger. 2003. *Distress Identification Manual for the Long-Term Pavement Performance Program*. FHWA-RD-03-031. Federal Highway Administration, Office of Infrastructure Research and Development, McLean, VA.
- Newcomb, D. E., M. Buncher, and I. J. Huddleston. 2001. Concepts of Perpetual Pavements. *Transportation Research Circular*, 503, pp. 4–11.
- NHI. 2000. *NHI Course #131053 Superpave Fundamentals Reference Manual*. FHWA-NHI-131053. National Highway Institute, Washington, DC.  
<https://idot.illinois.gov/Assets/uploads/files/Transportation-System/Manuals-Guides-&-Handbooks/T2/P028.pdf>.
- Prowell, B. D. and E. R. Brown. 2007. *NCHRP Report 573: Superpave Mix Design: Verifying Gyration Levels in the  $N_{design}$  Table*. National Cooperative Highway Research Program, Washington, DC.
- Qarouach, S. 2013. *An Investigation of the Effect of  $N_{design}$  Values on Performance of Superpave Mixtures*. MS thesis. North Carolina State University, Raleigh, NC.
- Roberts, F. L., P. S. Kandhal, E. R. Brown, D.-Y. Lee, and T. W. Kennedy. 1991. *Hot Mix Asphalt Materials, Mixture Design, and Construction*. 1st edition. National Asphalt Pavement Association (NAPA) Education Foundation, Lanham, MD.
- Schaefer, V. R., L. Stevens, D. White, and H. Ceylan. 2008. *Design Guide for Improved Quality of Roadway Subgrades and Subbases*. Iowa Statewide Urban Design and Specifications (SUDAS), Iowa State University, Ames, IA.  
[https://intrans.iastate.edu/app/uploads/2018/03/subgrade\\_subbase\\_tr525.pdf](https://intrans.iastate.edu/app/uploads/2018/03/subgrade_subbase_tr525.pdf).
- Schram, S., R. C. Williams, and A. Buss. 2014. Reporting Results from the Hamburg Wheel Tracking Device. *Transportation Research Record: Journal of the Transportation Research Board*, No. 2446, pp. 89–98.
- Smith, R. W. 1979. Purposes and Reasons for Compacting Asphalt Mixtures. In *Improved Asphalt Pavement Performance Through Effective Compaction*, pp. 9–11.
- Swanson, R. C., J. Nemecek, Jr., and E. Tons. 1965. Effect of Asphalt Viscosity on Compaction of Bituminous Concrete. *Highway Research Record*, No. 117, *Bituminous Materials, Mixtures, and Pavements*, Presented at the 44th Annual Meeting, January 11–15, pp. 23–52. <http://onlinepubs.trb.org/Onlinepubs/hrr/1966/117/117.pdf>.
- Tashman, L. S., E. Masad, B. Peterson, and H. Saleh. 2001. Internal Structure Analysis of Asphalt Mixes to Improve the Simulation of Superpave Gyrotory Compaction to Field Conditions (with Discussion). *Journal of the Association of Asphalt Paving Technologists*, Vol. 70. Asphalt Paving Technology 2001, March 19–21, Clearwater Beach, FL.
- Williams, R. C., A. Buss, M. G. J. Mercado, H. D. Lee, and A. Bozorgzad. 2016. *Validation of Gyrotory Mix Design in Iowa*. Asphalt Materials and Pavement Program (AMPP), Institute for Transportation, Iowa State University, Ames, IA.  
[https://intrans.iastate.edu/app/uploads/2018/03/gyrotory\\_mix\\_design\\_validation\\_w\\_cvr.pdf](https://intrans.iastate.edu/app/uploads/2018/03/gyrotory_mix_design_validation_w_cvr.pdf).

Witczak, M., K. Kaloush, T. Pellinen, M. El-Basyouny, and H. V. Quintus. 2002. *NCHRP Report 465: Simple Performance Test for Superpave Mix Design*. National Cooperative Highway Research Program, Washington DC.





**Iowa Department of Transportation**  
 Highway Division-Office of Materials  
 Proportion & Production Limits For Aggregates

County : Greene Project No.: ST\*N-4-2(36)-2J-37 Date: 10/02/06  
 Project Location: On IA 4 From US 30 To IA 175 In Calhoun County Mix Design No.: 1BD6-029  
 Contract Mix Formula: Intermediate Mix Size (in.): 1/2  
 Contractor: Henningsen Const Mix Type: HMA 1M Design Life ESAL's

Material	Ident #	% in Mix	Producer & Location	Type (A or B)	Friction Type	Beds	Gsb	%Abs
3/4 Stone	A94002	25.0%	Martin Marietta Fort Dodge Mine	A	4	36-42	2.644	0.81
3/8 Stone Chips	A94002	20.0%	Martin Marietta Fort Doge Mine	A	4	36-42	2.614	0.83
3/4 Screen Gravel	New Pit	37.0%	Becker Gravel Hauptert Pit	A	4		2.526	2.53
1/4 Conc Sand		18.0%	Hallett Jefferson	A	4		2.614	0.87

Type and Source of Asphalt Binder: PG 58-28 Flint Hills Algona

Material	Individual Aggregates Sieve Analysis - % Passing (Target)										
	1"	3/4"	1/2"	3/8"	#4	#8	#16	#30	#50	#100	#200
3/4 Stone	100	100	77	63	36	25	20	17	14	10	7.5
3/8 Stone Chips	100	100	100	100	24	8.0	5.0	3.5	2.5	2.0	1.7
3/4 Screen Gravel	100	100	91	88	73	59	45	29	14	6.9	5.2
1/4 Conc Sand	100	100	100	100	100	92	69	32	5.8	1.1	0.8

Preliminary Job Mix Formula Target Gradation											
Upper Tolerance	100	100	98	93	66	52	35	25	10	5.7	6.3
Comb Grading	100	100	91	86	59	47	35	21	10	5.7	4.3
Lower Tolerance	100	100	84	79	52	42	35	17	10	5.7	2.3
S.A.sq. m/kg	Total	4.93		+0.41	0.24	0.38	0.58	0.62	0.63	0.69	1.40

Production Limits for Aggregates Approved by the Contractor & Producer.										
Sieve Size in.	25.0% of mix 3/4 Stone		20.0% of mix 3/8 Stone Chips		37.0% of mix 3/4 Screen Gravel		18.0% of mix 1/4 Conc Sand			
	Min	Max	Min	Max	Min	Max	Min	Max		
1"	100.0	100.0	100.0	100.0	100.0	100.0	100.0	100.0		
3/4"	98.0	100.0	100.0	100.0	98.0	100.0	100.0	100.0		
1/2"	70.0	84.0	100.0	100.0	84.0	98.0	100.0	100.0		
3/8"	56.0	70.0	98.0	100.0	80.0	94.0	100.0	100.0		
#4	20.0	40.0	23.0	37.0	70.0	84.0	93.0	100.0		
#8	17.0	27.0	4.0	14.0	59.0	69.0	87.0	97.0		
#30	11.0	19.0	3.0	11.0	31.0	39.0	28.0	36.0		
#200	4.0	8.0	0.0	5.0	1.7	5.7	0.0	1.5		

Comments: \_\_\_\_\_  
 Copies to: Henningsen Const Dist 1 Lab

The above target gradations and production limits have been discussed with and agreed to by an authorized representative of the aggregate producer.

Signed: \_\_\_\_\_ Producer  
 Signed: \_\_\_\_\_ Contractor

**Figure 44. IA 4 formula (continued)**



**Iowa Department of Transportation**  
 Highway Division-Office of Materials  
 Proportion & Production Limits For Aggregates

County: Jasper Project No.: NHSN-320-1(24)-2R-50 Date: 06/19/06  
 Project Location: Ia 330 from Jasper County Line N. to US30 Mix Design No.: 1BD6-015  
 Contract Mix Tonnage: 28,500 Course: Surface Mix Size (in.): 1/2  
 Contractor: Cessford Construction Mix Type: HMA 10M Design Life ESAL's 10M

Material	Ident #	% in Mix	Producer & Location	Type (A or B)	Friction Type	Beds	Gsb	%Abs
Manf. Sand Combine	A64004	25.0%	Cessford - LeGrand	A	4	8-27	2.601	2.24
1/2 #220 Lmst.	A64004	38.0%	Cessford - LeGrand	A	4	8-27	2.607	1.88
5/8 5/8 X #4 Slag	A70008	12.0%	Linwood - Montpelier	A	2		3.721	1.32
3/8 Conc. Sand	A64502	25.0%	Martin Marietta - Marshalltown	A	4		2.627	0.66

Type and Source of Asphalt Binder: PG64-22 Bituminous Tama

Material	Individual Aggregates Sieve Analysis - % Passing (Target)										
	1"	3/4"	1/2"	3/8"	#4	#8	#16	#30	#50	#100	#200
Manf. Sand Combine	100	100	100	100	100	74	41	21	11	5.3	3.5
1/2 #220 Lmst.	100	100	99	80	41	22	16	13	11	9.8	8.8
5/8 5/8 X #4 Slag	100	100	96	55	3.2	1.8	1.6	1.4	1.3	1.1	1.0
3/8 Conc. Sand	100	100	100	100	98	88	73	44	9.2	1.2	0.8

Preliminary Job Mix Formula Target Gradation

Upper Tolerance	100	100	100	94	73	34	25				6.5
Comb Gradation	100	100	99	87	66	43	35	21	9.4	5.5	4.5
Lower Tolerance	100	100	92	80	59	44		17			2.5
S.A.sq. m/kg	Total	4.98		+0.41	0.27	0.40	0.57	0.61	0.58	0.67	1.49

Production Limits for Aggregates Approved by the Contractor & Producer.

Sieve Size in.	25.0% of mix		38.0% of mix		12.0% of mix		25.0% of mix			
	Manf. Sand Combine	1/2 #220 Lmst.	5/8 5/8 X #4 Slag	3/8 Conc. Sand	Min	Max	Min	Max		
1"	100.0	100.0	100.0	100.0	100.0	100.0	100.0	100.0		
3/4"	100.0	100.0	100.0	100.0	100.0	100.0	100.0	100.0		
1/2"	100.0	100.0	58.0	100.0	90.0	100.0	100.0	100.0		
3/8"	98.0	100.0	74.0	86.0	45.0	59.0	100.0	100.0		
#4	95.0	100.0	23.0	42.0	0.0	10.2	90.0	100.0		
#8	67.0	78.0	17.0	27.0	0.0	9.0	85.0	95.0		
#30	16.0	26.0	9.0	18.0	0.0	5.0	38.0	48.0		
#200	0.0	4.0	6.5	9.3	0.0	2.5	0.0	1.5		

Comments:

Copies to: Cessford Construction Marc Lamoreux Cheryl Baskin Central Materials  
 Jim Bailey Marshalltown RCE

The above target gradations and production limits have been discussed with and agreed to by an authorized representative of the aggregate producer.

Signed: \_\_\_\_\_ Producer  
 \_\_\_\_\_ Contractor

**Figure 46. IA 330 formula (continued)**





**APPENDIX B: QC/QA FIELD VOIDS DATA**

**Table 34. QC/QA data**

<b>ID</b>	<b>Iowa DOT Project No.</b>	<b>County</b>	<b>Thickness, mm</b>	<b>G<sub>mm</sub></b>	<b>Asphalt Binder%</b>	<b>VMA%</b>	<b>VFA%</b>	<b>AV%</b>	<b>ESAL</b>	<b>N<sub>design</sub></b>
IA 4	STPN-4-2(36)-2J-37	Calhoun	10.5	2.436	5.47	14.6	72.6	4.0	1M	76
IA 330	NHSN-330-1(24)-2R-50	Jasper	14.5	2.526	6.04	15.9	74.8	4.0	10M	96
I-235	IM-NHS-235-2(506)5-03-77	Polk	16	2.480	5.62	14.0	71.3	4.0	30M	109





## APPENDIX C: DYNAMAIC MODULUS TEST RESULTS

**Table 35. Dynamic modulus results**

<b>Mix</b>	<b>Temperature</b>	<b>25Hz</b>	<b>20Hz</b>	<b>10Hz</b>	<b>5Hz</b>	<b>2Hz</b>	<b>1Hz</b>	<b>0.5Hz</b>	<b>0.2Hz</b>	<b>0.1Hz</b>
I-235 Old N <sub>design</sub> Mix1	4	18230	17804	16771	15701	14121	12988	11930	10571	9647
I-235 Old N <sub>design</sub> Mix1	21	9894	9481	8258	7154	5809	4943	4137	3158	2589
I-235 Old N <sub>design</sub> Mix1	37	5122	4877	3970	3138	2308	1774	1277	878.6	729.7
I-235 Old N <sub>design</sub> Mix2	4	17888	17502	16371	15203	13663	12466	11334	9901	8904
I-235 Old N <sub>design</sub> Mix2	21	9789	9396	8210	7095	5804	4962	4182	3247	2686
I-235 Old N <sub>design</sub> n Mix2	37	5043	4734	3882	3169	2483	2070	1705	1401	1225
I-235 Old N <sub>design</sub> Mix3	4	17471	17051	15851	14666	13109	11945	10857	9468	8562
I-235 Old N <sub>design</sub> Mix3	21	9660	9269	8122	7006	5734	4915	4146	3218	2682
I-235 Old N <sub>design</sub> Mix3	37	4981	4695	3771	2996	2215	1741	1296	942.1	746
I-235 Old N <sub>design</sub> Mix4	4	16930	16778	15637	14590	13303	12340	11293	10097	9341
I-235 Old N <sub>design</sub> Mix4	21	9845	9486	8318	7216	5932	5066	4279	3320	2747
I-235 Old N <sub>design</sub> Mix4	37	5464	5154	4289	3536	2795	2347	1938	1575	1365
I-235 Old N <sub>design</sub> Mix5	4	16825	16284	14853	13806	12292	11057	10127	8802	7962
I-235 Old N <sub>design</sub> Mix5	21	9743	9373	8084	6944	5690	4850	4061	3148	2635
I-235 Old N <sub>design</sub> Mix5	37	4598	4312	3418	2654	1928	1494	1091	801.5	519.7

**Table 36. Dynamic modulus results (continued)**

<b>Mix</b>	<b>Temperature</b>	<b>25Hz</b>	<b>20Hz</b>	<b>10Hz</b>	<b>5Hz</b>	<b>2Hz</b>	<b>1Hz</b>	<b>0.5Hz</b>	<b>0.2Hz</b>	<b>0.1Hz</b>
I-235 New N <sub>design</sub> Mix1	4	14339	13933	12895	12012	10526	9599	8665	7509	6678
I-235 New N <sub>design</sub> Mix1	21	9400	9066	8059	7097	5982	5249	4576	3773	3308
I-235 New N <sub>design</sub> Mix1	37	5461	5227	4509	3909	3276	2894	2565	2199	1982
I-235 New N <sub>design</sub> Mix2	4	15157	14487	12499	11642	10700	9363	8335	6932	6194
I-235 New N <sub>design</sub> Mix2	21	8398	8122	7190	6323	5318	4656	4033	3366	2790
I-235 New N <sub>design</sub> Mix2	37	5116	3485	4061	3364	2642	2201	1811	1461	1251
I-235 New N <sub>design</sub> Mix3	4	16210	15857	14784	13693	12224	11088	10006	8527	7411
I-235 New N <sub>design</sub> Mix3	21	9179	8829	7825	6844	5732	5014	4335	3550	3071
I-235 New N <sub>design</sub> Mix3	37	4794	4540	3850	3280	2681	2331	2017	1725	1579
I-235 New N <sub>design</sub> Mix4	4	17827	17593	16635	15614	14167	13032	11912	10392	9191
I-235 New N <sub>design</sub> Mix4	21	9276	8967	7999	7083	6017	5325	4689	3935	3515
I-235 New N <sub>design</sub> Mix4	37	4792	4533	3799	3205	2589	2216	1876	1586	1404
I-235 New N <sub>design</sub> Mix5	4	18622	18330	17401	16401	14990	13970	12893	11416	10255
I-235 New N <sub>design</sub> Mix5	21	9709	9363	8359	7396	6297	5585	4927	4108	3647
I-235 New N <sub>design</sub> Mix5	37	5613	5375	4586	3946	3271	2870	2507	2137	1913

**Table 37. Dynamic modulus results (continued)**

<b>Mix</b>	<b>Temperature</b>	<b>25Hz</b>	<b>20Hz</b>	<b>10Hz</b>	<b>5Hz</b>	<b>2Hz</b>	<b>1Hz</b>	<b>0.5Hz</b>	<b>0.2Hz</b>	<b>0.1Hz</b>
IA 330 Old N <sub>design</sub> Mix1	4	15334	15036	14027	12936	11469	10393	9297	8027	7417
IA 330 Old N <sub>design</sub> Mix1	21	10449	10044	8932	7819	6478	5573	4704	3617	2913
IA 330 Old N <sub>design</sub> Mix1	37	5273	5064	4207	3441	2552	1979	1451	963	673
IA 330 Old N <sub>design</sub> Mix2	4	19253	18864	17857	16770	15322	14191	13041	11556	10486
IA 330 Old N <sub>design</sub> Mix2	21	10960	10489	9242	8072	6658	5715	4858	3798	3151
IA 330 Old N <sub>design</sub> Mix2	37	5631	5221	4284	3439	2531	1955	1422	957.8	697.3
IA 330 Old N <sub>design</sub> Mix3	4	17854	17673	16761	15709	14230	13239	12235	10987	10105
IA 330 Old N <sub>design</sub> Mix3	21	11220	10863	9659	8462	7008	6037	5122	3985	3255
IA 330 Old N <sub>design</sub> Mix3	37	6098	5821	4859	3962	2971	2329	1747	1205	893.1
IA 330 Old N <sub>design</sub> Mix4	4	15800	15463	14440	13378	11972	10971	9947	8648	8043
IA 330 Old N <sub>design</sub> Mix4	21	11596	11225	10070	8919	7533	6576	5719	4630	3929
IA 330 Old N <sub>design</sub> Mix4	37	6114	5821	4902	4053	3094	2480	1891	1313	984.1
IA 330 Old N <sub>design</sub> Mix5	4	18644	18283	17161	15957	14328	13089	11826	10338	9544
IA 330 Old N <sub>design</sub> Mix5	21	12601	12184	10906	9633	8091	7022	6037	4779	3997
IA 330 Old N <sub>design</sub> Mix5	37	6647	6309	5215	4237	3147	2454	1819	1215	877.4

**Table 38. Dynamic modulus results (continued)**

<b>Mix</b>	<b>Temperature</b>	<b>25Hz</b>	<b>20Hz</b>	<b>10Hz</b>	<b>5Hz</b>	<b>2Hz</b>	<b>1Hz</b>	<b>0.5Hz</b>	<b>0.2Hz</b>	<b>0.1Hz</b>
IA 330 New N <sub>design</sub> Mix1	4	17697	17330	16413	15576	14387	13454	12437	11218	10488
IA 330 New N <sub>design</sub> Mix1	21	11597	11244	10163	9088	7774	6847	5990	4933	4269
IA 330 New N <sub>design</sub> Mix1	37	6258	5970	5087	4283	3386	2817	2281	1687	1330
IA 330 New N <sub>design</sub> Mix2	4	17978	17860	16975	15996	14605	13484	12344	10956	10079
IA 330 New N <sub>design</sub> Mix2	21	10736	10376	9246	8166	6788	5852	4994	3949	3332
IA 330 New N <sub>design</sub> Mix2	37	5223	4929	4041	3269	2429	1894	1400	956.4	700.1
IA 330 New N <sub>design</sub> Mix3	4	18169	17873	16264	14912	14561	13561	12584	11377	10520
IA 330 New N <sub>design</sub> Mix3	21	10551	10172	9047	7918	6595	5690	4873	3860	3244
IA 330 New N <sub>design</sub> Mix3	37	5343	5066	4199	3422	2566	2016	1495	1015	731.1
IA 330 New N <sub>design</sub> Mix4	4	19825	19522	18580	17555	16154	15077	14001	12611	11610
IA 330 New N <sub>design</sub> Mix4	21	11230	10777	9596	8429	7027	6082	5217	4147	3484
IA 330 New N <sub>design</sub> Mix4	37	5903	5587	4635	3787	2846	2246	1688	1158	857.3
IA 330 New N <sub>design</sub> Mix5	4	17086	16663	15475	14279	12679	11457	10321	8949	8250
IA 330 New N <sub>design</sub> Mix5	21	11263	10869	9714	8578	7192	6264	5385	4333	3616
IA 330 New N <sub>design</sub> Mix5	37	5732	5444	4486	3639	2719	2122	1573	1069	786.5

**Table 39. Dynamic modulus results (continued)**

<b>Mix</b>	<b>Temperature</b>	<b>25Hz</b>	<b>20Hz</b>	<b>10Hz</b>	<b>5Hz</b>	<b>2Hz</b>	<b>1Hz</b>	<b>0.5Hz</b>	<b>0.2Hz</b>	<b>0.1Hz</b>
IA 4 Old N <sub>design</sub> Mix1	4	14671	14355	13443	12533	11255	10287	9378	8180	7345
IA 4 Old N <sub>design</sub> Mix1	21	7536	7219	6260	5368	4309	3621	3000	2290	1891
IA 4 Old N <sub>design</sub> Mix1	37	4016	3790	3085	2497	1908	1548	1239	973.9	1277
IA 4 Old N <sub>design</sub> Mix2	4	13609	13366	12494	11600	10381	9524	8598	7506	6801
IA 4 Old N <sub>design</sub> Mix2	21	7565	7267	6304	5422	4392	3717	3108	2408	2015
IA 4 Old N <sub>design</sub> Mix2	37	3923	3716	2992	2376	1733	1357	1009	921.2	727.6
IA 4 Old N <sub>design</sub> Mix3	4	15068	14741	13766	12724	11398	10435	9487	8289	7475
IA 4 Old N <sub>design</sub> Mix3	21	8373	8110	7195	6325	5295	4644	4049	3317	2906
IA 4 Old N <sub>design</sub> Mix3	37	3977	3778	3055	2438	1787	1403	1040	745.5	740.3
IA 4 Old N <sub>design</sub> Mix4	4	15716	15331	14355	13318	11937	10855	9791	8525	7637
IA 4 Old N <sub>design</sub> Mix4	21	8388	8019	6977	5994	4842	4081	3376	2549	2035
IA 4 Old N <sub>design</sub> Mix4	37	3940	3705	2947	2321	1673	1312	970.9	706.2	545.7
IA 4 Old N <sub>design</sub> Mix5	4	12453	12138	11248	10281	8969	8087	7208	6200	5646
IA 4 Old N <sub>design</sub> Mix5	21	7076	6778	5830	4952	3944	3297	2694	2023	1649
IA 4 Old N <sub>design</sub> Mix5	37	4165	3938	3219	2626	2027	1675	1361	1099	934.8

**Table 40. Dynamic modulus results (continued)**

<b>Mix</b>	<b>Temperature</b>	<b>25Hz</b>	<b>20Hz</b>	<b>10Hz</b>	<b>5Hz</b>	<b>2Hz</b>	<b>1Hz</b>	<b>0.5Hz</b>	<b>0.2Hz</b>	<b>0.1Hz</b>
IA 4 New N <sub>design</sub> Mix1	4	18030	17825	16862	15889	14547	13532	12517	11187	10326
IA 4 New N <sub>design</sub> Mix1	21	7999	7667	6706	5813	4789	4117	3509	2825	2428
IA 4 New N <sub>design</sub> Mix1	37	3740	3510	2800	2225	1657	1335	1179	1197	1027
IA 4 New N <sub>design</sub> Mix2	4	16088	15808	14841	14027	12714	11799	10789	9555	8894
IA 4 New N <sub>design</sub> Mix2	21	8476	8217	7161	6115	4840	4085	3460	2709	2274
IA 4 New N <sub>design</sub> Mix2	37	4098	3829	3092	2522	1958	1625	1330	1059	876.5
IA 4 New N <sub>design</sub> Mix3	4	17939	17639	16793	15814	14433	13476	12410	11148	10301
IA 4 New N <sub>design</sub> Mix3	21	8083	7754	6736	5842	4816	4109	3472	2773	2368
IA 4 New N <sub>design</sub> Mix3	37	4063	3809	3090	2485	1893	1547	1258	1015	866.1
IA 4 New N <sub>design</sub> Mix4	4	18122	17810	16877	15903	14595	13555	12489	11112	10192
IA 4 New N <sub>design</sub> Mix4	21	7928	7605	6654	5771	4758	4087	3476	2782	2383
IA 4 New N <sub>design</sub> Mix4	37	3702	3490	2782	2171	1547	1193	868.9	651.8	528.5
IA 4 New N <sub>design</sub> Mix5	4	18887	18605	17843	16963	15832	14981	14155	12976	12132
IA 4 New N <sub>design</sub> Mix5	21	8941	8620	7646	6715	5611	4877	4193	3393	2911
IA 4 New N <sub>design</sub> Mix5	37	4870	4632	3876	3209	2501	2070	1683	1336	1129

## APPENDIX D: HAMBURG WHEEL TRACKING TEST RESULTS

Table 41. HWTT results

Mix	No. of Wheel Passes	Rut Depth (mm)				Max Impression (mm)	Creep Slope (mm/1,000 passes)	Strip Slope (mm/1,000 passes)	SIP
		8,000 passes	10,000 passes	15,000 passes	20,000 passes				
H330 L1-2	20,000	2.76	3	3.5	4.06	4.29	0.0915	0.1313	20,000
H330 L3-4	20,000	2.76	3	3.5	4.06	4.29	0.0915	0.1313	20,000
H330 R5-6	20,000	2.12	2.32	2.66	3.07	3.53	0.0599	0.1153	20,000
H330 R7-8	20,000	2.12	2.32	2.66	3.07	3.53	0.0599	0.1153	20,000
HWY 330 L4-5	19,300	2.43	2.68	3.38	4.31	6.64	0.0971	0.188	17,664
HWY 330 L6-7	19,950	2.33	2.58	3.15	4.08	5.73	0.1064	0.2353	17,231
HWY 330 R9-10	20,000	1.57	1.68	1.79	1.99	2.44	0.026	0.0457	20,000
HWY 330 R11-12	20,000	1.57	1.68	1.79	1.99	2.44	0.026	0.0457	20,000
I-235 BI L1	20,000	2.41	2.6	2.91	3.27	3.99	0.0532	0.0766	20,000
I-235 BI L2	20,000	2.5	2.76	3.26	3.85	4.54	0.0902	0.1402	20,000
I-235 BI L3	20,000	2.74	2.87	3.26	3.73	4.43	0.0772	0.1004	20,000
I-235 BI L4	20,000	2.43	2.58	2.92	3.17	3.87	0.0543	0.0819	20,000
I-235 R1	20,000	2.32	2.47	2.8	2.98	3.7	0.0402	0.0642	20,000
I-235 R2	20,000	2.22	2.32	2.56	2.73	3.28	0.0327	0.0613	20,000
I-235 R3	20,000	1.91	2.02	2.24	2.39	2.83	0.0346	0.0469	20,000

**Table 42. HWTT results (continued)**

<b>Mix</b>	<b>No. of Wheel Passes</b>	<b>Rut Depth (mm)</b>				<b>Max Impression (mm)</b>	<b>Creep Slope (mm/1,000 passes)</b>	<b>Strip Slope (mm/1,000 passes)</b>	<b>SIP</b>
		<b>8,000 passes</b>	<b>10,000 passes</b>	<b>15,000 passes</b>	<b>20,000 passes</b>				
I-235 R4	20,000	1.76	1.87	2.11	2.33	3.23	0.0367	0.0536	20,000
H 4 L1	20,000	2.08	2.26	2.61	2.98	3.49	0.0622	0.0878	20,000
H 4 L2	20,000	2	2.15	2.50	2.88	3.64	0.0565	0.0809	20,000
H 4 L3	20,000	1.83	1.98	2.27	2.55	3.06	0.0404	0.071	20,000
H 4 L4	20,000	1.91	2.07	2.32	2.5	2.95	0.0262	0.0938	20,000
HWY 4 R1	20,000	2.11	2.26	2.54	2.75	3.41	0.047	0.0658	20,000
HWY 4 R2	20,000	1.86	2.03	2.32	2.48	3.1	0.0356	0.0672	20,000
HWY 4 R3	20,000	1.85	2.03	2.26	2.6	3.23	0.0498	0.0836	20,000
HWY 4 R4	20,000	1.97	2.15	2.43	2.59	3.05	0.0457	0.0488	20,000



## APPENDIX E: DCT RESULTS

**Table 43. DCT Results**

<b>Mix</b>	<b>Fracture Energy (J/m<sup>2</sup>)</b>	<b>Peak Load (kN)</b>
Old IA 4 DCT1	252	2.469
Old IA 4 DCT2	278	2.645
Old IA 4 DCT3	271	2.671
Old IA 4 DCT4	327	2.516
New IA 4 DCT1	266	2.762
New IA 4 DCT2	236	2.548
New IA 4 DCT3	239	2.329
New IA 4 DCT4	214	2.469
Old IA 330 DCT1	189	2.477
Old IA 330 DCT2	229	2.482
Old IA 330 DCT3	281	2.608
Old IA 330 DCT4	302	2.363
New IA 330 DCT1	290	2.557
New IA 330 DCT2	236	2.594
New IA 330 DCT3	275	2.712
New IA 330 DCT4	334	2.779
Old I-235 DCT1	567	2.888
Old I-235 DCT2	320	2.443
Old I-235 DCT3	311	2.486
Old I-235 DCT4	437	2.453
New I-235 DCT1	497	2.615
New I-235 DCT2	693	2.633
New I-235 DCT3	453	2.448
New I-235 DCT4	521	2.569



## APPENDIX F: BEAM FATIGUE TEST RESULTS

**Table 44. Beam fatigue results**

Mix Type		Microstrain ( $\mu\epsilon$ )	Initial Flexural Stiffness (MPa)	50% of Initial Flexural Stiffness (MPa)	Flexural Stiffness at end of test (MPa)	Cycles to Failure ( $N_f$ )	Cumulative dissipated energy ( $\text{MJ/m}^3$ )	
IA 330	old	1	900	5416	2708	2389	7020	38.9
		2	900	5680	2840	2239	3700	20.8
		3	700	7058	3529	3209	8490	36.7
		4	700	5408	2704	2384	7880	26.7
		5	500	6047	3023.5	2807	35540	69.6
		6	500	4990	2495	2345	68860	73.5
	new	1	900	5776	2888	2378	3360	19.7
		2	900	4906	2453	2019	4500	21.2
		3	700	5814	2907	2589	15610	56.4
		4	700	5845	2922.5	2551	15620	53.1
		5	500	6307	3153.5	2867	49430	93.4
		6	500	6168	3084	2885	63580	116.4

**Table 45. Beam fatigue results (continued)**

Mix Type		Microstrain ( $\mu\epsilon$ )	Initial Flexural Stiffness (MPa)	50% of Initial Flexural Stiffness (MPa)	Flexural Stiffness at end of test (MPa)	Cycles to Failure ( $N_f$ )	Cumulative dissipated energy ( $\text{MJ/m}^3$ )	
I-235	old	1	900	4272	2136	1752	16760	63.6
		2	900	3179	1589.5	1316	7980	24
		3	700	2852	1426	1306	58260	100.4
		4	700	2601	1300.5	1144	51190	74.9
		5	500	2098	1049	928	529880	309
		6	500	3859	1929.5	1732	512350	546
	new	1	900	2893	1446.5	1166	10770	27.3
		2	900	3979	1989.5	1592	9030	32.8
		3	700	3275	1637.5	1416	47970	92
		4	700	3422	1711	1487	36020	71.2
		5	500	3469	1734.5	1549	311760	332.1
		6	500	4046	2023	1906	732820	851.7

**Table 46. Beam fatigue results (continued)**

Mix Type		Microstrain ( $\mu\epsilon$ )	Initial Flexural Stiffness (MPa)	50% of Initial Flexural Stiffness (MPa)	Flexural Stiffness at end of test (MPa)	Cycles to Failure ( $N_f$ )	Cumulative dissipated energy (MJ/m <sup>3</sup> )	
IA 4	old	1	900	3948	1974	1591	5970	21.9
		2	900	3092	1546	1253	8800	25
		3	700	3994	1997	1728	21890	51.3
		4	700	4687	2343.5	1992	16390	44.7
		5	500	3805	1902.5	1711	135080	147.5
		6	500	4728	2364	2121	117380	160.3
	new	1	900	4463	2231.5	1779	8980	36
		2	900	4135	2067.5	1674	6770	25.7
		3	700	3451	1725.5	1469	38140	56
		4	700	3813	1906.5	1650	24570	53.4
		5	500	4502	2251	1999	74680	104
		6	500	4589.3	2294.65	2092	41560	77.9



## APPENDIX G: AASHTOWARE PAVEMENT ME DESIGN INPUTS

**Table 47. Binder input**

<b>Pavement</b>	<b>PG</b>	<b>Temp</b>	<b>G* (Pa)</b>	<b><math>\delta</math> (°)</b>
I-235	64-22	58	15814	75.47
		64	7120	78.52
		70	3280	81.24
IA 4	58-28	52	7771	79.42
		58	3406	82.35
		64	1541	84.68
IA 330	64-22	58	9761	79.99
		64	4254	82.52
		70	1912	84.66

**Table 48. 2014 ME Design inputs summary**

Pavement Name	New or Old N-Design	Binder Types	Traffic (AADTT) 2 way	No. of lanes in design direction	% of trucks in design direction	% of trucks in design lane	operational speed (mph)
I-235	Old	PG 64-22	5047	4	50.00%	0.78	60
I-235	New	PG 64-22	5047	4	50.00%	0.78	60
HWY 4	Old	PG 58-28	642	2	50.00%	1	55
HWY 4	New	PG 58-28	642	2	50.00%	1	55
HWY 330	Old	PG 64-22	707	2	50.00%	1	65
HWY 330	New	PG 64-22	707	2	50.00%	1	65



**Table 49. 2014 ME Design inputs summary (continued)**

Pavement Name	New or Old N-Design	Subgrade	AC Surface Pavement Thickness	Total Concrete Base Thickness	Climatic Location	Initial Year Built	Field Data Collected	Service Life
I-235	Old	A-4 (90%)	6	10	Polk	2006	2014	8
I-235	New	A-4 (90%)	6	10	Polk	2006	2014	8
HWY 4	Old	A-7-5 (70%)	3	8	Calhoun	2006	2014	8
HWY 4	New	A-7-5 (70%)	3	8	Calhoun	2006	2014	8
HWY 330	Old	A-6 (80%)	5	10	Jasper	2006	2014	8
HWY 330	New	A-6 (80%)	5	10	Jasper	2006	2014	8

**Table 50. 2016 ME Design inputs summary**

Pavement Name	New or Old N-Design	Binder Types	Traffic (AADTT) 2 way	No. of lanes in design direction	% of trucks in design direction	% of trucks in design lane	operational speed (mph)
I-235	Old	PG 64-22	5478	4	50.00%	0.78	60
I-235	New	PG 64-22	5478	4	50.00%	0.78	60
HWY 4	Old	PG 58-28	515	2	50.00%	1	55
HWY 4	New	PG 58-28	515	2	50.00%	1	55
HWY 330	Old	PG 64-22	755	2	50.00%	1	65
HWY 330	New	PG 64-22	755	2	50.00%	1	65

**Table 51. 2016 ME Design inputs summary (continued)**

Pavement Name	New or Old N-Design	Subgrade	AC Surface Pavement Thickness	Total Concrete Base Thickness	Climatic Location	Initial Year Built	Field Data Collected	Service Life
I-235	Old	A-4 (90%)	6	10	Polk*	2006	2018	12
I-235	New	A-4 (90%)	6	10	Polk*	2006	2018	12
HWY 4	Old	A-7-5 (70%)	3	8	Calhoun*	2006	2018	12
HWY 4	New	A-7-5 (70%)	3	8	Calhoun*	2006	2018	12
HWY 330	Old	A-6 (80%)	5	10	Jasper*	2006	2018	12
HWY 330	New	A-6 (80%)	5	10	Jasper*	2006	2018	12





**THE INSTITUTE FOR TRANSPORTATION IS THE FOCAL POINT FOR TRANSPORTATION  
AT IOWA STATE UNIVERSITY.**

**InTrans** centers and programs perform transportation research and provide technology transfer services for government agencies and private companies;

**InTrans** contributes to Iowa State University and the College of Engineering's educational programs for transportation students and provides K–12 outreach; and

**InTrans** conducts local, regional, and national transportation services and continuing education programs.



**IOWA STATE  
UNIVERSITY**

Visit [InTrans.iastate.edu](http://InTrans.iastate.edu) for color pdfs of this and other research reports.